

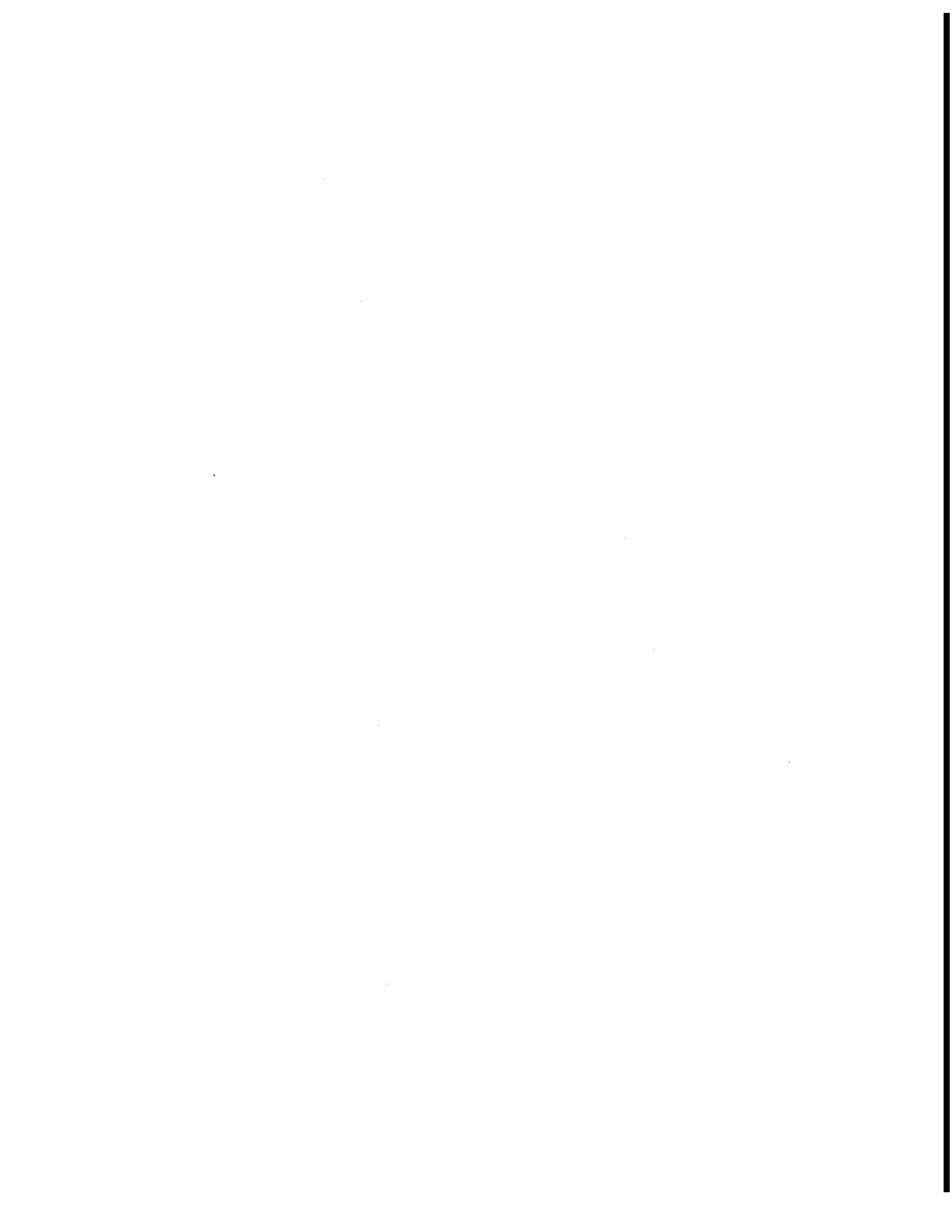
AIRCRAFT ALTITUDE MEASUREMENT USING  
A VECTOR MAGNETOMETER

Research Report

R. Peitila & W. R. Dunn, Jr.

December 1, 1977

NASA Grant NGR 05-017-031



AIRCRAFT ATTITUDE  
MEASUREMENT USING A  
VECTOR MAGNETOMETER

Preface

The following report is based on work performed as a part of NASA Grant 05-017-031 by the University of Santa Clara, Department of Electrical Engineering and Computer Science.

Inquiries regarding this work can be directed to:

Dr. W. R. Dunn  
c/o Department of Electrical Engineering & Computer Science  
University of Santa Clara  
Santa Clara, California 95053

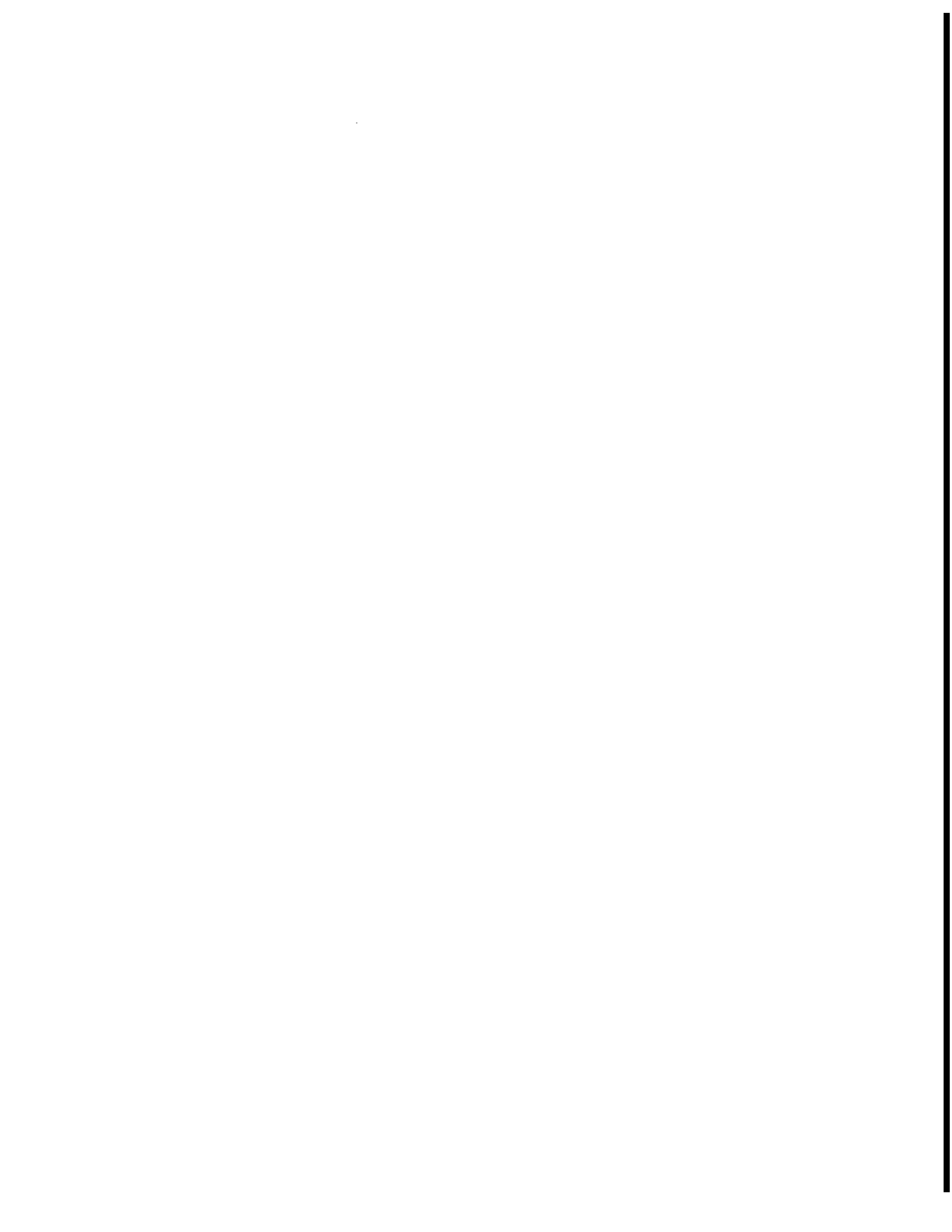


TABLE OF CONTENTS

Acknowledgment . . . . .	iii
Abstract . . . . .	iv
I A VECTOR AUTOPILOT SYSTEM	
1-1 Introduction . . . . .	1
1-2 Attitude Determination . . . . .	2
1-3 Attitude Determination Employing Magnetic Field Components . . . . .	6
1-4 A Possible System Configuration . . . . .	8
1-5 Other Considerations . . . . .	15
1-6 Conclusions . . . . .	19
II AN ATTITUDE INDEPENDENT REMOTE MAGNETIC INDICATOR	
2-1 Introduction . . . . .	20
2-2 An Algorithm to Compute Aircraft Heading . . . . .	21
2-3 Mechanization of the Heading Algorithm . . . . .	27
2-4 Conclusions . . . . .	28
III DESIGN OF A MICROPROCESSOR BASED HEADING INSTRUMENT	
3-1 Introduction . . . . .	30
3-2 Hardware Design Considerations . . . . .	31
3-3 Software Design Considerations . . . . .	37
3-4 Design of Subroutines . . . . .	39
3-5 Conclusions . . . . .	50
IV HEADING INSTRUMENT ERROR ANALYSIS	
4-1 Introduction . . . . .	54
4-2 Sensor Errors . . . . .	55
4-3 Analog Subsystem Error Analysis . . . . .	74
4-4 Processing Errors . . . . .	90
4-5 Measurement Error Summary . . . . .	97
4-6 Sample Error Analysis . . . . .	99
4-7 Conclusions . . . . .	102

Table of Contents (Continued)

V	LABORATORY EVALUATION OF THE ATTITUDE INDEPENDENT REMOTE MAGNETIC INDICATOR AND HEADING INSTRUMENT	
5-1	Introduction . . . . .	104
5-2	Test Apparatus . . . . .	105
5-3	Heading Measurements With No Offset Correction	109
5-4	Heading Measurements to investigate Orthogon- ality Error . . . . .	113
5-5	Conclusions . . . . .	114
Appendix A:	Instruction Set of the Signetics 2650 microprocessor chip . . . . .	127
Appendix B:	Assembly Language Program . . . . .	130
Appendix C:	Table Generating Programs . . . . .	156

## CHAPTER I

## A VECTOR AUTOPILOT SYSTEM

## 1-1 INTRODUCTION

An essential requirement of an aircraft attitude control system is that deviation of the body axes relative to a reference axes frame must be sensed. In addition, to overcome the ever-present possibility of errors or failure of the sensors, various configurations of redundant sensors are usually employed to assist in detection and correction of errors. To this end, there has been a continuing effort to improve existing sensors, to develop new sensor configurations, and to develop new sensor devices.

This chapter discusses the role of a vector magnetometer<sup>1</sup> as a new instrument for aircraft attitude determination. Although magnetometers have played a role in the attitude measurement of missiles and satellites [Ref. 1-1], there is an apparent lack of application in aircraft systems. By providing independent measures of attitude, the solid state vector magnetometer sensor system can not only assist in improving accuracy and reliability of existing systems but can also reduce component count with obvious benefits in weight and cost. Additionally, since a large number of aircraft heading reference systems depend on measurement of the Earth's magnetic field, it can be shown that by substituting a three-axis magnetometer for the remote sensing unit; both heading and attitude measurement functions can be derived using common elements, thereby further reducing the component count.

---

<sup>1</sup>Aviation use to date has been essentially scalar magnetometry.

To investigate the feasibility of the above system, this chapter will proceed by developing a technique to determine attitude given magnetic field components. Sample calculations are then made using the Earth's magnetic field data acquired during actual flight conditions. Results of these calculations are compared graphically with measured attitude data acquired simultaneously with the magnetic data. The role and possible implementation of various reference angles are discussed along with other pertinent considerations. Finally, it is concluded that the Earth's magnetic field as measured by modern vector magnetometers can play a significant role in attitude control systems.

## 1-2 ATTITUDE DETERMINATION

Coordinate systems are usually defined by orthogonal right-handed sets of three unit vectors. An example of such a set is illustrated in Fig. 1-1 where the orientation of the body fixed frame used in this paper is delineated. Angular rotations are conventionally defined as rotations in the plane normal to a unit vector with the positive sense of rotation defined by the right-hand rule [Ref. 1-2].

To derive relationships of attitude variations as a function of magnetic vector component variation, we can proceed by considering matrix representations of an orthogonal transformation. If  $H_x$ ,  $H_y$ , and  $H_z$  are the magnetic components measured at a desired airframe attitude and  $H_x'$ ,  $H_y'$ , and  $H_z'$  are the components measured after any rotation of the body, vector  $H' = [H_x' \ H_y' \ H_z']^T$  can be related to vector  $H = [H_x \ H_y \ H_z]^T$  by an orthogonal linear transformation  $H' = AH$ . Here  $A$  must satisfy the orthogonality condition  $AA^T = I$ , where  $A^T$  is the transpose of  $A$ ; additionally, the determinant of  $A$  must be unity [Ref. 1-3, 1-4].



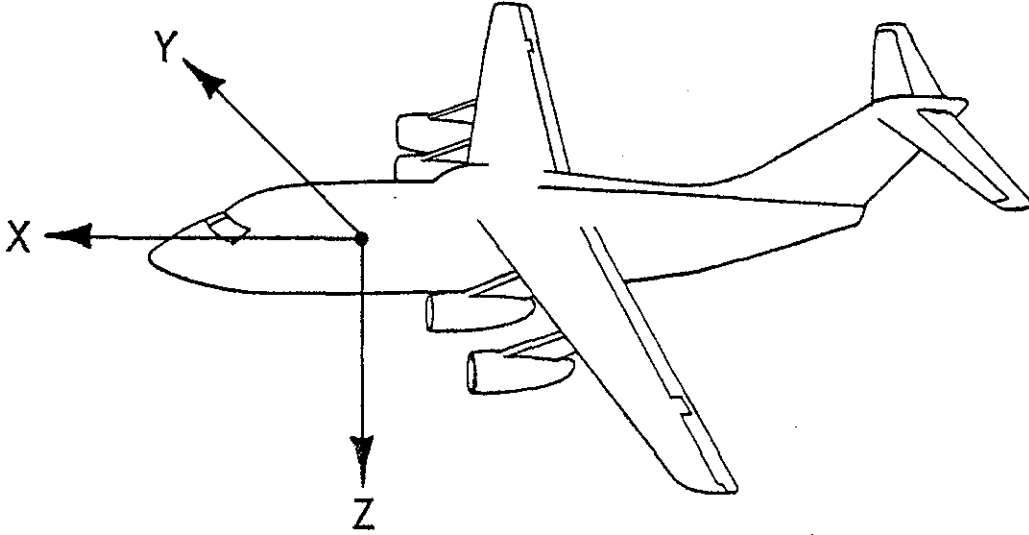


Fig. 1-1 AXIS ORIENTATION

Rotations about the z axis in Fig. 1-1 result in yaw deviations ( $\psi$ ) and in new components ( $H'$ ), as shown by

$$\begin{bmatrix} Hx' \\ Hy' \\ Hz' \end{bmatrix} = \begin{bmatrix} \cos \psi & \sin \psi & 0 \\ -\sin \psi & \cos \psi & 0 \\ 0 & 0 & 1 \end{bmatrix} \begin{bmatrix} Hx \\ Hy \\ Hz \end{bmatrix} \quad (1-1)$$

Similarly, independent rotations about the y axis and the x axis result in pitch ( $\theta$ ) and roll ( $\phi$ ) dependent variations in the measured H components, as shown by

$$\begin{bmatrix} Hx' \\ Hy' \\ Hz' \end{bmatrix} = \begin{bmatrix} \cos \theta & 0 & -\sin \theta \\ 0 & 1 & 0 \\ \sin \theta & 0 & \cos \theta \end{bmatrix} \begin{bmatrix} Hx \\ Hy \\ Hz \end{bmatrix} \quad (1-2)$$

$$\begin{bmatrix} Hx' \\ Hy' \\ Hz' \end{bmatrix} = \begin{bmatrix} 1 & 0 & 0 \\ 0 & \cos \phi & \sin \phi \\ 0 & -\sin \phi & \cos \phi \end{bmatrix} \begin{bmatrix} Hx \\ Hy \\ Hz \end{bmatrix} \quad (1-3)$$

The effect of a combined rotation can be expressed by using the product of the transformation matrices. In addition, if the rotations are small, the total rotation experienced by applying sequential rotations is independent of the order in which the rotations are performed [Ref. 1-3,1-4].

$$\begin{bmatrix} Hx' \\ Hy' \\ Hz' \end{bmatrix} = \begin{bmatrix} \cos \psi & \sin \psi & 0 \\ -\sin \psi & \cos \psi & 0 \\ 0 & 0 & 1 \end{bmatrix} \begin{bmatrix} \cos \theta & 0 & -\sin \theta \\ 0 & 1 & 0 \\ \sin \theta & 0 & \cos \theta \end{bmatrix} \begin{bmatrix} 1 & 0 & 0 \\ 0 & \cos \phi & \sin \phi \\ 0 & -\sin \phi & \cos \phi \end{bmatrix} \begin{bmatrix} Hx \\ Hy \\ Hz \end{bmatrix} \quad (1-4a)$$

$$\begin{bmatrix} Hx' \\ Hy' \\ Hz' \end{bmatrix} = \begin{bmatrix} \cos \psi \cos \theta & \sin \psi \cos \theta & \sin \theta \cos \psi \\ -\sin \psi \cos \theta & \cos \psi \cos \theta & -\sin \theta \sin \psi \\ \sin \theta & -\cos \theta \sin \psi & \cos \theta \end{bmatrix} \begin{bmatrix} Hx \\ Hy \\ Hz \end{bmatrix}$$

$$\begin{bmatrix} \sin \phi \sin \psi & -\sin \theta \cos \psi \\ \cos \psi \sin \phi & +\sin \psi \sin \theta \\ \cos \phi \cos \theta & \cos \phi \end{bmatrix} \begin{bmatrix} Hx \\ Hy \\ Hz \end{bmatrix} \quad (1-4b)$$

Assume that the angular variations  $\theta$ ,  $\psi$ , and  $\phi$  are small enough so that the small angle approximations

$$\begin{aligned}\sin \theta &\approx \theta, \quad \sin \psi \approx \psi, \quad \sin \phi \approx \phi, \\ \cos \theta &\approx \cos \psi \approx \cos \phi \approx 1\end{aligned}$$

can be made. Then, if the products of small angles (in radians) can be assumed to be much smaller than the angles alone, the expression reduces to

$$\begin{bmatrix} Hx' \\ Hy' \\ Hz' \end{bmatrix} = \begin{bmatrix} 1 & \psi & -\theta \\ -\psi & 1 & \phi \\ \theta & -\phi & 1 \end{bmatrix} \begin{bmatrix} Hx \\ Hy \\ Hz \end{bmatrix} \quad (1-5)$$

Further modifications in the form of the matrices result in

$$\begin{bmatrix} Hx' \\ Hy' \\ Hz' \end{bmatrix} = \begin{bmatrix} -Hz & Hy & 0 \\ 0 & -Hx & Hz \\ Hx & 0 & -Hy \end{bmatrix} \begin{bmatrix} \theta \\ \psi \\ \phi \end{bmatrix} + \begin{bmatrix} Hx \\ Hy \\ Hz \end{bmatrix} \quad (1-6)$$

By subtracting, we arrive at an expression for the difference in H components as functions of angular deviation.

$$\begin{bmatrix} Hx' \\ Hy' \\ Hz' \end{bmatrix} - \begin{bmatrix} Hx \\ Hy \\ Hz \end{bmatrix} = \begin{bmatrix} \Delta Hx \\ \Delta Hy \\ \Delta Hz \end{bmatrix} = \begin{bmatrix} -Hz & Hy & 0 \\ 0 & -Hx & Hz \\ Hx & 0 & -Hy \end{bmatrix} \begin{bmatrix} \theta \\ \psi \\ \phi \end{bmatrix} \quad (1-7)$$

It is significant to note at this point that the transformation matrix is singular implying that solutions for  $\theta$ ,  $\psi$ , and  $\phi$  are not independently available.

### 1-3 ATTITUDE DETERMINATION EMPLOYING MAGNETIC FIELD COMPONENTS

A given orthogonal set of three unit vectors can be displaced in Euclidean space by rotating the system through any angle  $\delta$  about a directed rotation axis. It is also customary to represent this rotation vectorially as a directed line segment whose length is proportional to the rotation angle. This rotation is analogous to the rotation experienced by the body fixed frame of Fig. 1-1 as the aircraft experiences combined pitch, yaw, and roll variation. During flight the body fixed set rotates about this rotation axis assuming new (possibly erroneous) attitudes in space. The task of the attitude sensing system is to provide measures of compounded pitch, yaw, and roll that would result in the same attitude assuming that the rotations occurred sequentially about the x, y and z axes rather than the actual rotation axis.

It was shown in the previous section that a compounded rotation of an orthogonal set can be described by a product of respective transformation matrices. Additionally it was noted that for small angular rotations the order of multiplication is unimportant. Using the relationships of (1-7), expressions for the angular deviations in terms of measured magnetic vector components can be derived.

$$\Delta H_x = -H_z\theta + H_y\psi \quad (1-8a)$$

yields

$$\theta = (H_y\psi - \Delta H_x)/H_z \quad (1-8b)$$

$$\psi = (\Delta H_x + H_z\theta)/H_y \quad (1-8c)$$

Similarly,

$$\Delta H_y = -H_x \psi + H_z \phi \quad (1-9a)$$

yields

$$\psi = (H_z \phi - \Delta H_y) / H_x \quad (1-9b)$$

$$\theta = (\Delta H_y + H_x \psi) / H_z \quad (1-9c)$$

and

$$\Delta H_z = H_x \theta - H_y \phi \quad (1-10a)$$

yields

$$\theta = (\Delta H_z + H_y \phi) / H_x \quad (1-10b)$$

$$\phi = (H_x \theta - \Delta H_z) / H_y \quad (1-10c)$$

Assuming that  $H_x$ ,  $H_y$  and  $H_z$  are nominal vector components as measured in a reference attitude and that  $H_x'$ ,  $H_y'$  and  $H_z'$  are new field components at the new attitude, then  $\Delta H_x = H_x' - H_x$ ,  $\Delta H_y = H_y' - H_y$ ,  $\Delta H_z = H_z' - H_z$  are expressions of the incremental changes in field components. Additionally, before using (1-8), (1-9) or (1-10) to solve for attitude variations (pitch, yaw, or roll), one additional angle from an auxiliary sensor<sup>2</sup> must be supplied. Using one additional angle of rotation (about any one axis) the remaining two rotations can then be calculated.

To illustrate this point, flight data acquired during the flight of a NASA flown Convair 900 instrumented with a three-axis magnetometer and a Litton inertial navigation system were used to calculate roll, pitch, and yaw.

---

<sup>2</sup>It was noted following (1-7) that a unique solution for attitude variation is not possible using magnetic field data alone.

Attitude variation about each of the three axes was calculated using measured magnetic field components supported by one angle from the inertial system. The results of these calculations are plotted in Figs. 1-2 through 1-4.

It is significant to note that the rotations shown occurred simultaneously (i.e., time base is the same for all three figures). The flight was at an altitude of approximately 5000 ft at an airspeed of approximately 250 nmi/h.

Although the data used to plot the attitudes shown in Figs. 1-2 through 1-4 were not acquired specifically for this purpose, the correlations in measured and calculated attitude clearly show that; within the limits of instrument accuracy, signals proportional to attitude variation can be derived using flight data.

#### 1-4 A POSSIBLE SYSTEM CONFIGURATION

Since the intent of this chapter is to introduce the notion that magnetometer technology has advanced to the point where three-axis magnetometers can be incorporated in aircraft attitude sensing systems on a cost effective basis, the system discussion will be limited in scope to describing a possible combined heading and attitude measurement method.

Heading references fall into three classes; 1) those that depend on the Earth's magnetic field, 2) those that depend on the use of low-drift gyroscope to retain a preset azimuth, and 3) those (gyrocompasses) that depend on sensing the Earth's rotation [Ref.1-5]. By far the greatest number of aircraft heading systems depend on the Earth's magnetic field, although many of these include gyroscopes to improve the performance characteristics.

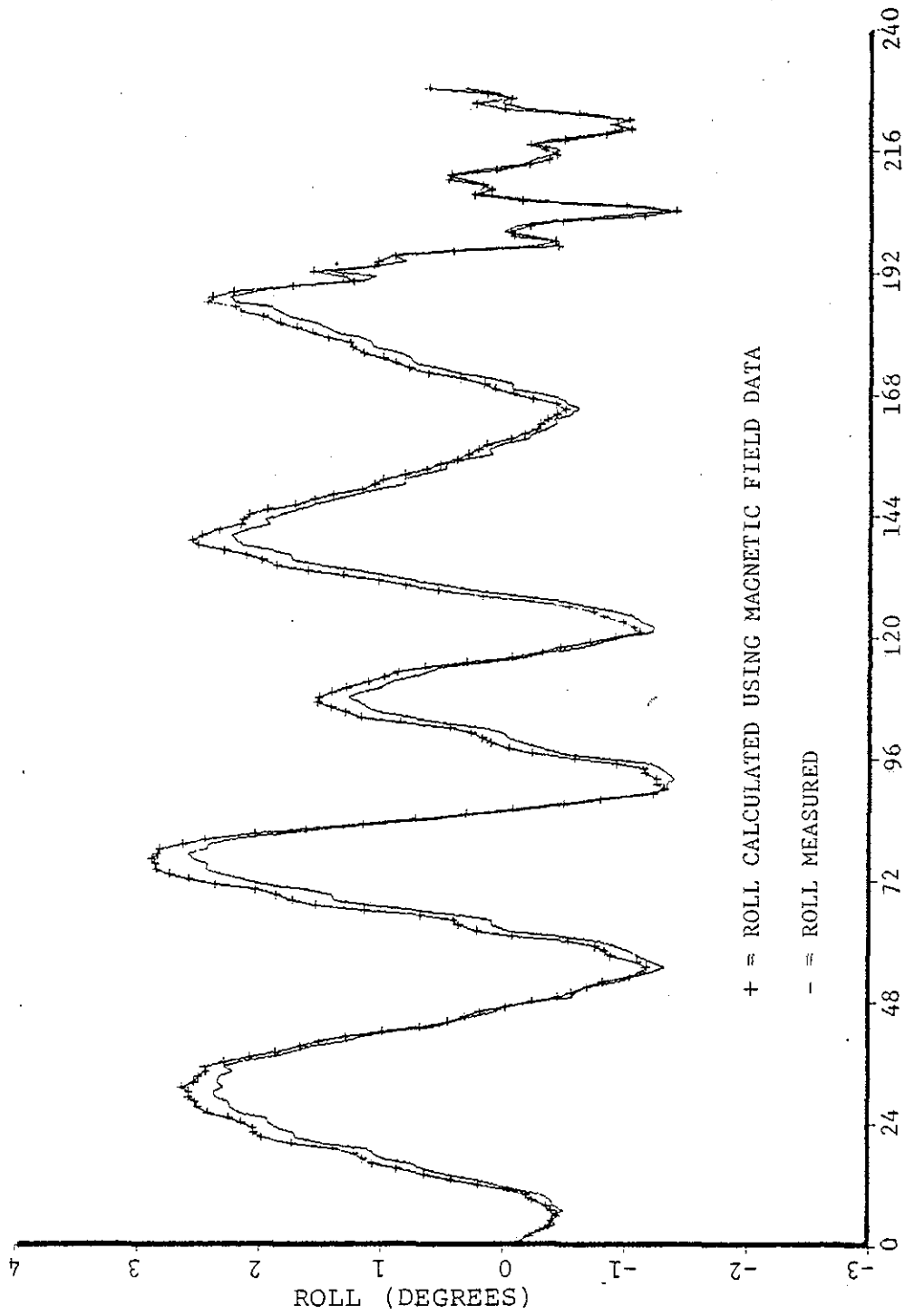


FIGURE 1-2 ROLL AXIS

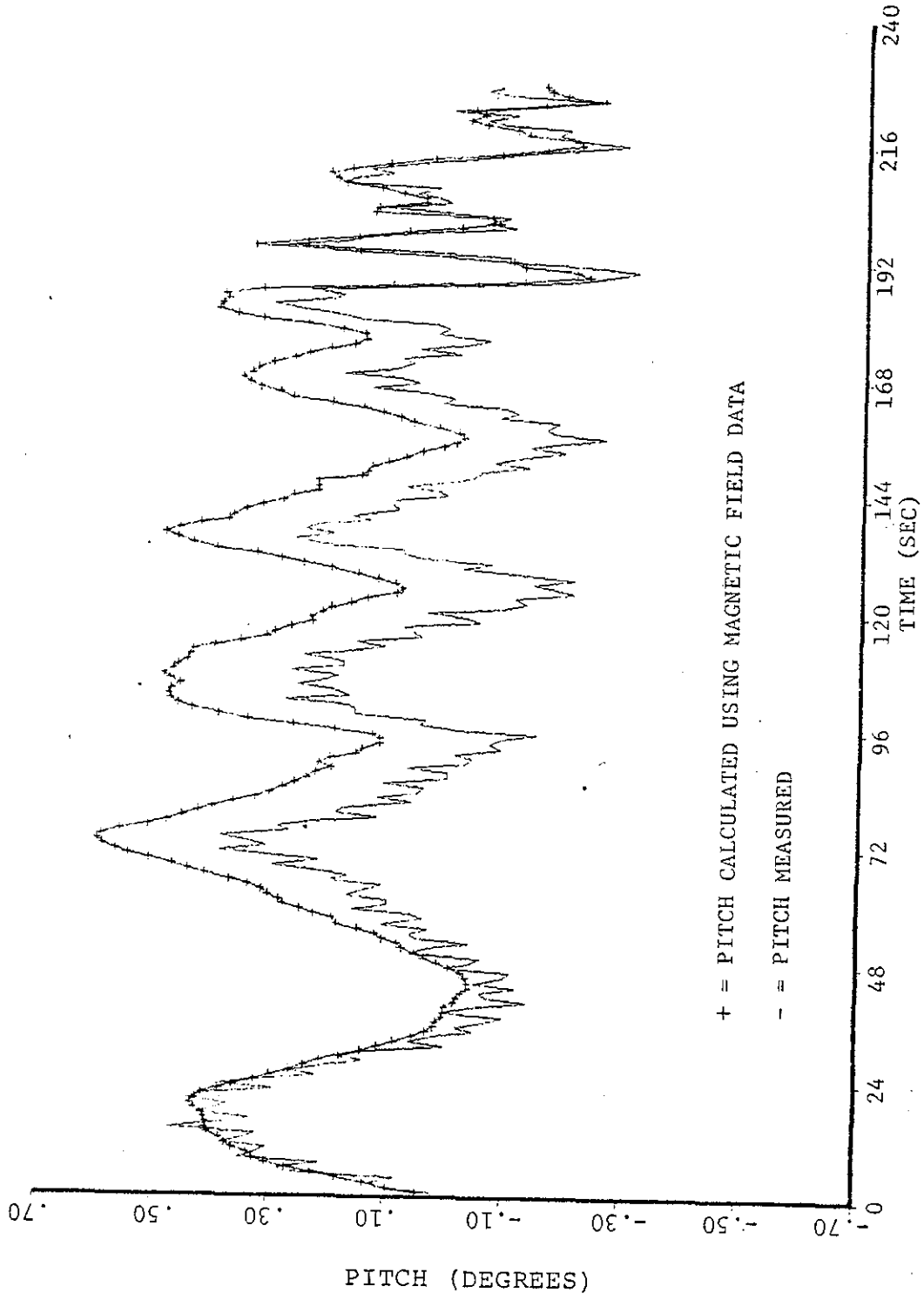


FIGURE 1-3 PITCH AXIS



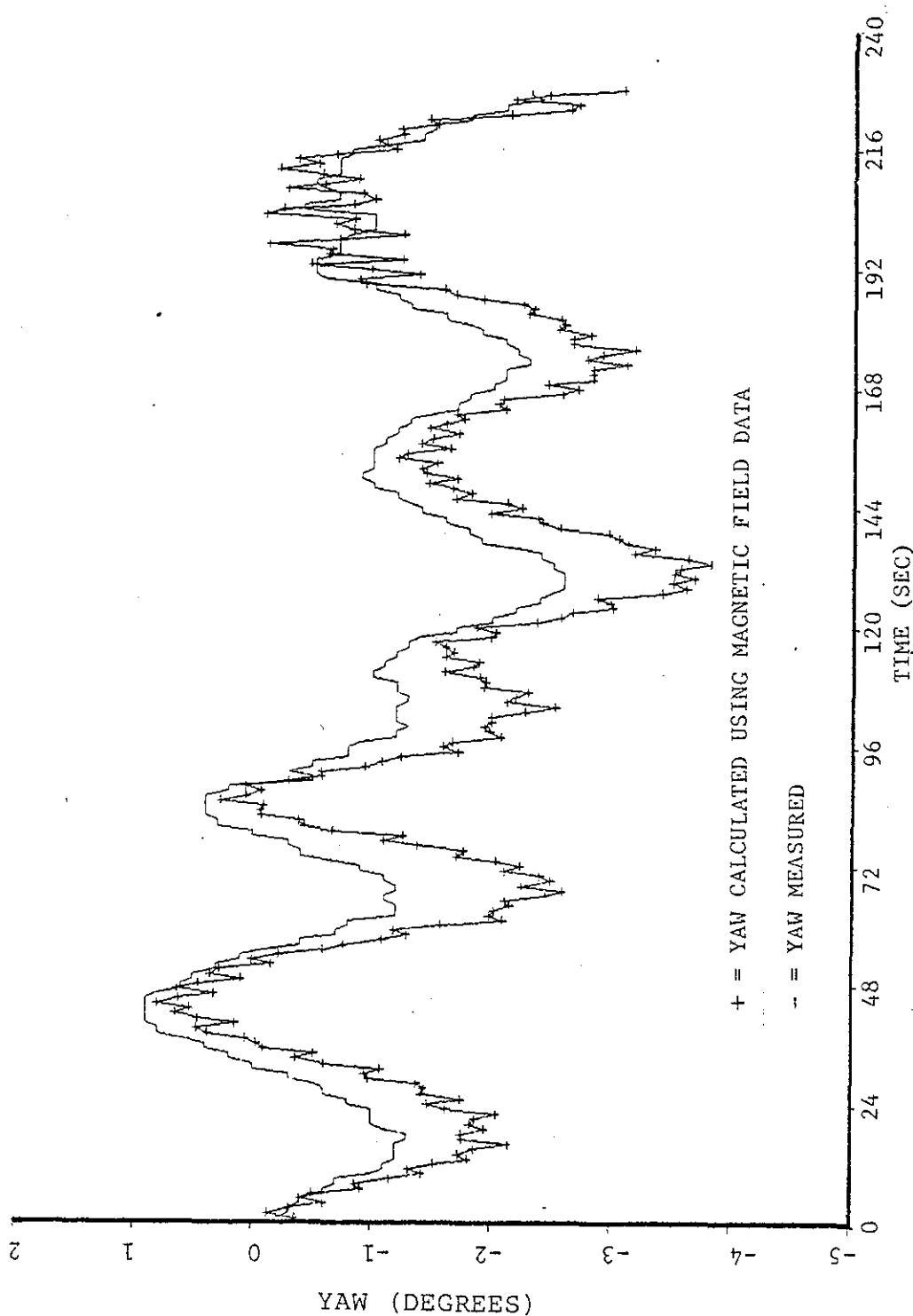


FIGURE 1-4 YAW AXIS

A popular system combination (with no gyro) is to combine a pendulous remote magnetic sensor and a synchro receiver in a null seeking circuit. The philosophy being to attempt to measure only the horizontal component of the Earth's magnetic field and to swing the receiver into alignment with it. Under acceleration, departures of the sensor unit from the horizontal result in angular heading errors  $\epsilon$  [Ref. 1-5].

$$\epsilon = (aH/g) \tan\gamma \sin\theta$$

where  $aH$  is the horizontal acceleration,  $g$  is the acceleration due to gravity,  $\theta$  is the angle between the acceleration vector and magnetic north, and  $\gamma$  is the magnetic field dip angle;  $\arctan$  (vertical field/horizontal field).

Accuracy of this system can be improved by incorporating a strapped-down solid state magnetic sensing unit (free of acceleration errors) that measures and displays the angle of the Earth's horizontal magnetic component relative to the aircraft. This system can be implemented as follows:

1) Determine the direction of the magnetic vector  $F$  relative to the sensors (and the airframe), by measuring the  $x$ ,  $y$  and  $z$  components (Figs. 1-1 and 1-5). The direction cosines  $\cos\alpha$ ,  $\cos\beta$ ,  $\cos\gamma$  are the cosines of the angles  $\alpha$ ,  $\beta$ ,  $\gamma$  between the magnetic vector and the positive  $x$ ,  $y$  and  $z$  axes. Additionally,

$$\cos\alpha = x/(x^2 + y^2 + z^2)^{\frac{1}{2}}$$

$$\cos\beta = y/(x^2 + y^2 + z^2)^{\frac{1}{2}}$$

$$\cos\gamma = z/(x^2 + y^2 + z^2)^{\frac{1}{2}}$$

- 2) Using either a vertical reference<sup>3</sup> or knowledge of aircraft attitude, we can effectively rotate the body axes such that the x-y plane is horizontal (see Chapter II).
- 3) Simple application of direction cosines will yield the direction of magnetic north in the aircraft's x-y plane.

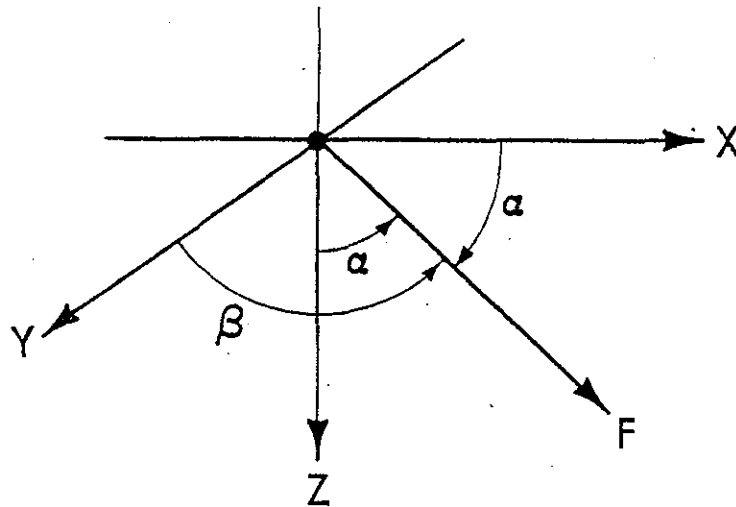


Fig. 1-5 FIELD VECTORS AND DIRECTION COSINES

Although the preceding discussion implies that heading can be determined by using a strapped-down magnetometer, there remains the problem of attitude determination. Another widely used system for obtaining a heading reference

---

<sup>3</sup>Not necessarily derived inertially [Ref. 1-11].

is to combine the relatively excellent short term stability of a directional gyroscope with the long term stability of magnetic field measurements. By slaving the directional gyroscope to the magnetic field [Ref. 1-5, sec. 10.4.7], gyroscopes with relatively large free drift error can be used to provide an excellent heading reference.

Replacement of the pendulous remote sensing unit of this type of system with a strapped-down vector magnetometer would result in both heading and attitude information on a continuous basis. This combination would operate as follows:

- 1) The system is initialized by determining a reference attitude (perhaps by using a primary inertial attitude system).
- 2) The angular position of the horizontal magnetic field component is computed as above and used to slave the directional gyroscope.
- 3) The directional gyroscope, with relatively good short term stability (devices with free drift of less than 0.5 deg/h have been designed), is used to determine yaw ( $\psi$ ) errors.
- 4) For small angle deviations, (1-8), and (1-9), and (1-10) can be employed to recalculate aircraft attitude. The process loops back to step 2) closing the loop on a combined attitude and heading reference system.

The sampling frequency required to maintain an acceptable level of error is of course determined by the aircraft performance expected (angular rates) and by the gyro error (drift rate plus errors due to additional sources such as

gyroscope tilt from vertical). The overall system is such that heading can be determined as before with errors due to sensor departures from horizontal substituted for long term accumulation of attitude uncertainty (this can be corrected by looping to step 1) at a frequency dependent on error rates). Additionally one gains measurements of attitude with minimal computation and replacement of a mechanical remote sensing unit with a solid state strapped-down magnetometer sensor.

#### 1-5 OTHER CONSIDERATIONS

The characteristics of the Earth's magnetic field and its variations have long been established [Ref. 1-6-1-10]. Since the field is to be used as a reference in the attitude measurement scheme, there is a need here to discuss its adverse characteristics. Although the field does experience variation, most of the variation is either in amplitude (ionospheric contributions) or has time constants that make the variation negligible (secular variation).

In traversing local anomalies, there will, however, be deflections in the ambient field due to the additive effect of local dipoles or monopoles. The effect of local terrain caused anomalies can be visualized by picturing the main field vector oriented in space with a second modulating vector rotating at its tip. Maximum angular error would occur when this modulating vector has maximum magnitude and is positioned at right angles to the main vector.

To illustrate the effect of local anomalies one can calculate the level of anomaly required to cause an error. Since the Earth's main field is typically in the order of 0.50 G it is readily apparent that a local anomaly of approximately 0.01 G at right angles to the local field is

required to cause an error of 1 deg. Furthermore, the local anomaly would have to be aligned with one of the aircraft body axes to result in one degree of attitude error in any one axis. Fortunately, anomalies with components of this magnitude positioned at right angles to the main field are extremely rare. In addition, the anomalies are localized over ore bodies or other geophysical irregularities, have magnitudes that diminish as the cube of altitude, and tend to average to zero over relatively short distances. In summary, the probability of encountering an anomaly that would cause as much as a 1 degree error is relatively small. The error, if introduced, will be short lived and, unlike drift error, will average to zero.

Fundamental to a magnetic field referenced system is the ability to measure orthogonal components of the field vector. Precision and accuracy of measurement of the components is of course specified by the desired control specifications.

Since the Earth's magnetic field varies in magnitude on a global basis between 0.3 G and 0.6 G (30,000 gamma to 60,000 gamma), it is apparent that full scale measurements of 0.6 G can be expected. Sensors mounted at right angles to the field will monitor no measureable field and thus define the lower limit of measurement to be zero. For the continental United States the declination varies between 60 and 80 deg, resulting in a range in horizontal component of 0.15 to 0.25 G with vertical component in the range of 0.4 to 0.55 G. Heading variations (yaw) result in changes of the horizontally sensed field components and would specify the maximum precision required. In addition, flight at  $45 \text{ deg} \pm (n \times 90 \text{ deg})$  (where n is any whole number) with respect to magnetic north results in minimum sensitivity of the x and y

axes measurements. In this case sensor inputs would range between 0.106 and 0.177 G with minimum field at the north. Assuming the preceding ambient measurements, variations in component magnitude of approximately 0.0180 to 0.0305 G/deg for small angle variations can be expected.

A brief survey of commercial magnetometer manufacturers reveals that triaxial magnetometers that measure from zero to 0.6 G with linearities of 0.5 percent, noise less than  $\pm 1$  mG and sensitivities of at least 2.5 V per 600 mG are currently available. In addition, these devices have a bandwidth of direct current to at least 500 Hz and are rated to have less than 1 deg error in orthogonality.

From a precision standpoint, it is apparent that variations in yaw for this worst case situation can be sensed to better than 0.1 deg with currently available magnetometer technology. The sensor technology required to implement an attitude sensing system of reasonable specifications is available (more detailed analysis is presented in Chapter III).

Although the preceding calculations indicate that for small angular variations attitude can be calculated using measured magnetic data, there is a need to consider the effects of larger finite rotations. In this case the small angle assumptions would not be valid and an Euler transformation would have to be made. Measurement of three axes of field components could be used to develop the direction cosines required to determine the orientation of the axis of rotation, the angular rotation about it, and the three angular rotations of pitch, roll, and yaw.

For the special case where the axis of rotation aligns with the magnetic vector, there would of course be no

measured component changes.<sup>4</sup> By measuring the attitude of a second vector (not in alignment with the magnetic vector), we could resolve the ambiguous situation cited above and provide additional redundancy.

The optimum auxiliary vector would be one that could be sensed without using inertial devices. The Earth's electric field can be considered. The main reason for considering this field as a means of providing an auxiliary angular reference is that the resultant system has the potential of being completely solid state. The electric field vector can be used to determine attitude variation in a manner analogous to the magnetic vector system. Inherent limitations of each single vector system can be obviated if the vectors are not coincident.

Although Hill [Ref. 1-11] reported success in controlling pitch and roll using the electrostatic field alone, comments by Markson [Ref. 1-12] indicate that the electrostatic field is not always a reliable vertical reference. Employment of the electrostatic field for this attitude measurement system is limited to augmenting the magnetic field measurements by eliminating ambiguity of motion around the magnetic vector. The requirement of vertical electrostatic field is thus removed and replaced by a requirement that the field direction is relatively stable.

By using two independently derived vectors we have sufficient data to obviate the ambiguity just cited and we have the potential of providing redundancy as well.

---

<sup>4</sup>An example of this would be yaw rotation while flying straight and level over the magnetic poles or roll rotation while flying towards a pole at the magnetic equator.



## 1-6 CONCLUSION

This chapter has identified a novel method of measuring aircraft attitude using relatively inexpensive, well developed instrumentation. It has recognized that magnetic field sensing systems have been used to some extent in attitude sensing and control of space vehicles; it has also suggested, however, that with appropriate support, magnetometers can find increased application in aircraft attitude measurement systems.

This claim is corroborated by actual flight test data. Magnetometers have evolved to a point where three axis measurements of the Earth's magnetic field can be made with sufficient precision and accuracy to enable measurement of small angle attitude variations.

This chapter has also discussed a possible system configuration combining heading determination and attitude measurement functions. By replacing the conventional remote sensing unit with a three-axis magnetometer, it has been suggested that both functions can be obtained with the hardware required previously for heading measurement alone.

As with any system, there are limitations imposed. The main limitation for a vector magnetometer system seems to be the inability to sense rotations around the magnetic vector itself. This problem is not unlike the ambiguity experienced by magnetic heading systems at high latitudes. By judiciously incorporating auxiliary instruments, not only can the ambiguities be removed but a degree of redundancy can be added while still maintaining a cost and weight advantage over comparable systems.

## CHAPTER II

### AN ATTITUDE INDEPENDENT REMOTE MAGNETIC INDICATOR

#### 2-1 INTRODUCTION

Preliminary investigation [Ref.2-1] revealed that aircraft attitude can be calculated using measurements of earth's magnetic field vector and a single auxiliary rotation angle. An algorithm to compute the two remaining aircraft rotational angles was developed. Using flight data, it was demonstrated that an excellent correlation in computed versus actual aircraft attitude could be achieved. In addition to providing measurements of the magnetic field for redundant attitude computations (to improve accuracy and reliability of existing autopilot systems), it was noted that the vector magnetometer could substitute for the remote magnetic sensing unit. In this manner both heading and attitude measurements could be derived using common elements with obvious benefits in weight and cost.

This chapter discusses the mechanization of a microprocessor based computer system that uses a three axis magnetometer plus gyro data to compute heading. The magnetometer is a three axis solid state device that can be mounted in a strapped down configuration resulting in an attitude independent remote magnetic indicator. Gyro measurements of pitch and roll angle plus three axis magnetic measurements are used by the algorithm to compute aircraft heading. The system can function independently to compute heading or by simply increasing the stored program could implement the attitude computing algorithm of [Ref. 2-1] as well.

The chapter proceeds by developing an algorithm to compute aircraft heading using the strapped down magnetometer

and two gyro measured angles. Practical aspects of designing the system including both hardware and software are then presented. In addition, the limitations in instrument accuracy and operation as determined by sensor errors, signal processing errors, arithmetic precision and computation speed are discussed. Considerable computational capability inherent in the system enables minimization of systematic errors. It is demonstrated that inexpensive sensors can be employed with offset and orthogonality errors compensated by microprocessor programming. Finally, it is concluded that a microprocessor based computer with a solid state magnetometer can play a significant role in aircraft instrumentation.

## 2-2 AN ALGORITHM TO COMPUTE AIRCRAFT HEADING

Coordinate frames are usually defined by orthogonal right-hand sets of three unit vectors. An example of such a set is illustrated in Fig. 1-1 where the orientation of the body fixed frame used in this chapter is delineated. The reference coordinate frame referred to in this chapter is oriented with axes  $x$  and  $y$  in the horizontal plane and axis  $z$  vertical ( $z$  down is positive). Pitch attitude angle ( $\theta$ ) of an aircraft is defined [Ref. 2-2] as the angle between some preferred longitudinal axis and the horizontal reference. In this chapter, pitch angle is the angle between the  $x$  axis of the aircraft and the  $x$ - $y$  plane of the reference axis set. Since angular rotations are conventionally defined as rotations in the plane normal to a unit vector with the positive sense of rotation defined by the right-hand rule [Ref. 1-2], we will define positive pitch angle ( $\theta$ ) as the "nose up" or positive rotation about the  $y$  axis when the  $y$  axis is horizontal. The roll and yaw angles ( $\phi$  and  $\psi$ ) will then simply be rotations about the  $x$  and  $y$  axes respectively.

By aligning the three magnetometer axes with the respective x, y and z axes of the aircraft, we can measure magnetic field components of the aircraft at any attitude. For the trivial case where pitch ( $\theta$ ) and roll ( $\phi$ ) are both zero degrees, Hx and Hy are the horizontal field components and we can compute yaw from the horizontal vectors as follows:

$$\psi_1 = \cos^{-1}(Hx/(Hx^2 + Hy^2)^{\frac{1}{2}}) \quad (2-1a)$$

or

$$\psi_1 = \sin^{-1}(Hy/(Hx^2 + Hy^2)^{\frac{1}{2}}) \quad (2-1b)$$

We select either (2-1a) or (2-1b) based on the relative magnitudes of Hx and Hy. By minimizing the numerator of the argument we guarantee that the inverse trigonometric operation results in an angle between zero and forty-five degrees with maximum sensitivity ensured. Heading is then computed using the signs of Hx and Hy to select the appropriate equation from Table 2-1.

Hx Hy	NEGATIVE	POSITIVE
Negative	$\psi = 180 - \psi_1$	$\psi = \psi_1$
Positive	$\psi = \psi_1 + 180$	$\psi = 360 - \psi_1$

Table 2-1. Formulae to Compute Heading

For most cases, the pitch and roll angles are not zero and inverse rotations are required to determine the actual horizontal field components Hx and Hy. Since any aircraft attitude can be represented as a sequence of rotations about each axis beginning at some reference attitude, we can

determine the reference Hx and Hy field components by performing an inverse roll followed by an inverse pitch computation<sup>1</sup>.

The inverse roll computation can be developed by considering vector components of an arbitrary vector  $\bar{H}$  in Fig. 2-1. The first set ( $x_2, y_2, z_2$ ) represents the vector components measured in a reference orientation. The second set has common origin and aligns with common x axis component. It is rotated (rolled) about the x axis resulting in new y and z values. We can describe vector  $\bar{H}$  in both coordinate frames as

$$\bar{H} = x_2 \cdot \hat{i}_2 + y_2 \cdot \hat{j}_2 + z_2 \cdot \hat{k}_2 \quad (2-2)$$

and

$$\bar{H} = x_3 \cdot \hat{i}_3 + y_3 \cdot \hat{j}_3 + z_3 \cdot \hat{k}_3 \quad (2-3)$$

Since the vector  $\bar{H}$  is unique, we note that equations (2-2) and (2-3) are equal. Furthermore if we form dot products we solve for the horizontal components  $x_2, y_2,$  and  $z_2$  in terms of the rotated values and the roll angle ( $\phi$ ).

From (2-2) we obtain

$$\bar{H} \cdot \hat{i}_2 = x_2 (\hat{i}_2 \cdot \hat{i}_2) + y_2 (\hat{j}_2 \cdot \hat{i}_2) + z_2 (\hat{k}_2 \cdot \hat{i}_2) \quad (2-4a)$$

$$\bar{H} \cdot \hat{i}_2 = x_2 \quad (2-4b)$$

and from (2-3) we obtain

$$\bar{H} \cdot \hat{i}_2 = x_3 (\hat{i}_3 \cdot \hat{i}_2) + y_3 (\hat{j}_3 \cdot \hat{i}_2) + z_3 (\hat{k}_3 \cdot \hat{i}_2) \quad (2-5a)$$

$$\bar{H} \cdot \hat{i}_2 = x_3 \quad (2-5b)$$

<sup>1</sup>Since pitch is defined as the angle between the x axis and the horizontal plane we can assume that at any heading, aircraft attitude results due to a pitch followed by a roll.

then

$$x_2 = x_3 \quad (2-6)$$

Similarly,

$$\bar{H} \cdot \hat{j}_2 = y_2 = x_3(\hat{i}_3 \cdot \hat{j}_2) + y_3(\hat{j}_3 \cdot \hat{j}_2) + z_3(\hat{k}_3 \cdot \hat{j}_2) \quad (2-7a)$$

$$y_2 = y_3 \cos \phi - z_3 \sin \phi \quad (2-7b)$$

and

$$\bar{H} \cdot \hat{k}_2 = z_2 = x_3(\hat{i}_3 \cdot \hat{k}_2) + y_3(\hat{j}_3 \cdot \hat{k}_2) + z_3(\hat{k}_3 \cdot \hat{k}_2) \quad (2-8a)$$

$$z_2 = y_3 \sin \phi + z_3 \cos \phi \quad (2-8b)$$

These expressions can be summarized as

$$\begin{bmatrix} x_2 \\ y_2 \\ z_2 \end{bmatrix} = \begin{bmatrix} 1 & 0 & 0 \\ 0 & \cos \phi & -\sin \phi \\ 0 & \sin \phi & \cos \phi \end{bmatrix} \cdot \begin{bmatrix} x_3 \\ y_3 \\ z_3 \end{bmatrix} \quad (2-9)$$

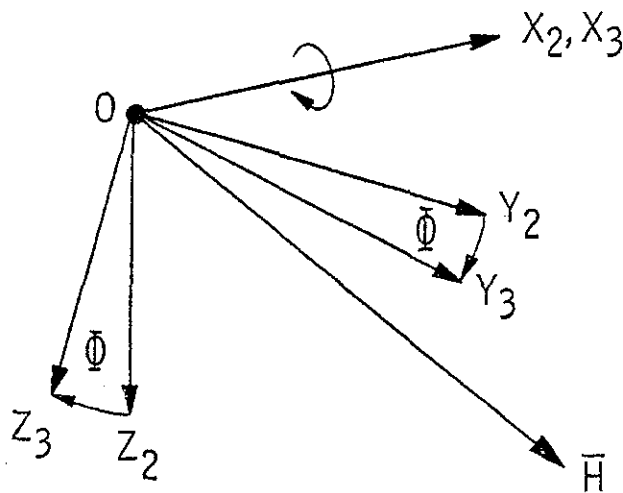


Fig. 2-1 AXES ROTATED IN ROLL

Similarly, considering an axis set rotated in pitch as shown in Fig. 2-2, we can express the reference set  $x_1, y_1, z_1$  in terms of the rotated set  $x_2, y_2, z_2$  as follows

$$\begin{bmatrix} x_1 \\ y_1 \\ z_1 \end{bmatrix} = \begin{bmatrix} \cos \theta & 0 & \sin \theta \\ 0 & 1 & 0 \\ -\sin \theta & 0 & \cos \theta \end{bmatrix} \cdot \begin{bmatrix} x_2 \\ y_2 \\ z_2 \end{bmatrix} \quad (2-10)$$

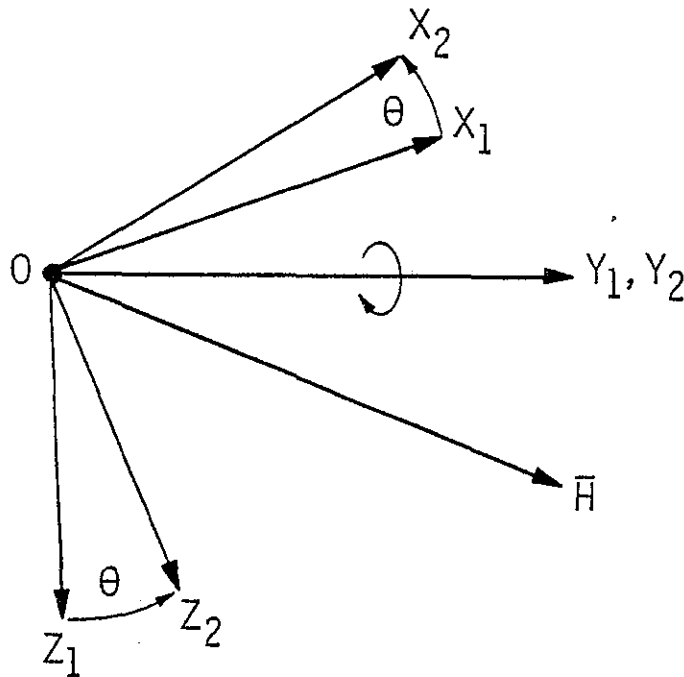


Fig. 2-2 AXES ROTATED IN PITCH

Finally, if we assume that the axis set subscripted with <sup>3</sup> represents components of Earth's magnetic vector measured at an arbitrary aircraft attitude, we can derive the magnetic components ( $H_{xh}, H_{yh}, H_{zh}$ ) in the horizontal plane for a given heading

$$\begin{bmatrix} H_{xh} \\ H_{yh} \\ H_{zh} \end{bmatrix} = \begin{bmatrix} \cos \theta & 0 & \sin \theta \\ 0 & 1 & 0 \\ -\sin \theta & 0 & \cos \theta \end{bmatrix} \begin{bmatrix} 1 & 0 & 0 \\ 0 & \cos \phi & -\sin \phi \\ 0 & \sin \phi & \cos \phi \end{bmatrix} \cdot \begin{bmatrix} H_{x_3} \\ H_{y_3} \\ H_{z_3} \end{bmatrix} \quad (2-11a)$$

$$\begin{bmatrix} H_{xh} \\ H_{yh} \\ H_{zh} \end{bmatrix} = \begin{bmatrix} \cos \theta & (\sin \theta \sin \phi) & \sin \theta \cos \phi \\ 0 & \cos \phi & -\sin \phi \\ -\sin \theta & (\cos \theta \sin \phi) & \cos \phi \cos \theta \end{bmatrix} \cdot \begin{bmatrix} H_{x_3} \\ H_{y_3} \\ H_{z_3} \end{bmatrix} \quad (2-11b)$$

The algorithm to be implemented with the microprocessor would therefore require operations as outlined in Fig. 2-3. Details of programming method, modifications to the above equations to facilitate programming and computation speed versus accuracy tradeoffs are discussed in following sections.

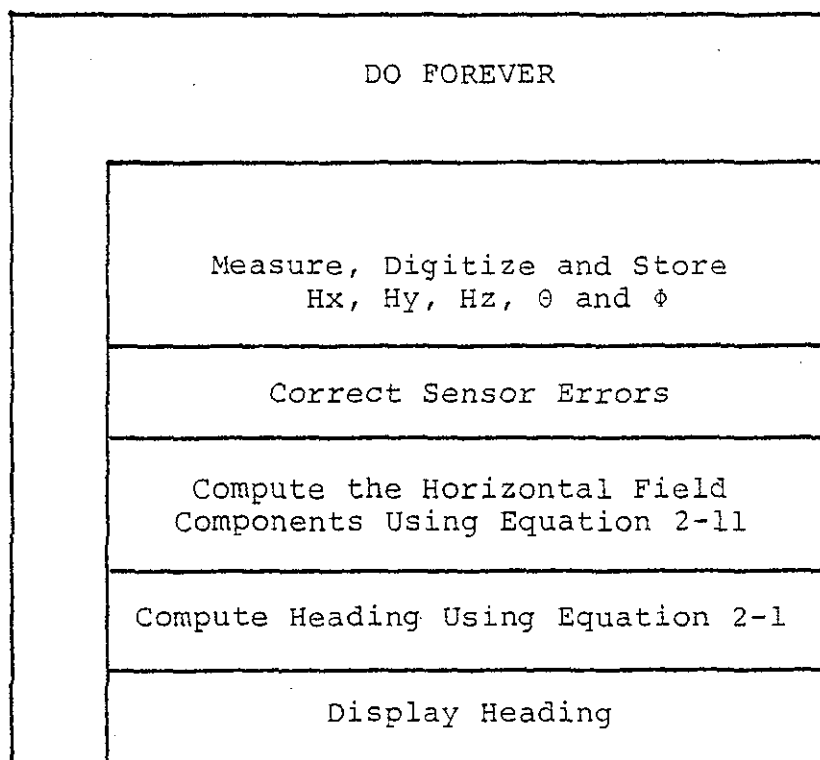


Fig. 2-3 LOGICAL OPERATIONS REQUIRED TO COMPUTE HEADING



## 2-3 MECHANIZATION OF THE HEADING ALGORITHM

### A. General Considerations

To evaluate the performance of an integrated system experimentally, an instrument was designed to implement the algorithm developed above. Several approaches were considered to implement the heading instrument for experimentation:

1) A minicomputer implementation incorporating an HP-2100 minicomputer supported by peripheral interface and analog circuitry. Programming of the HP-2100 would have enabled the computer to control multiplexing and processing of sensor data as suggested by Parish and Lee [Ref. 2-3].

2) A hybrid system composed of a remote data acquisition system to collect data from sensors for subsequent processing by a computer (possibly an HP-2100).

3) A digital/analog electronic implementation incorporating the design of a special purpose computer to perform the required functions of a heading instrument.

The first two approaches were abandoned since it was desirable to perform the experiments at various locations remote from a computer facility and to have data available immediately without having to rely on off-line computations at a later date. The design task then evolved to the design of a special purpose computer system to implement the algorithm, provide a means for evaluating the performance of the proposed algorithm and to allow modifications to the system if required.

### B. Design Criteria

Having decided on the general approach to implementing

the algorithm it became necessary to consider the performance criteria desired of the instrument.

1) Accuracy

As a design goal, an absolute accuracy of  $\pm 1.0^\circ$  in heading uncertainty was selected for the laboratory implementation. This accuracy is compatible with commercially available heading systems.

2) Computation Speed

The bandwidth of the system is determined mainly by the computation speed of the computer<sup>2</sup>. As a design goal, complete heading updates once per second was established.

3) Flexibility

A desirable feature of the laboratory evaluation instrument was considered to be flexibility. Revisions or additions to the algorithm as predicted by experimental data should be incorporated with minimal redesign of the instrument.

## 2-4 CONCLUSIONS

An instrument designed to implement the heading algorithm developed above uses a three axis magnetometer to measure magnetic field data in the vicinity of an aircraft. Since the magnetometer proposed is a solid state three axis fluxgate device and is permanently mounted in a strapped down configuration, the implementation results in an attitude independent

---

<sup>2</sup>The response times of the various sensors and analog circuitry are orders of magnitude greater than the desired one second sample interval.

remote magnetic indicator<sup>3</sup>.

Several factors will contribute to system inaccuracy. Although the major error sources can be evaluated mathematically (Chapter IV), there is a need to evaluate the implementation experimentally. Systematic errors that arise can be reduced by instrument computation. This capability (inherent with a computer based system) enables incorporation of less expensive sensors in the heading instrument with less concern with factors such as temperature regulation, sensor orthogonality and sensor offset<sup>4</sup>.

Since the algorithm can be implemented using a microprocessor as the major computer element, the resulting instrument will have inherent computation capability, be small in size and consume relatively little power. These factors make the instrument an ideal device for aircraft application where the need for redundant distributed processing capability is invaluable.

---

<sup>3</sup>Current remote magnetic indicators are pendulous and rely on gravity to enable measurements of the horizontal magnetic vector (not attitude independent).

<sup>4</sup>Assuming that the sensors have repeatable or measurable characteristics, algorithms can be developed to correct previously measured erroneous data.

## CHAPTER III

### DESIGN OF A MICROPROCESSOR BASED HEADING INSTRUMENT

#### 3-1 INTRODUCTION

Progress in device and component technologies during the 1970's has led to an assortment of sophisticated integrated circuits (IC) devices [Ref. 3-1] which enable the design of instruments with a high degree of sophistication and accuracy. Of these devices, the microprocessor has to date been the most exploited component in industrial control and instrumentation applications [Ref. 3-2 through 3-7]. There have been many papers presented addressing the general application and feasibility of applying microcomputers to particular design tasks [Ref. 3-8 through 3-21].

Although much of the literature to date on microprocessors has addressed the design of commercial products (usually the final result of a carefully orchestrated effort beginning with a market survey), the design of a laboratory instrument for algorithm evaluation differs in design philosophy. In particular, the laboratory instrument is designed to evaluate a proposed algorithm under laboratory conditions. The traditional benchmark evaluations and attempts to match the microprocessor to the application is not only difficult but unnecessary. If the processor is much more powerful than necessary, the "overkill" is little noticed; but if an insufficiently endowed microprocessor is selected, the effects can be devastating. Not only will the program be difficult to write and voracious of memory, it would be difficult to change to a more powerful microprocessor part way through the project. With these considerations in mind, a general purpose, flexible microprocessor with powerful architecture and instruction set the Signetics 2650 microprocessor [Ref. 3-22] was selected.

### 3-2 HARDWARE DESIGN CONSIDERATIONS

The design of a microprocessor based system begins by considering the total system level block diagram to be implemented (Fig. 3-1). Inputs from five sensors including x, y and z axis magnetic data plus pitch and roll angles ( $H_x$ ,  $H_y$ ,  $H_z$ ,  $\theta$  and  $\phi$ ) are to be multiplexed, sequentially sampled and converted to a digital representation prior to processing (executing the algorithm developed above). The main subsystem of Fig. 3-1, the central processing unit (CPU), operates under control of instructions stored in the system memory and interfaces with the input and output subsystems via data ports.

At this early stage in the design, it is significant to note that the block diagram of Fig. 3-1 differs slightly from that of a classical discrete hardware solution. The input subsystem (composed of analog multiplexer, sample and hold, and analog to digital converter) differs from a conventional data acquisition in that it is devoid of a control section. The microprocessor will control the data acquisition sampling and conversion in addition to performing the arithmetic function associated with the algorithm.

Having established a tentative block diagram of the instrument, the design continues by addressing relevant characteristics and limitations of each subsystem. These characteristics will then in turn be considered in configuring the final system and program to be executed.

#### 1) The Analog Subsystem

Composed of the analog multiplexer, sample/hold and analog to digital converter, the analog subsystem of Fig. 3-1 affects both system accuracy and throughput rate. The

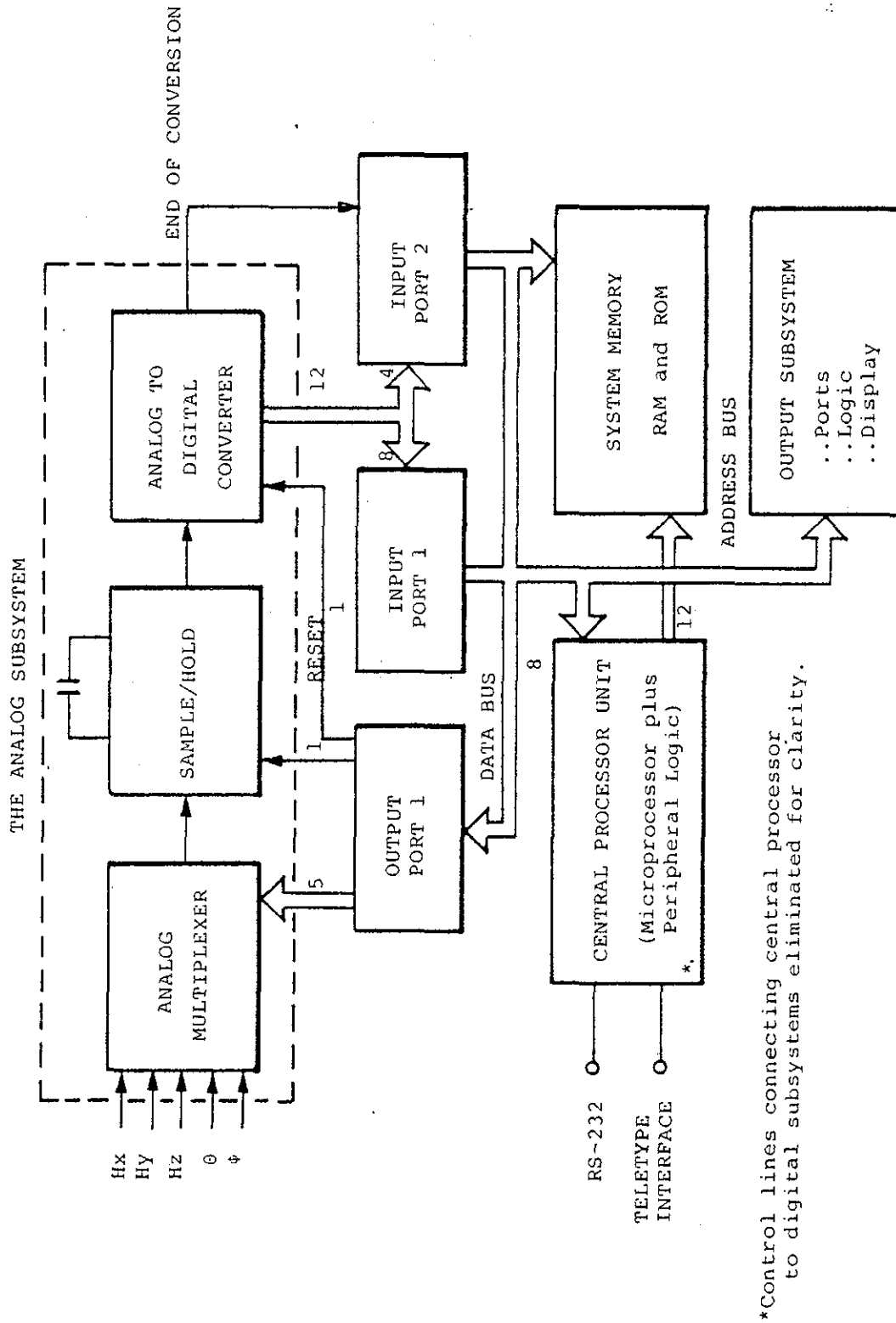


Fig. 3-1. SYSTEM BLOCK DIAGRAM

well-known Shannon theorem [Ref. 3-23, 3-24] on sampling theory defines one of the basic limits on throughput rate stating that the minimum frequency for sampling must be double the highest significant frequency of the signal, including the noise on the signal. This minimum frequency is necessary, the theorem states, if the sampled signal is to contain all of the information needed for undistorted reconstruction. At a lower sampling frequency aliasing can occur<sup>1</sup>. The minimum sampling rate for data to be used in this heading instrument (based on the design goal of Chapter II) then results in a system bandwidth of 30 hertz. The analog signals from each sensor are low pass filtered to reduce frequency content above 60 hertz. A survey of commercially available multiplexers, sample and hold modules and analog to digital convert modules (ADC) [Ref. 3-25 to 3-28] reveals that subsystems with throughput characteristics exceeding the requirements of a system sampled at one second intervals are readily available (pertinent specifications are discussed in more detail in Chapter IV). The limiting parameter determining total system speed performance will then be the execution time of the algorithm (a programming consideration). A further system consideration is the ability to adjust analog system offset and gain. These adjustments are made using variable resistors (trim pots) connected to appropriate leads on the sample and hold and analog to digital converter modules.

## 2) The Central Processing Unit (CPU)

The central processing unit (Fig. 3-2) is composed of the microprocessor (Signetics 2650) supported by peripheral logic elements (Fig. 3-2). Design of this subsystem involved medium

---

<sup>1</sup>That is, the sampled data derived from a sine wave of frequency  $f$  sampled at a frequency less than  $2f$  can be fitted with sine waves of a frequency other than  $f$ .

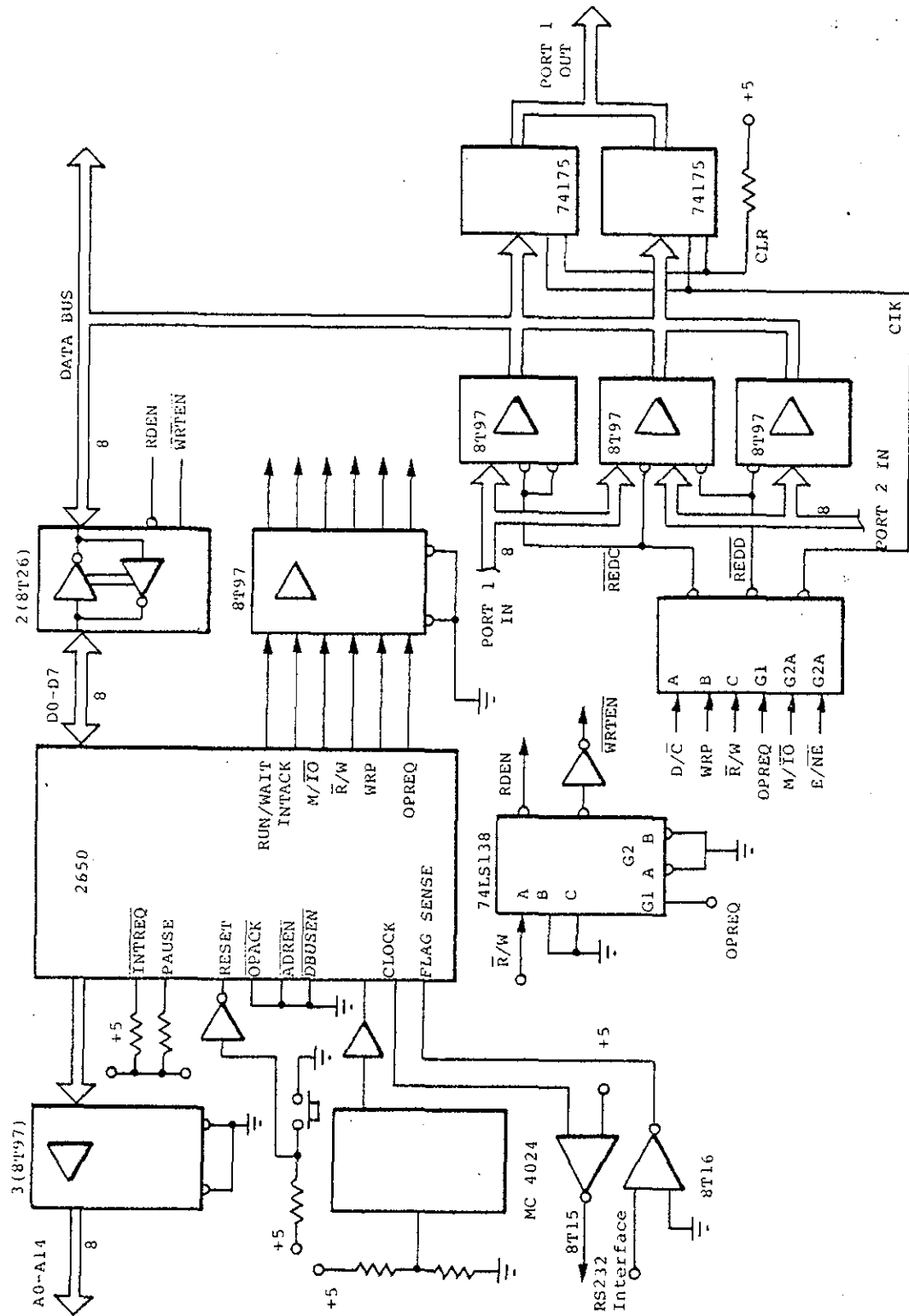


Fig. 3-2. THE CPU SUBSYSTEM



and small scale integrated circuits using well-known [Ref. 3-29 through 3-31] design techniques. To facilitate system development several features were included in the design of the CPU subsystem (features that would not necessarily be required in a production instrument). These include:

- a) System reset, single step and normal run mode operation controlled by switches and logic elements.
- b) An RS-232 teletype interface is included to enable manual intervention and development capability during program development. The program was developed by loading and executing instructions into the random access memory (RAM) under control of the PIPBUG<sup>2</sup> program.

### 3) The Memory Subsystem

The memory subsystem (Fig. 3-3) was organized onto cards each with two thousand byte capability. In this manner system memory could easily be expanded (or reduced) in increments of 2K bytes. The memory chips selected were organized as 256 four bit words and feature pin for pin compatibility with commercially available random access (RAM) and programmable read only memory (PROM) chips. Program segments could then be developed in RAM and finally "burned" into PROM chips for a permanent, nonvolatile operation. In this manner the system development begins with 1K bytes of memory devoted to the resident PIPBUG program (in ROM chips) with the remainder of memory allocated as RAM for both program and scratch pad usage.

---

<sup>2</sup>Signetics tradename for the 2650 resident loader and monitor program.

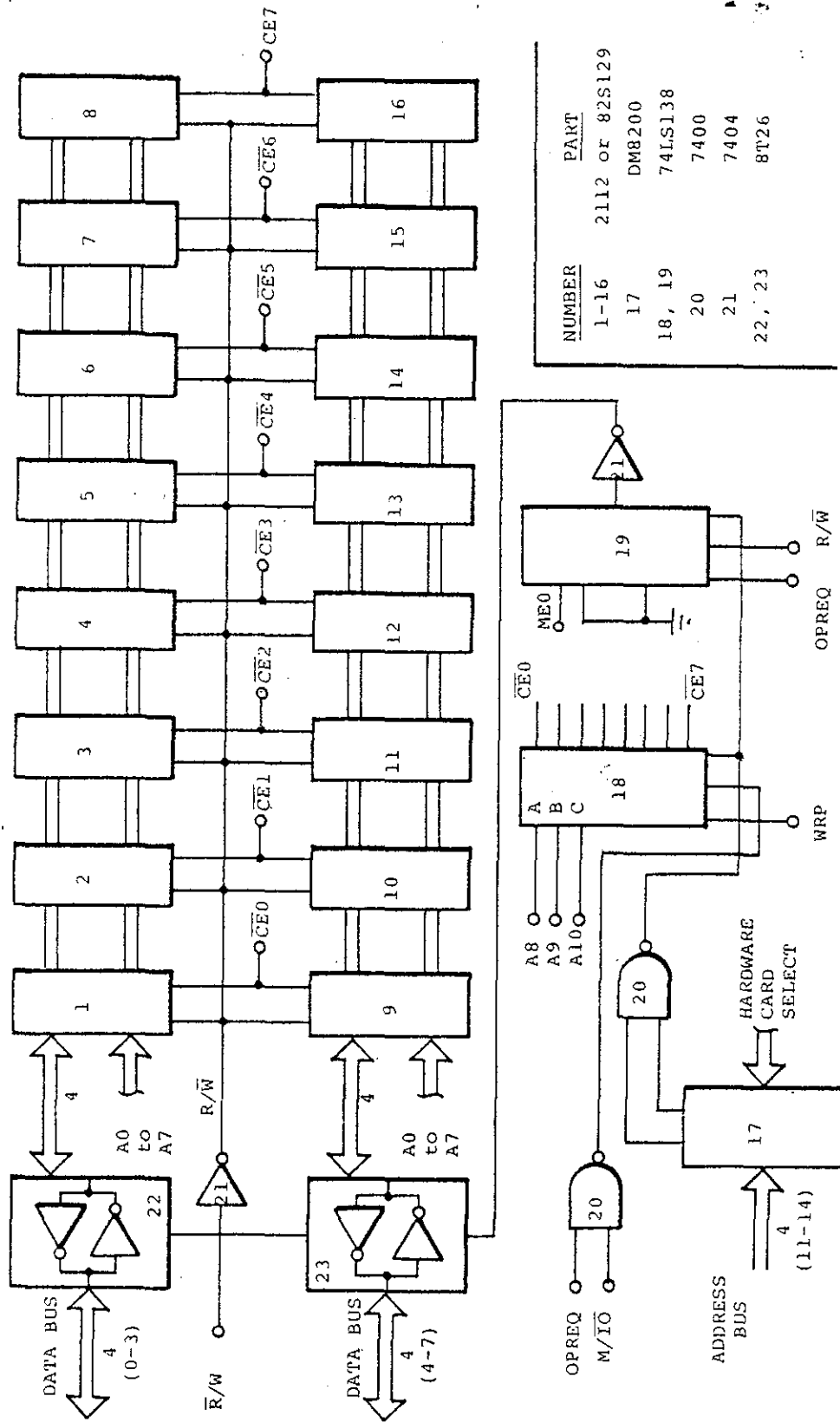


Fig. 3-3. MEMORY SUBSYSTEM (1 Card)

As the program is developed, additional memory is added in increments of 2K bytes per card or 256 bytes on the card. Modifications to the program can be easily made using the PIPBUG program and teletype.

#### 4) The Output Subsystem

For laboratory development the output subsystem of Fig. 3-4 was designed to provide seven segment visual output of the aircraft heading with three significant digits displayed. To expediate the design cycle and to enhance system throughput rate, the outputs were designed as ports with latches and decoder driver functions provided by hardware. In other applications a hardware/software tradeoff could be made with the data decoding and driving implemented using table lookup and multiplexing controlled by the CPU.

### 3-3 SOFTWARE DESIGN CONSIDERATIONS

The general purpose processor selected to implement the CPU was designed to implement programmed logic and to perform conventional computer operations. This heading instrument takes advantage of both areas. Since the instrument is actually a special purpose computer under control of a stored program, the functional specialization resides in the program rather than the hardware logic. Modifications can be made relatively easily, satisfying the flexibility design goal of Chapter II.

Having decided on the tentative hardware structure described in Section 3-2 above, the program development leading to the final listing in Appendix B proceeded as follows:

- 1) Structured flow charts were developed depicting the total system operation as an ordered sequence of operations. Each

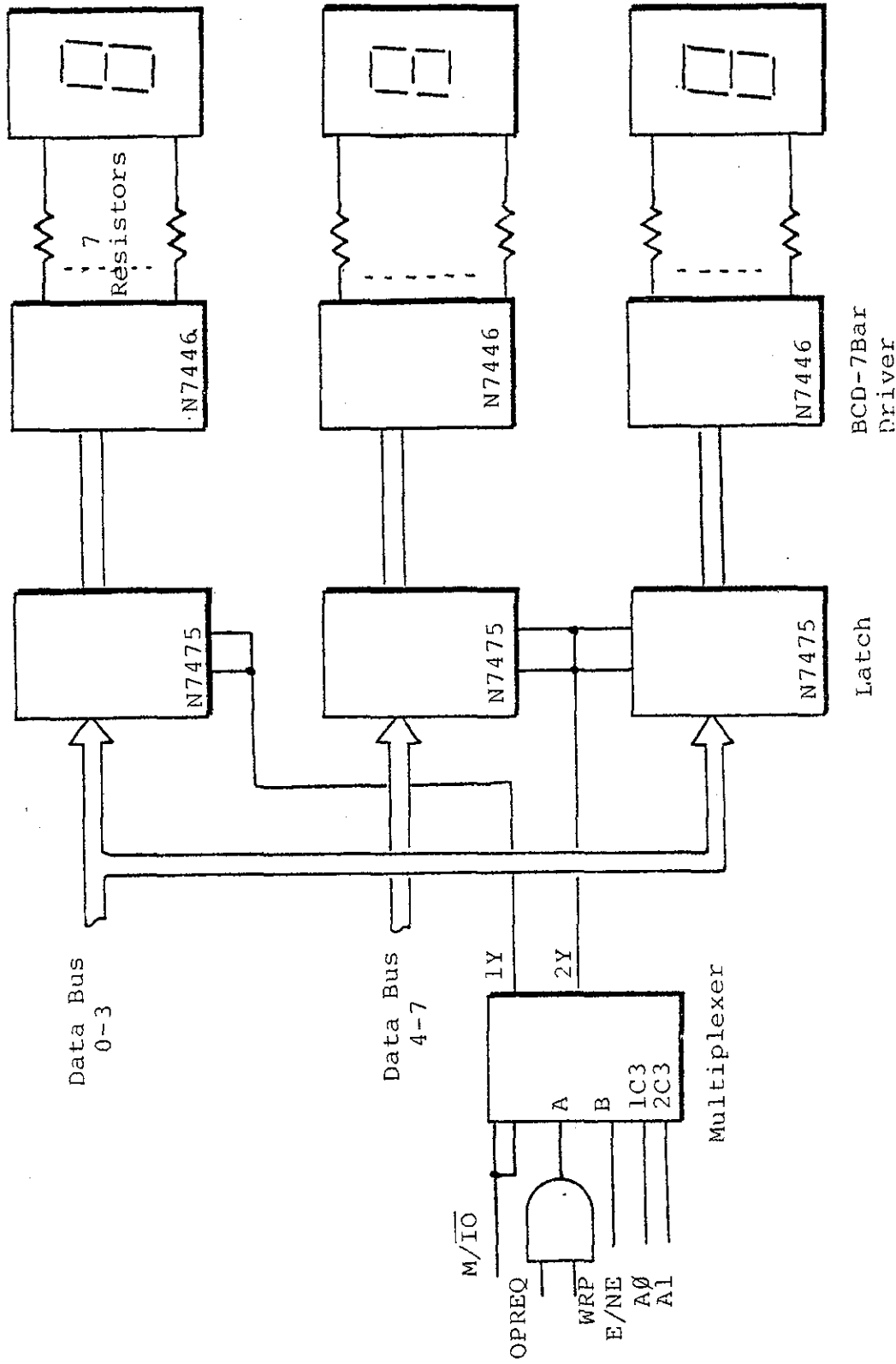


Fig. 3-4 THE OUTPUT SUBSYSTEM

operation is identified as a separate subroutine which in turn can have "nested" subroutines of its own (Fig. 3-5).

2) System accuracy requirements were next investigated (discussed in detail in Chapter IV) to ascertain the precision requirements<sup>3</sup> of the various subroutines.

3) The respective subroutines outlined in 1) above were developed and implemented using a cross assembler program [Ref. 3-32]. Each subroutine was then loaded into the development hardware and "debugged" prior to total program integration. The above program development depicts a top down strategy of program development [Ref. 3-33] and leads to an expedient system development with subroutines being individually developed to yield a modular program construction.

#### 3-4 DESIGN OF SUBROUTINES

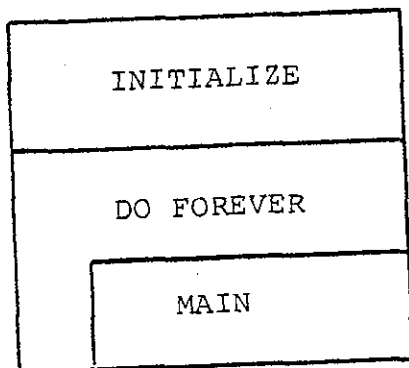
The total program consists of an overall system program composed of nested subroutines. The discussion in this section is limited in scope to the design of the more complex subroutines required to implement the solid state remote magnetic heading algorithm.

##### 1) Subroutine "SAMP" (Fig. 3-6a)

The first portion of this subroutine is dedicated to the control function of selecting an analog channel via the multiplexer, sampling and holding the data, resetting and reading data from the analog to digital converter (ADC). Prior to or during the programming of this section, data fields in

---

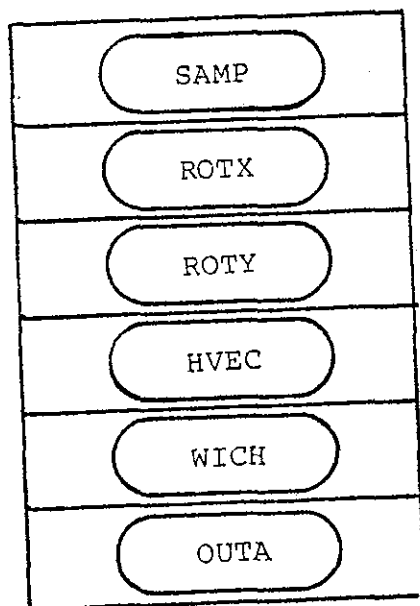
<sup>3</sup>This step is vital to determine whether the operations outlined in 1) above are to be carried out in a single or multi-precision manner.



Power on reset of all registers and subsystems

Compute the aircraft heading

Fig. 3-5a. SYSTEM PROGRAM



Sample all analog channels

Compute the horizontal Hx field

Compute the horizontal Hy field

Compute the horizontal field vector

Compute heading

Output the data

Fig. 3-5b. SUBROUTINE "MAIN"

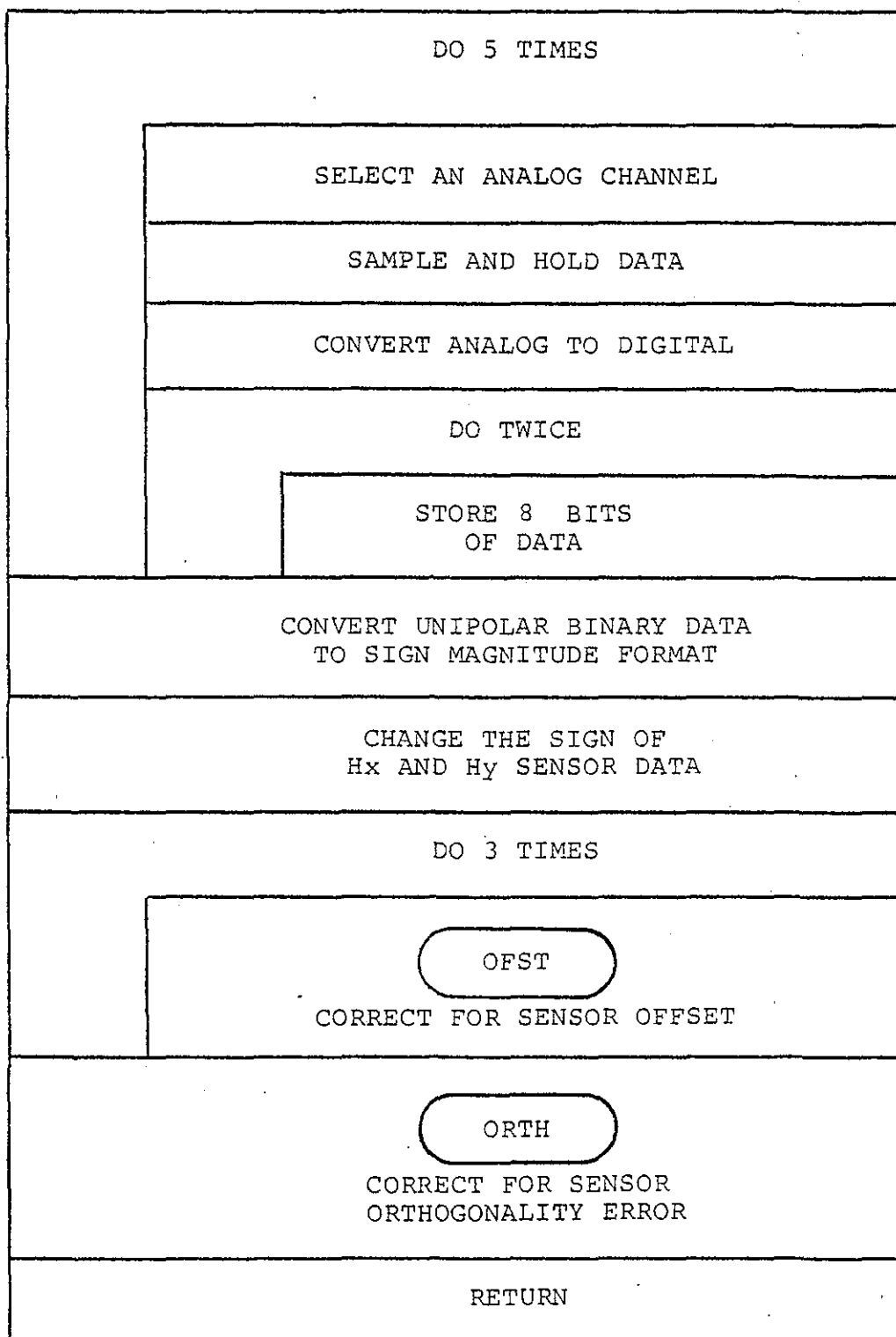


Fig. 3-6a. SUBROUTINE "SAMP"

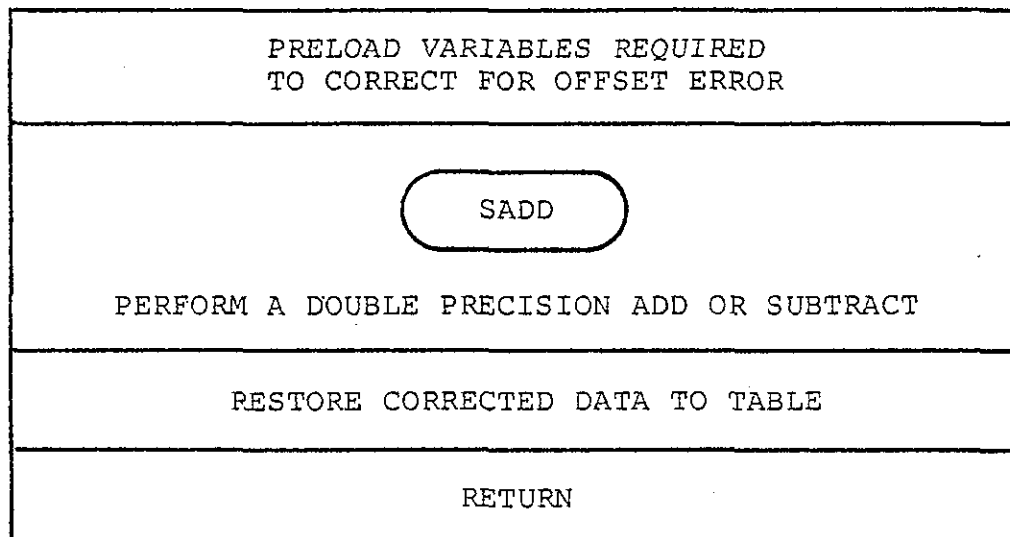


Fig. 3-6b. SUBROUTINE "OFST"

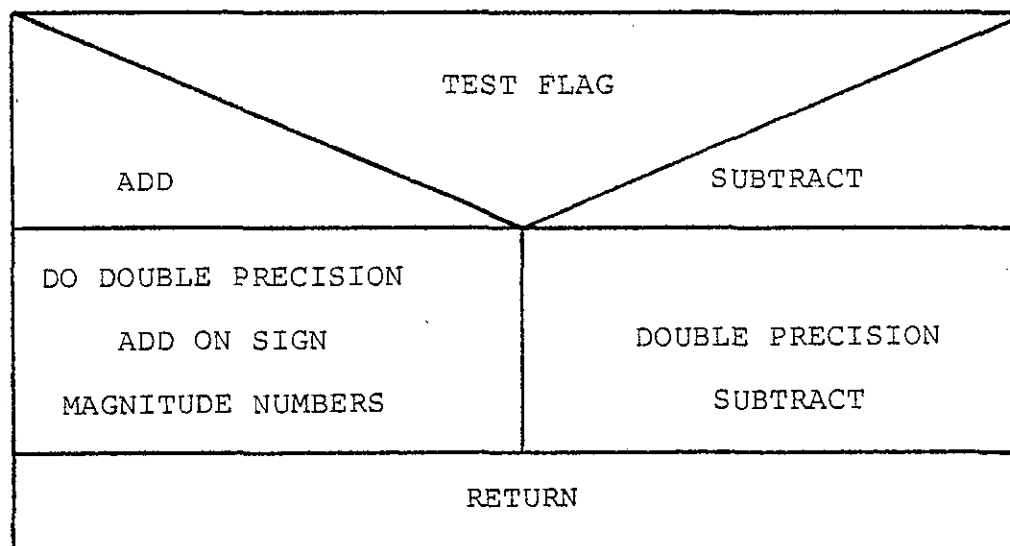


Fig. 3-6c. SUBROUTINE "SADD"



input ports 1 and 2 and output port 1 of Fig. 3-1 are allocated. Control information is then passed to the peripheral module by writing control words to output port 1. Analog to digital converter status and the 12 bit data field are sampled by reading input ports 1 and 2.

Sensor outputs were biased at +2.5 Volts with transfer characteristics as depicted in Fig. 3-7a [Ref. 3-34]. The ADC selected for this laboratory instrument had a binary output data format related to analog input as shown in Fig. 3.7b [Ref. 3-35]. The second function of the sampling subroutine "SAMP" was to convert data from a unipolar binary format to a sign magnitude format. Since the total transfer function from sensor input to ADC output (Fig. 3-7a and b) indicates an offset of 2.5 Volts or 1/2 the ADC output range, the sign magnitude format can be generated as shown in Fig. 3-8.

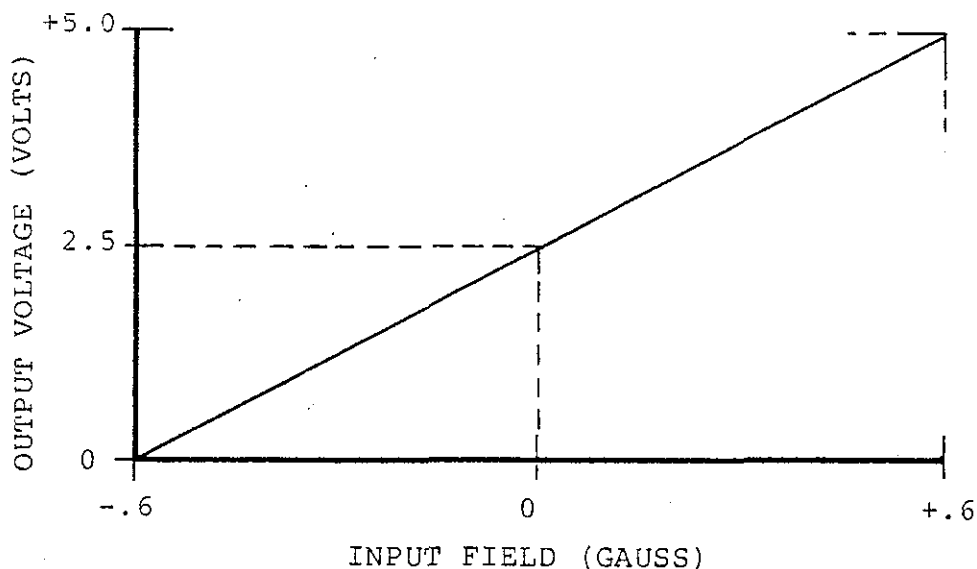


Fig. 3-7a. SENSOR TRANSFER CHARACTERISTIC

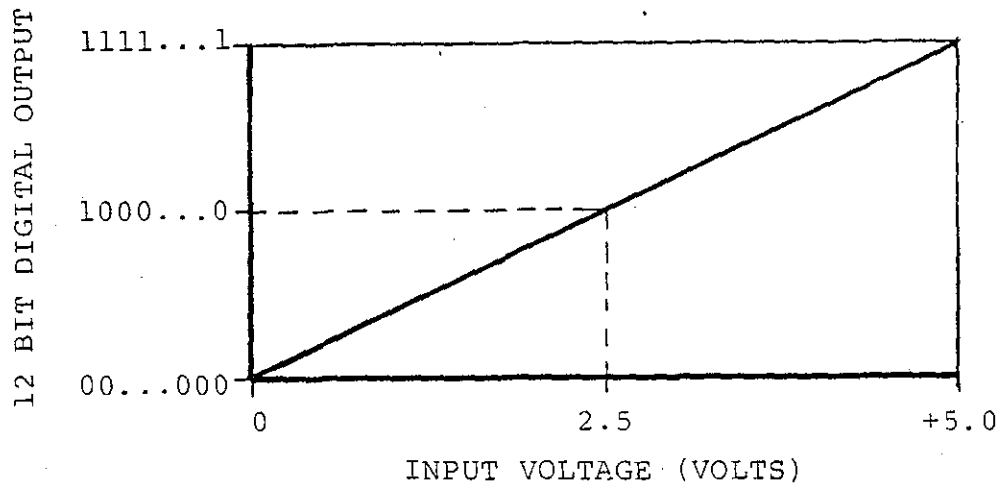


Fig. 3-7b. VDC TRANSFER CHARACTERISTICS

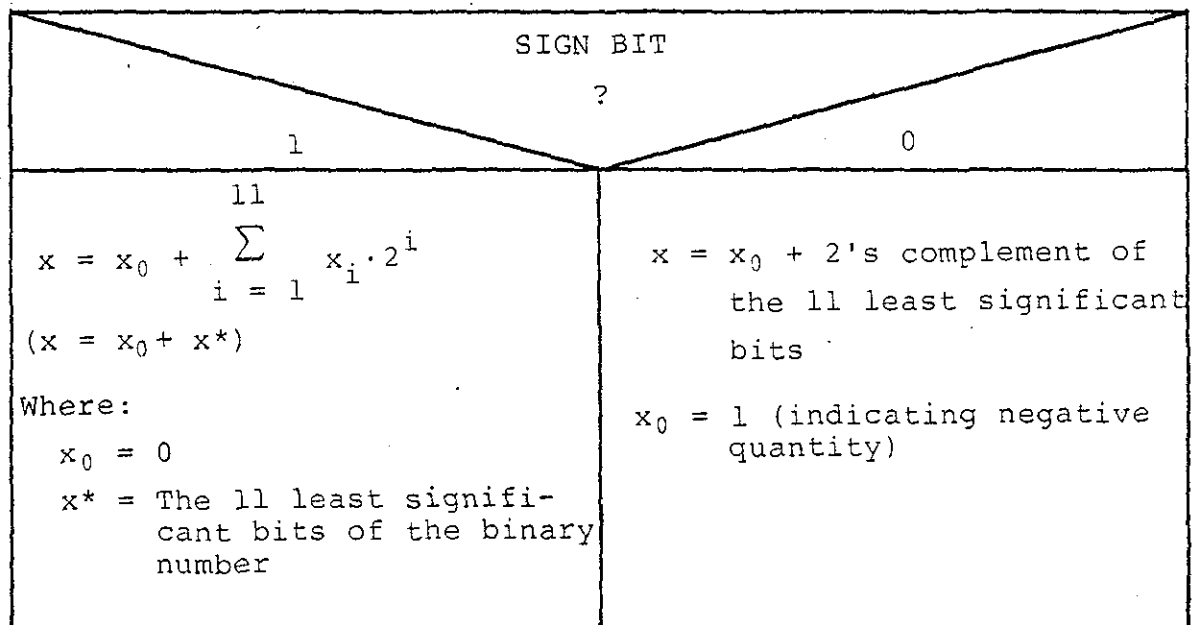


Fig. 3-8 CONVERSION OF DATA

The third function of the "SAMP" subroutine was to reverse the sign of the Hx and Hy data (to correct a test fixture problem) and to correct for sensor offsets. Although analog subsystem offsets are corrected by adjusting either the sample and hold module or the ADC, the independent sensors themselves have offsets<sup>4</sup>. Offset errors for the laboratory instrument were compensated by determining the offset correction term for each sensor (method described in detail in Chapter V) and then either adding or subtracting the term to the respective data during the sample subroutine. By characterizing the sensor errors<sup>5</sup>, actual datum could be improved further during this step.

The final function of the "SAMP" subroutine was to correct for sensor orthogonality error (subroutine "ORTH"). Although the sensors were physically aligned and specified to have orthogonality characteristic [Ref. 3-34] less than +1 degree relative to the base coordinates, this nonorthogonality contributes appreciably to total system error (see error analysis in Chapter IV). The physical misalignment of the sensors was determined experimentally (Chapter V) and determined to be mainly a misalignment of sensor x in the x-y plane as illustrated in Fig. 3-9.

The actual data measured with the x axis sensor is then related to the true Hx and Hy values as

$$Hx^1 = Hx \cos \epsilon - Hy \sin \epsilon .$$

---

<sup>4</sup>With zero stimulus applied the sensors have a finite nonzero output. This error in the fluxgate magnetometer is a function of temperature, voltage and magnetic remanence in the sensor magnetics [Ref. 3-36].

<sup>5</sup>Sensor characteristics relating the temperature and power supply coefficients of offset error and nonlinearity can be derived empirically.

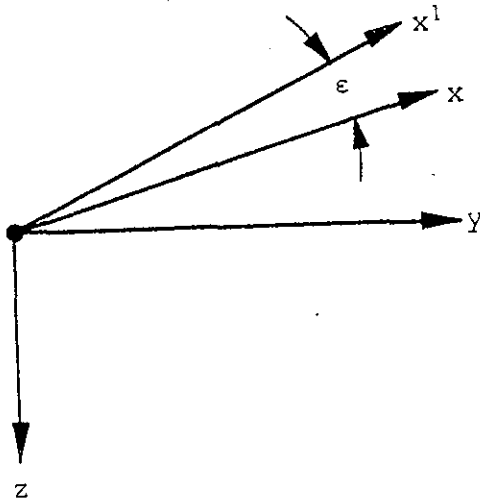


Fig. 3-9 X AXIS NONORTHOGONALITY

Using small angle approximations, we can solve for the desired true value of  $H_x$

$$H_{x'} = H_x - H_y \sin \epsilon \quad (3-1a)$$

$$H_x = H_{x'} + H_y \sin \epsilon \quad (3-1b)$$

By measuring  $\epsilon$  (Chapter V) and storing the angle as a constant, the x axis data was then restored using equation 3-1b above in subroutine "ORTH".

## 2) Subroutines ROTX and ROTY

These subroutines compute arithmetic values for  $H_{xh}$  and  $H_{yh}$  of equation 2-11b using sign magnitude quantities and table lookup to determine solutions for the transcendental functions. Subroutines "SADD" and "SMPY" are nested and used to perform double precision add and multiply as required.

## 3) Subroutine HVEC

Following computation of the horizontal X and Y axis magnetic vector, the subroutine "MAIN" calls subroutine "HVEC" to compute the square of the horizontal vector. Vectors Hx and Hy are squared by calling subroutine "SQU" then added, yielding  $H(\text{HORIZONTAL})^2$ .

## 4) Subroutine WICH

To compute heading, equation 2-1 (or a similar form) must be solved using the horizontal magnetic field vector and either the x or y axis horizontal field component. Although the square root operation implied in equation 2-1 could be implemented using a numerical technique [Ref. 3-37, 3-38], the computation time is decreased by using a table lookup method. Subroutine "WICH" (Fig. 3-10) compares the absolute magnitude of the two horizontal field vectors Hx and Hy to determine the relative heading of the aircraft<sup>6</sup> with respect to the north-south and east-west axes (Fig. 3-11).

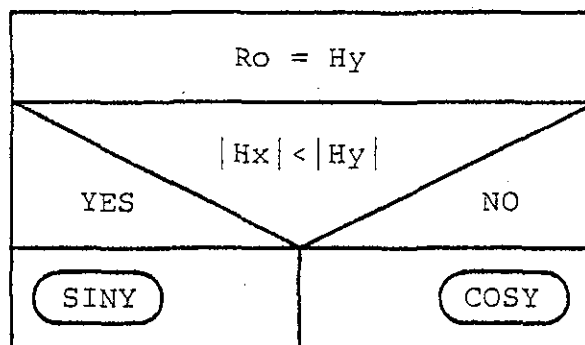


Fig. 3-10. SUBROUTINE "WICH"

<sup>6</sup>If  $|Hx| < |Hy|$ , then an equation similar in form to 2-1a must be used.

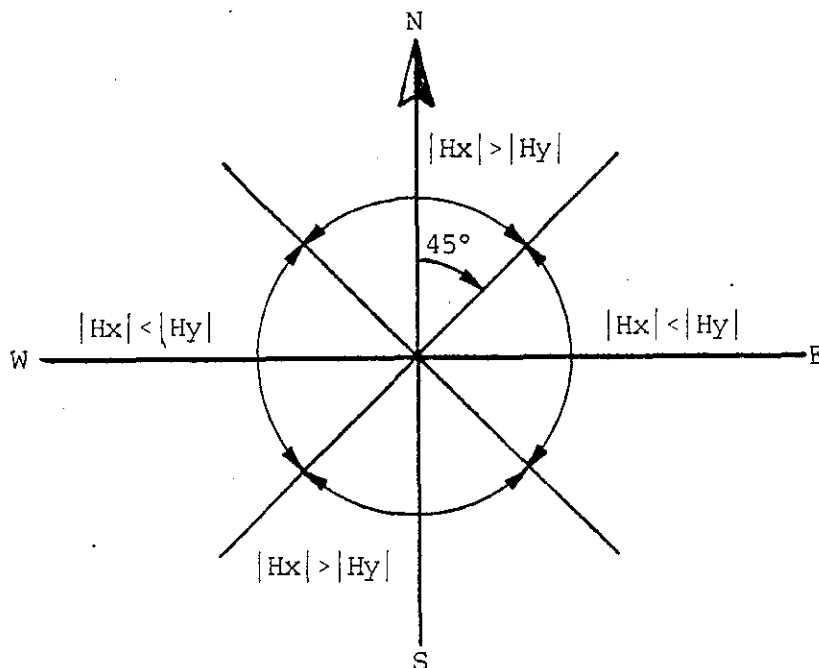


Fig. 3-11. MAGNITUDES OF  $H_x$  AND  $H_y$  RELATED AIRCRAFT HEADING

5) Subroutines COSY and SINY (Fig. 3-12, 3-13)

Depending on the relative absolute magnitudes of  $H_x$  and  $H_y$ , either "COSY" or "SINY" is called to compute aircraft heading. These subroutines invoke subroutine "DIVI" to form the quotient of the axis vector squared and the horizontal field vector squared (a double precision operation). Subroutine "ANGL" is then called to perform an associative table lookup operation using successive approximation and interpolation to complete the inverse cos squared operation. The double precision binary quantity is then converted to three digit binary coded decimal format (BCD) prior to computation of aircraft heading (subroutine "HDG").

The subroutine "SINY" of Fig. 3-12 includes a subtraction of the computed angle from 90 degrees following conversion to BCD format. This operation ensures that the angle passed to

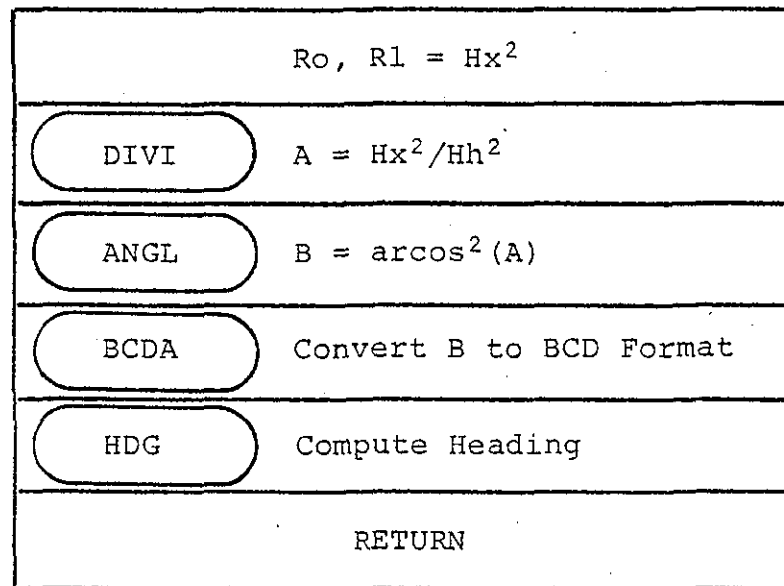


Fig. 3-12. SUBROUTINE "COSY"

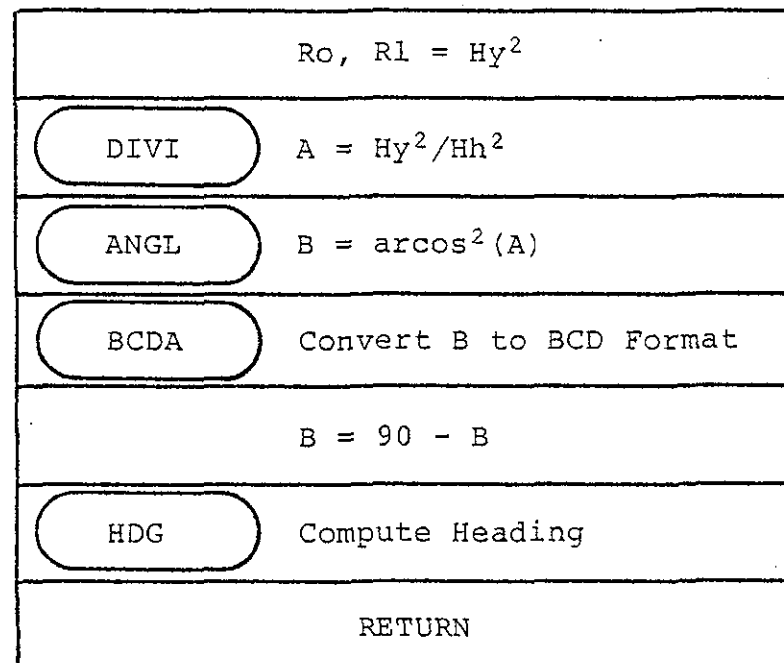


Fig. 3-13. SUBROUTINE "SINY"

the calling subroutine upon exiting either "SINY" or "COSY" is an aircraft heading angle relating sensor x to the north-south axis.

#### 6) Subroutine HDG (Fig. 3-14)

The function of this subroutine is to compute aircraft heading having established the angle between the x axis sensor and the north-south geodetic axis. Determination of the actual heading is accomplished by comparing the signs of both the x and y axis horizontal vectors prior to computing heading (Fig. 3-15). It should be noted that all of the preceding computations leading to horizontal vector data were on sign magnitude quantities preserving the correct horizontal vector polarities<sup>7</sup>.

### 3-5 CONCLUSIONS

This chapter has outlined the practical aspects of designing an instrument to evaluate both the heading algorithms and solid state magnetic indicator proposed in previous chapters. The chapter outlined a design approach that can be used to implement a microprocessor based instrument. In particular, the need to consider the total system hardware requirements while simultaneously considering the programming requirements was identified. Design proceeded by outlining a system block diagram (Fig. 3-1) with major subsystems considered. The instrument required a special purpose computer with an analog subsystem to sample and digitize five sensor signals. Timing and control of the analog subsystem plus digital processing of data was controlled by a microprocessor based central processing unit (CPU). Memory for permanent storage of

---

<sup>7</sup>It is possible at certain attitudes to require sign reversals when computing horizontal vectors.



SIGN OF Hx ?			
POSITIVE		NEGATIVE	
SIGN OF Hy		SIGN OF Hy	
POSITIVE	NEGATIVE	POSITIVE	NEGATIVE
HDG = 360 - ANGLE	HDG = ANGLE	HDG = 180 + ANGLE	HDG = 180 - ANGLE
HDG =360      360			
HDG = 0			
RETURN			

Fig. 3-14. SUBROUTINE "HDG"

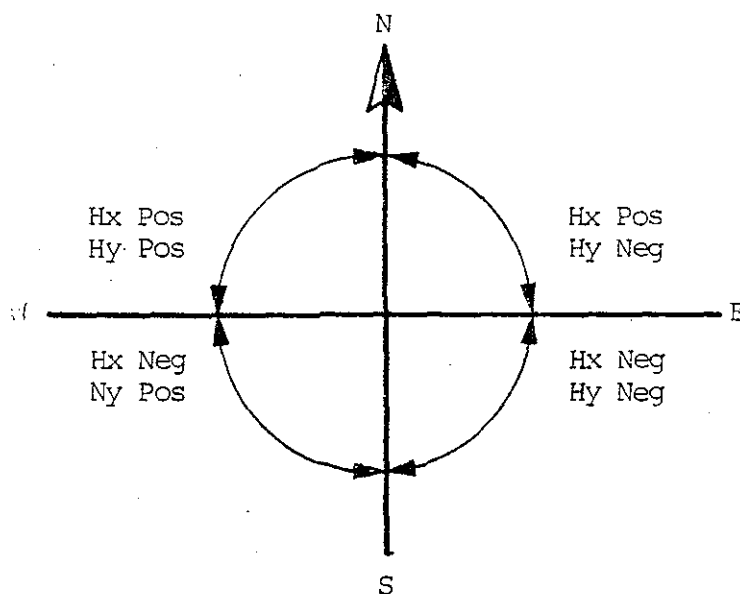


Fig. 3-15. POLARITIES OF HORIZONTAL VECTORS RELATED TO AIRCRAFT HEADING

instructions and temporary storage of data was implemented using memory chips organized on cards with 2048 byte capacity. The particular memory chips selected feature pin compatibility<sup>8</sup> with both read only and volatile random access versions. System inputs consisted of sensor signals from a three axis solid state fluxgate magnetometer plus two analog signals simulating gyroscope outputs. System outputs consist of visual seven segment readout displaying computed heading. In addition, an RS-232 teletype interface was provided to facilitate system development and experimentation.

By identifying the total system in block diagram form at the very beginning, the role and requirements of each subsystem as well as the supporting software were identified. The design then evolved on a modular basis with each subsystem and its supporting program developed in parallel. In this manner pin assignments for input/output ports and critical timing requirements that involved both hardware and software consideration were handled efficiently. By outlining the program requirements in flow chart form (analogous to the block diagram of the hardware subsystem), subroutines were identified facilitating a modular program development. Where possible, subroutines were shared in a nested manner avoiding replication of programming and waste of memory.

Details of error analysis and calculation of overall system throughput rate were deferred to Chapter IV. It was pointed out however, that errors induced by imprecision of data plus truncation and roundoff during processing of the algorithm were to be considered early in the design phase. These data were required to select the sensors and the analog to digital

---

<sup>8</sup>Memory integrated circuit (IC) devices of both types can be used in the same mechanical sockets with actual chip type being used transparent to the remainder of the system.

converter as well as to design the supportive software for the analog subsystem. In addition, the data precision requirements were necessary prior to programming the algorithm<sup>9</sup>.

By incorporating a microprocessor as the main CPU element, considerable sophistication in both control and computing performance was achieved. The overall system was designed relatively quickly, provided a convenient laboratory instrument for evaluation of the proposed algorithms and featured inherent flexibility.

---

<sup>9</sup>Some of the subroutines required double precision manipulations to maintain overall system accuracy.

## CHAPTER IV

## HEADING INSTRUMENT ERROR ANALYSIS

## 4-1 INTRODUCTION

The heading instrument designed to evaluate the heading and solid state remote magnetic indicator algorithms is prone to error from many sources. These errors will accumulate and degrade the accuracy of aircraft heading or yaw angle computations. This chapter addresses the various error sources to determine their relative magnitudes and effects on the overall computation.

Prior to beginning the hardware design of the microprocessor based instrument many of these potential error sources were considered. Their effects were considered in establishing parameters such as word lengths, A/D converter precision, computation speeds, sampling rates, magnetometer sensor accuracies, system noise tolerance, etc. As the design of the microprocessor based system evolved, the error analysis refined. Ultimately, important limitations in instrument design and operation were identified by combined error analysis and empirical data. By carefully analyzing the source and extent of the limiting parameters (such as sensor offset and non-orthogonality), the magnitude of errors unique to this laboratory sensor array were identified. Specialized software was then added (with empirically derived constants) to correct for the otherwise limiting sensor irregularities improving the total system performance.

In this manner, it is apparent that error analysis is an integral part of instrument design. Not only are important parameters identified early in the design cycle (prior to system block diagram development), but shortcomings in conventional

sensors can be improved by judicious application of error correcting algorithms. In this case, data constants were determined after the final instrument became operational. The sensor peculiarities were analyzed empirically using the instrument itself.

The chapter begins by first identifying and carefully analyzing potential error sources in the sensors. This analysis is followed by a similar consideration of errors originating in the analog subsystem. Processing errors that originate due to the finite word length and precision of the microprocessor along with the effects of simplifications made to the algorithms are finally analyzed. The chapter then concludes with a summary of measurement errors, a sample error analysis, a comparison of predicted to measured error and a summary.

#### 4-2 SENSOR ERRORS

The heading computation algorithm employing the remote magnetic indicator (Chapter II) is prone to error proportional to both fluxgate magnetometer sensor and gyroscope measurement errors. Errors inherent in the fluxgate magnetometer are summarized on the data sheet [Ref. 3-34]. Since the experimentation employed simulated gyroscope sensors with voltage levels accurately represented, the analysis of sensor errors will assume ideal gyroscope sensors to predict experimental data.

##### A) Sensor Offset Error

Magnetometer sensors exhibit error caused by both electronic and magnetic phenomena. Errors in the Develco sensors were outlined by Workentine [Ref. 4-1]. These offset errors are induced in the Develco sensors by both electronic offset voltages and currents in the respective sensor electronics and

by residual magnetic fields in the magnetic mass of the sensor assemblies. Although the physical and electronic design attempts to reduce offset error, a finite non-zero output can exist when a zero input is applied.

Offset error for each sensor in the Develco model 9200C three axis magnetometer assembly is specified [Ref. 3-34] as "Zero Field Bias +2.5 Volts  $\pm 1.0\%$ ". This offset translates into a worst case maximum error voltage of

$$E_{\text{OFFSET}} = \pm(2.5\text{V} \times 0.01) = \pm 25\text{mV}$$

Since the offset error is sensor dependent, correction cannot be made at a single physical point (as for analog subsystem offsets described in Section 4-3). Corrections can however be made to the measured data by simply adding or subtracting a constant equal to the offset magnitude following each data measurement<sup>1</sup>.

Offset values for each sensor used in the experiment were obtained by rotating the sensor into alignment with earth's magnetic field vector to measure both positive and negative maximum values. The difference in magnetic measurement (assuming negligible analog subsystem error) is related to system offset error composed of sensor electronic and sensor plus test fixture induced magnetic offset error. The actual offset error can be calculated using these two measurements

---

<sup>1</sup>Offset corrections were made in the sample subroutine "SAMP" illustrated in Fig. 3-6a.

$$\begin{aligned}
 |E_{\max}| &= E_f + E_o \\
 |E_{\min}| &= E_f - E_o \\
 |E_{\max}| - |E_{\min}| &= (E_f + E_o) - (E_f - E_o) = 2 E_o \\
 E_o &= (1/2) (|E_{\max}| - |E_{\min}|)
 \end{aligned}$$

where

$E_{\max}$  = The maximum positive voltage recorded when the sensor aligns with earth's field vector.

$E_{\min}$  = The maximum negative voltage recorded when the sensor aligns 180° with earth's field vector.

$E_f$  = The magnitude of earth's magnetic vector represented in volts.

$E_o$  = The sensor offset voltage due to both electronic and magnetic phenomena

Data recorded during x, y and z axis offset measurements as described above are recorded in Table 4-1. Since the offset error is a function of sensor magnetic permeability, the actual offset value will vary with time depending on induced magnetic fields<sup>2</sup>.

Final offset correction values were determined by rotating two sensors in the horizontal plane around the third vertical axis and measuring offsets in two sensors at a time. Recorded data for each sensor was previously corrected for orthogonality error by the sample subroutine "SAMP" (discussion

---

<sup>2</sup>For example, magnetized screwdrivers or other tools used near the sensor will alter the residual magnetic field.

---

SENSOR AXIS	DATA RECORDED (HEXADECIMAL)		OFFSET (HEXADECIMAL PLUS SIGN)
	Emax	Emin	
X	628	E78	+40
Y	640	E5D	-15
Z	637	E68	-25

---

Table 4-1    OFFSET DATA DERIVED BY MEASURING  
EARTH'S FIELD



of this correction follows in Section 4-2B). Data recorded in this manner appears in Tables 4-2 and 4-3. Final correction terms for correcting sensor offset error were calculated using these data. Offset terms to be added or subtracted from respective data channels are tabulated in Table 4-4.

By correcting system offset errors in this manner, the effective error contribution can be reduced appreciably (see final data discussion Chapter V). For a flight instrument, sensor offset characteristics as a function of temperature variation and supply voltage can be derived empirically and appropriate offset corrections made by computing the value of the correction term variable. Magnetically induced offsets can be reduced by degaussing the sensor assembly periodically.

#### B) Axis Alignment Errors

The error specification of [Ref. 3-34] indicates that the maximum axis alignment error is +1 degree relative to base referenced coordinates. This error results in sensor directional uncertainty as illustrated in Fig. 4-1. Each sensor is located within a right circular cone with axis along the true sensor axis and vertex at the common sensor origin. Although this alignment uncertainty contributes no error in determining the total magnetic vector

$$\bar{H} = (\bar{H}_x^2 + \bar{H}_y^2 + \bar{H}_z^2)^{\frac{1}{2}},$$

there is considerable uncertainty in attempting to resolve the true magnetic field component along any axis of the reference coordinate system. This alignment uncertainty of magnetic sensors limits system performance of conventional field direction measuring apparatus [Ref. 4-1].

Protractor Heading Measurement (Degrees)	Data Measured Hx Hy (Units)		Protractor Heading Measurement (Degrees)	Data Measured Hx Hy (Units)		Error Due To Offset X Y (Units)	
	Hx	Hy		Hx	Hy	X	Y
0	8	-759	180	83	720	75	-39
345	199	-743	165	-112	704	87	-39
330	383	-677	150	-292	638	91	-39
315	540	-569	135	-448	527	92	-42
300	666	-421	120	-573	381	93	-40
285	749	-249	105	-658	206	91	-43
270	783	-62	90	-696	14	87	-48
255	770	132	75	-681	-179	89	-47
240	706	314	60	-616	-362	90	-48
225	597	473	45	-504	-521	93	-48
210	449	601	30	-359	-645	90	-44
195	273	687					
180	(DATA UNAVAILABLE DUE TO TEXT FIXTURE LIMITATION)						
165							
TOTAL OFFSETS						978	477
AVERAGE OFFSETS						88.9	43.4

Table 4-2 X AND Y AXIS ERROR MEASURED BY ROTATING  
X, Y AROUND Z IN THE HORIZONTAL PLANE

Protractor Heading Measurement (Degrees)	HZ Data Measured (Units)	Protractor Heading Measurement (Degrees)	HZ Data Measured (Units)	Offset Error (Units)
0.5	0	180.5	-56	-56
315.5	-527	135.5	469	-58
270.5	-763	90.5	707	-56
225.5	-571	45.5	513	-58
TOTAL OFFSET				-228
AVERAGE OFFSET				-57

Table 4-3 Z AXIS OFFSET ERROR MEASURED BY ROTATING  
THE Z AXIS AROUND THE VERTICAL X AXIS

Sensor Axis	Total Average Offset (Units)	Required Correction	Amount of Correction		
			Decimal	Binary	Hex
X	88.9	Subtraction	45	00101101	02D0
Y	43.4	Addition	22	00010110	0160
Z	47.0	Addition	29	00011101	01D0

Table 4-4 OFFSET CORRECTION VALUES

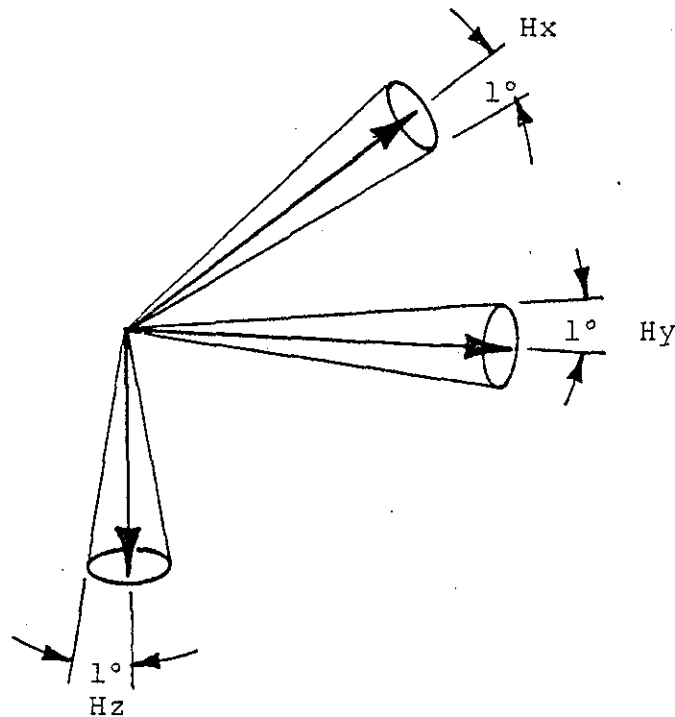


Fig. 4-1 SENSOR ALIGNMENT UNCERTAINTY

Although this error source can be reduced by physically aligning the sensors more accurately during assembly, cost of the sensors increases. Ultimately, directionality of the magnetic sensors becomes a function of the physical sensor itself and more accurate sensors are required as pointed out by Gise [Ref. 4-2]. A heading system that tolerates sensor misalignment is therefore a very desirable alternative to requiring precise alignment or more elaborate sensors.

During assembly of the Develco fluxgate magnetometer sensor array, sensor misalignment is determined by using earth's magnetic field and a precision mechanical rotation assembly. A sensor (assume the X axis) is aligned with earth's magnetic

vector by positioning the sensor to maximize electrical output<sup>3</sup>. One of the other sensors (assume the y axis) is aligned with the rotation axis of the precision calibration assembly (Fig. 4-2) and perpendicular to the first by rotating the sensor array around the second sensor axis (y axis in this case) and adjusting its relative position until a null output is achieved at all rotation angles. Mechanical orthogonality of the sensors is then limited only by the mechanical imprecision of the calibration device (orthogonality within  $\pm 0.01$  degrees can be easily achieved in the calibration tool) and by the directional characteristics of the physical sensors.

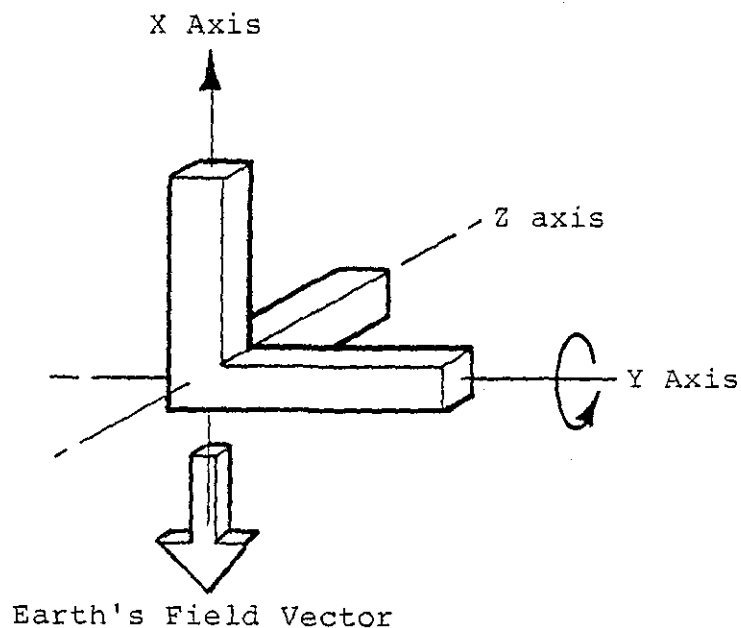


Fig. 4-2 MECHANICAL ORIENTATION OF THE MAGNETOMETER SENSORS DURING CALIBRATION

In addition to functioning as an alignment apparatus, the calibration device described above provides a convenient means

<sup>3</sup>By maximizing or nulling a measurement, the mechanical positioning is a function of only the field and the resolution of the voltage measuring device obviating errors due to physical position measurement.

to characterize sensor assemblies after final assembly adjustments are made. Any misalignment of the second sensor relative to the first results in a coning of the second sensor around the rotation axis<sup>4</sup> with a sinusoidal output voltage that is a function of total earth's magnetic field and axis alignment error. The peak to peak voltage resulting from sensor coning is recorded during the final alignment test and made available to sensor purchasers. Coning voltages developed for the sensor assembly used with this experiment were obtained from Develco [Ref. 4-3] and are recorded in Table 4-5. Sensor misalignment for each axis can be derived using additional data provided by Develco along with additional empirical data derived by experimentation.

The total ambient magnetic field at the Develco laboratory is measured using the three sensors (applying equation 4-1) and is supplied as digital data. In our case, the total field measured was 1573 units or

$$\frac{1573 \text{ units}}{2048 \text{ units Full Scale (F.S.)}} \times 60,000 \text{ gamma F.S.} = 46,084 \text{ gamma } (\gamma)$$

$$\text{Sensitivity of the sensor} = \frac{2.5 \text{ Volts F.S.}}{60,000 \gamma \text{ F.S.}} = 42 \mu\text{Volts}/\gamma$$

Considering the X axis sensor, coning resulted in a signal of 38 mV peak to peak (or 19mV peak). Misalignment of the X axis sensor from the Y-Z plane can then be calculated as

---

<sup>4</sup>Assume that the first axis is initially adjusted for maximum output to align it with earth's field and the rotation axis is perpendicular to the field.

SENSOR ASSEMBLY NO. S/N 1043-013

Rotation Axis	Coning Voltage (Peak-Peak mV)	Orthogonality Error (Degrees)
X	38	0.57
Y	8	≈0
Z	51	0.76

Table 4-5 MAGNETOMETER ORTHOGONALITY MEASUREMENTS

Peak Signal = 19 mV or 456 gamma angular misalignment

$$\epsilon_x = \sin^{-1} \frac{456}{46,084}$$

$$\epsilon_x = 0.57 \text{ degrees}$$

Similarly, the Y and Z axis have misalignment errors of  $\epsilon_y \approx 0$  and  $\epsilon_z = 0.76$  degrees with respect to the X-Z and X-Y planes respectively (sensor orthogonality errors are tabulated in Table 4-5).

Having established that sensor orthogonality errors exist, the remaining task is to identify the direction that the sensor axis points relative to the other two sensor axes. Since the Y axis has relatively little orthogonality error, it will be assumed to be perpendicular to the X-Z plane. In addition, since the Hz data enters into the algorithm in a second order manner relative to the Hx and Hy measured data, correction and characterization of the Hx sensor was considered to be of primary concern. Orientation of the X axis sensor relative to the Y and Z axes was determined empirically.

Angular position of the X axis sensor can be described using the error angles  $\epsilon_{xy}$  and  $\epsilon_{xz}$  as delineated in Fig. 4-3. Characterization of sensor orthogonality error in terms of these two angles would enable algorithmic corrections of measured data.

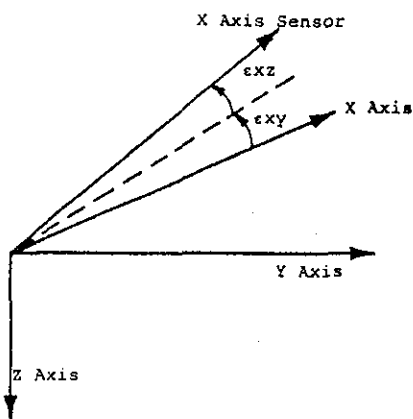


Fig. 4-3 X AXIS SENSOR ORIENTATION



1) Empirical Determination of  $\epsilon_{xz}$

The angle  $\epsilon_{xz}$  (angle between the x axis sensor and the z axis of the geodetic coordinate system) was determined in several steps using the test apparatus described in Chapter V.

- i) The x and y sensors were oriented in the horizontal plane with the z axis sensor vertical downward.
- ii) The x and y sensors were rotated around the z axis with magnetic data measurements (corrected for sensor offset error as described in Section 4-2A) recorded in Table 4-6 for incremental rotation angles.
- iii) The total horizontal field at each angular position was calculated

$$H_{ht} = (H_x^2 + H_y^2)^{\frac{1}{2}}$$

- iv) Average horizontal field  $H_{av}$  was computed by averaging the results of iii) above.
- v) The horizontal field deviation  $H_d$  was computed for each angular position; tabulated in Table 4-6 and plotted on Fig. 4-4.

$$H_d = (H_{av} - H_{ht})$$

The horizontal field deviation or error (as shown on Fig. 4-4) was now examined. An angular error  $\epsilon_{xz}$  should cause the horizontal field error curve to peak at 90 and 180 degrees. Since this obviously was not the case, it was concluded that major error in x axis orthogonality was due to the component  $\epsilon_{xy}$ .

Physical* Heading (Degrees)	Displayed** Heading (Degrees)	Measured Data (Units)		Total Computed Horizontal Field (Hht) (Units)	Hd (Hav-Hht) (Units)
		Hx	Hy		
355	90	12	-727	727	-3
335	70	258	-682	729	-1
315	50	477	-555	732	2
295	30	637	-362	733	3
275	10	720	-127	731	1
255	350	718	127	729	-1
235	330	628	363	725	-5
215	310	464	569	734	4
195	290	242	687	728	-2
175	270	-10	731	731	1
155	250	-258	686	733	3
135	230	-476	557	733	3
115	210	-635	362	731	1
95	190	-721	123	731	1
75	170	-718	-133	730	0
55	150	-628	-371	729	-1
35	130	-460	-565	729	-1

Total Hht = 12415

Average (Hav) = 730

\*Measured using a protractor on the test apparatus.  
 \*\*Computed and displayed digitally by the instrument.

Table 4-6 MEASUREMENT OF HORIZONTAL FIELD

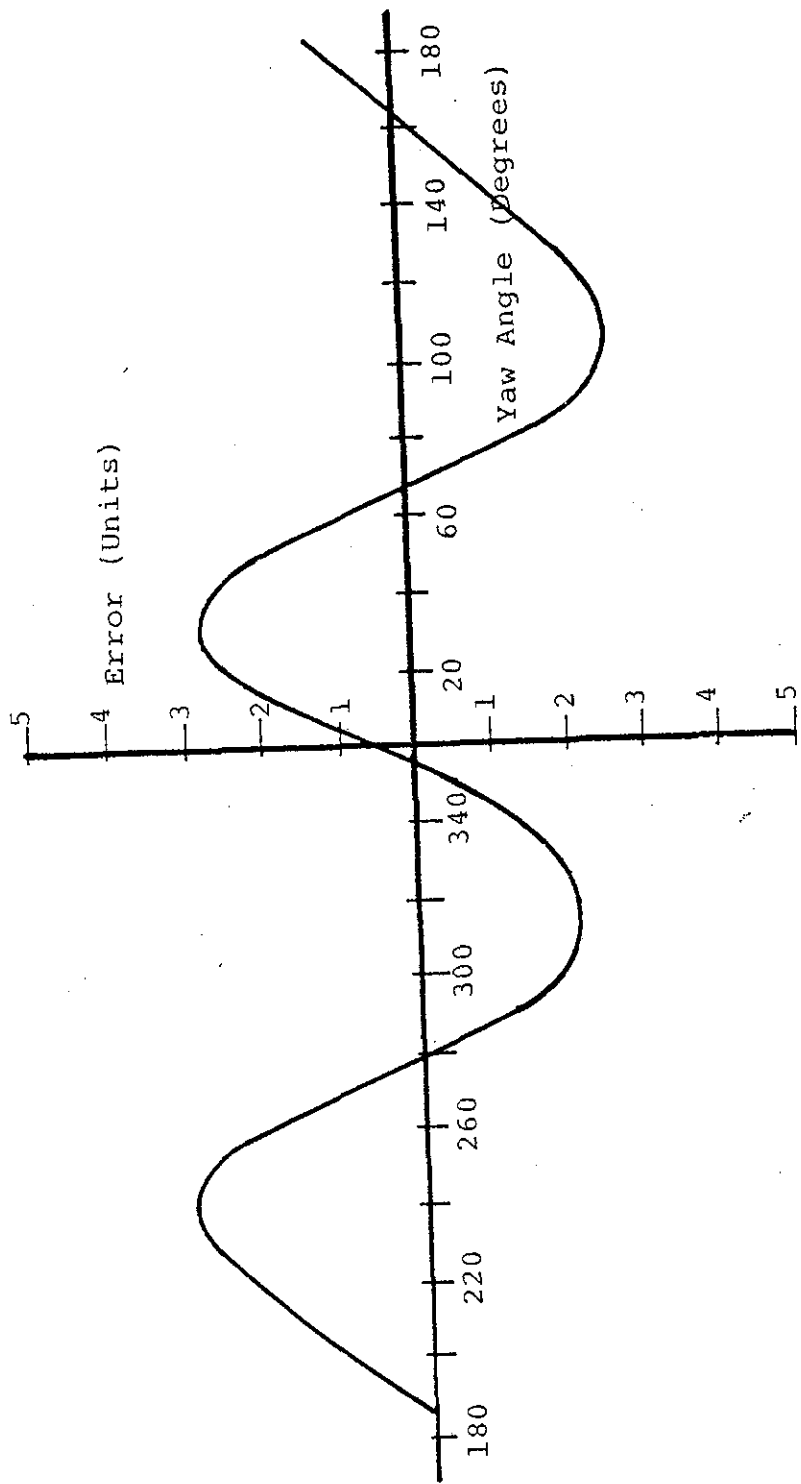


Fig. 4-4 DEVIATIONS OF THE HORIZONTAL FIELD MEASUREMENT FROM THE MEAN

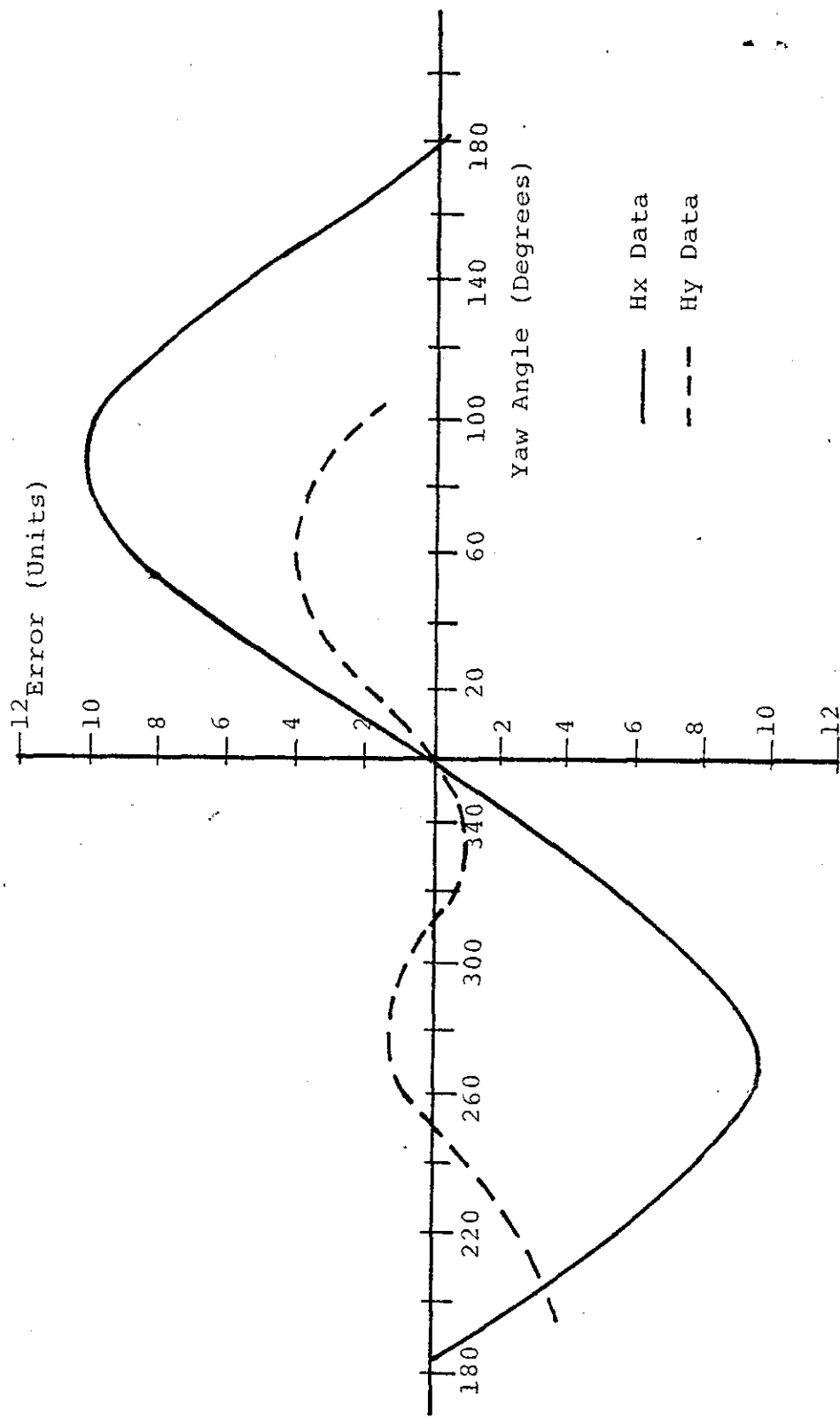


Fig. 4-5 DEVIATION OF Hx AND Hy DATA FROM THE COMPUTED FIELD COMPONENTS AS A FUNCTION OF YAW

## 2) Empirical Determination of $\epsilon_{xy}$

The angle  $\epsilon_{xy}$  representing x axis sensor misalignment relative to axis y was measured as follows:

Steps i) and ii) above were repeated with the exception that the calculated values for  $H_x$  and  $H_y$  ( $H_{xc}$  and  $H_{yc}$  respectively) were recorded with measured  $H_x$  and  $H_y$  data ( $H_{xm}$  and  $H_{ym}$  respectively) in Table 4-7. The calculated values were obtained by assuming that the angle  $\epsilon_{xz}$  as determined above was negligible and that the y axis sensor was perpendicular to the x-z plane. With these assumptions, we note that at the heading of zero degrees (extrapolated between display of 10 and 350 degrees of Table 4-7 and Fig. 4-5), there is no error in yaw due to either  $H_x$  or  $H_y$ . By physically rotating the sensors in fixed intervals from yaw = 0 degrees and noting that the horizontal field  $H_h = 730$  units, we can then compute expected  $H_x$  and  $H_y$  data at respective yaw orientations.

Physical orientation of the x axis sensor is easily determined by considering orientation at the maximum error excursions. These observations are illustrated in Fig. 4-6. We note that the only possible orientation of the x axis sensor satisfying the data in Fig. 4-5 is that of Fig. 4-6.

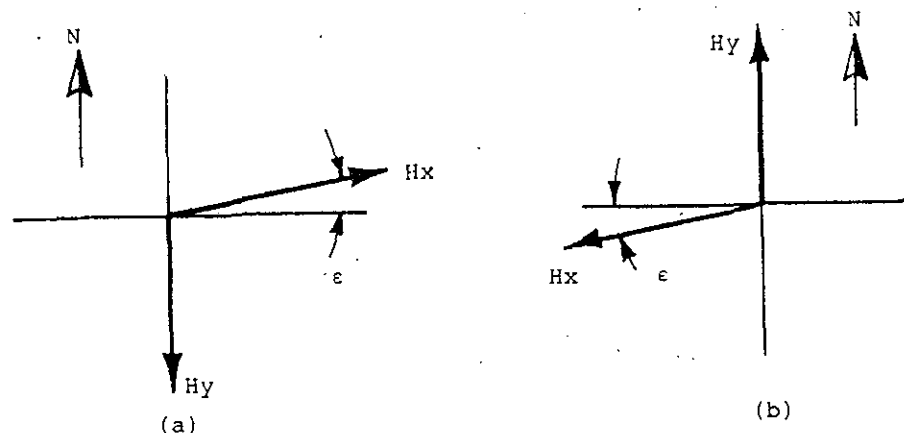


Fig. 4-6 (a) SENSORS ORIENTED AT YAW = +90 degrees  
 (b) SENSORS ORIENTED AT YAW = +270 degrees

Physical* Heading (Degrees)	Displayed** Heading (Degrees)	Measured Data (Units)		Computed Data (Units)		Deviation (Units) (Hxm-Hxc) (Hym-Hyc)	
		Hxm	Hym	Hxc	Hyc	(Hxm-Hxc)	(Hym-Hyc)
355	90	12	-727	0	-730	+12	+ 3
335	70	258	-682	250	-686	+ 8	+ 4
315	50	477	-555	469	-559	+ 8	+ 4
295	30	637	-362	632	-365	+ 5	+ 3
275	10	720	-127	719	-127	+ 1	0
255	350	718	127	719	+127	- 1	0
235	330	628	363	632	365	- 4	- 2
215	310	464	569	469	559	- 5	10
195	290	242	687	250	686	- 8	1
175	270	-10	731	0	730	-10	1
155	250	-258	686	-250	686	- 8	0
135	230	-476	557	-469	559	- 7	- 2
115	210	-635	362	-632	365	- 3	- 3
95	190	-721	123	-719	+127	- 2	- 4
75	170	-718	-133	-719	-127	1	- 6
55	150	-628	-371	-632	-365	4	- 6
35	130	-460	-565	-489	-559	9	- 6

\* Measured using a protractor on the test apparatus.

\*\* Computed and displayed digitally by the instrument.

Table 4-7 MEASURED AND COMPUTED HX AND HY DATA  
IN THE HORIZONTAL PLANE

Magnitude of the angle  $\epsilon_{xy}$  can be computed as follows using data from Fig. 4-5

Max. delta from Fig. 4-5 = 10 units  
Average horizontal field = 730 units

$$\epsilon_{xy \text{ max}} = \sin^{-1} \frac{10}{730}$$

$$= 0.79 \text{ degrees}$$

We note that the angle of 0.79 degrees is approximately the same as determined by Develco during manufacture of the sensors (Table 4-5). The added error is due to test set inaccuracy.

C) Fluxgate Sensor Noise Induced Error

The analog output from the fluxgate sensors can exhibit an error due to signal uncertainty resulting from noise. Although the data sheet [Ref. 3-34] indicates that 5mV peak to peak of ripple can exist on the output, the frequency content centers in the 550 kHz range (driver frequency of the fluxgate magnetometer) and no appreciable ripple<sup>5</sup> exists below 60 Hz (especially when the sensor output is filtered prior to data sampling). The noise specification of less than 1 gamma peak to peak in the 1 Hz bandwidth region is also negligible. In summary, no appreciable error due to noise on the magnetometer signal lines is evident.

D) Magnetometer Gain Error

The magnetometer is specified to have gain (sensitivity) of 2.5 Volts/600 milligauss,  $\pm 1\%$  which translates into a maximum signal uncertainty of

<sup>5</sup>Verbally confirmed by Workentine of Develco [Ref. 4-1].

$$\pm(2.5V \times 0.01) = \pm 25 \text{ mV.}$$

This represents a sensor transfer function of 4.16 Volts/gauss or 0.24 gauss per volt. The uncertainty then can be expressed as

$$\begin{aligned} \pm(0.24 \text{ gauss} \times 0.01) &= \pm 2.4 \text{ milligauss} \\ &= \pm(2.4 \times 10^2) \text{ gamma} \end{aligned}$$

Since this error is not corrected in the laboratory instrument it will be considered in total in the final error analysis. It is worth noting however, that should the magnetometer gain uncertainty be characterized, gain corrections for each sensor could be made during computation by the computer. In addition the error term is proportional to actual signal level applied.

#### E) Magnetometer Linearity Error

D.C. linearity of the magnetometer is specified to be  $\pm 0.5\%$  of signal level. This uncertainty at full scale can be expressed as  $\pm(2.5 \text{ Volts} \times 0.005) = \pm 12.5 \text{ mV}$ . Alternately, linearity error can cause a signal uncertainty of  $\pm 1.2$  milligauss or  $\pm(1.2 \times 10^2)$  gamma. Linearity error is also not corrected during computation and is considered in the final error analysis. By simply characterizing and correcting the linearity characteristics of each sensor, considerable improvement in system accuracy could be achieved.

### 4-3 ANALOG SUBSYSTEM ERROR ANALYSIS

The analog subsystem of the instrument is outlined in block diagram form in Fig. 4-7. This subsystem accepts analog signals from magnetometer and gyroscope transducers, performs a time division multiplexing between the signals and digitizes



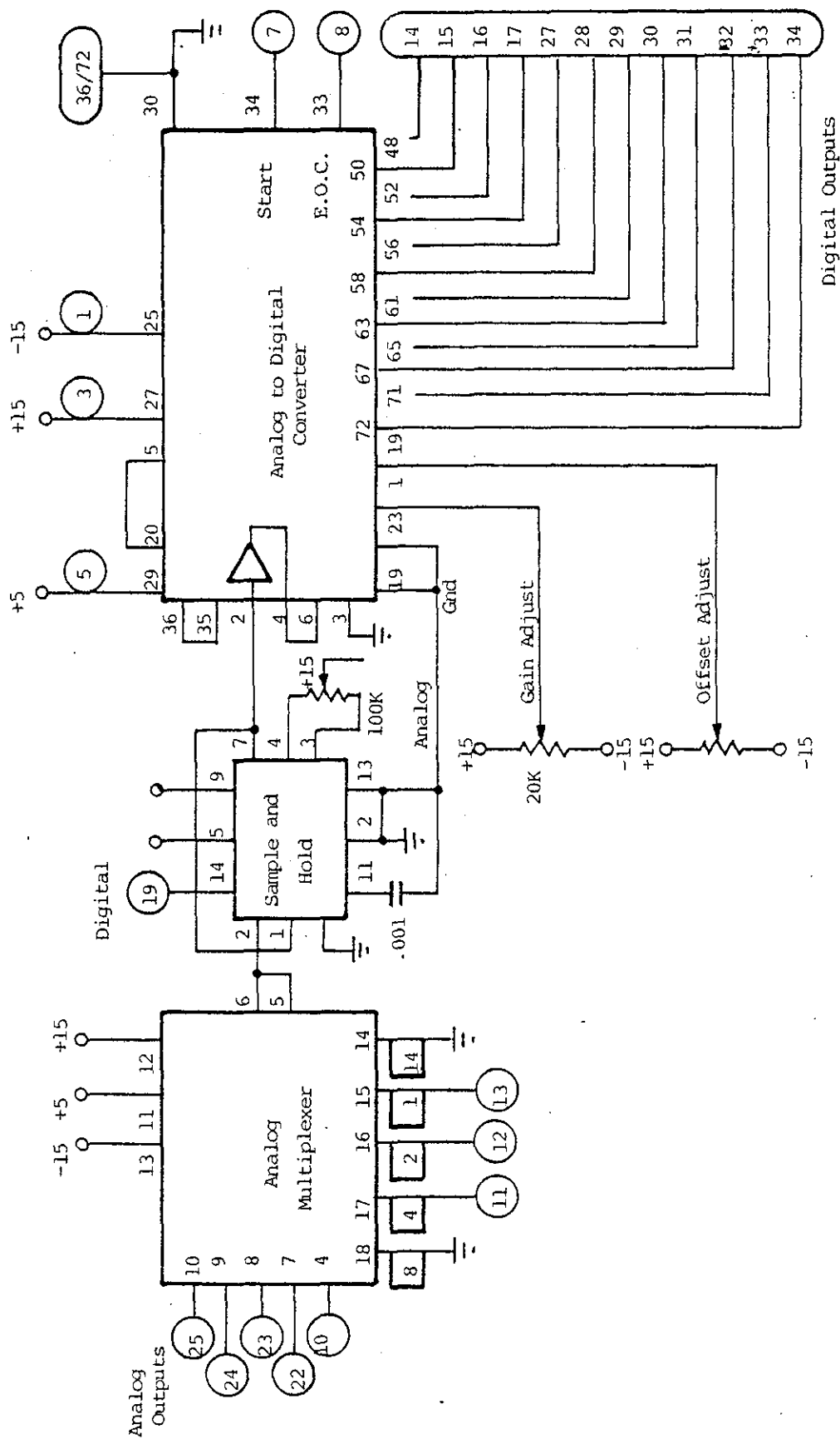


Fig. 4-7 THE ANALOG SUBSYSTEM

the respective signals prior to subsequent processing by the computer. During this data acquisition and conversion process, errors are introduced into each of the signals. This section addresses the potential error sources and computes the respective error contributions to be expected during operation of the instrument.

Although the multiplexer and sample and hold blocks of Fig. 4-7 could be eliminated (eliminating possible error sources) by digitizing each signal with a unique analog to digital converter, it can be shown that such a system would be expensive and difficult to implement. The analog to digital converter (A/D) quantizes an analog signal in a finite amount of time. Speed of conversion is predicted in a finite amount of time by both the resolution of the converter and the frequency of the signal to be converted. Time required to perform a conversion is generally called the "aperature time".

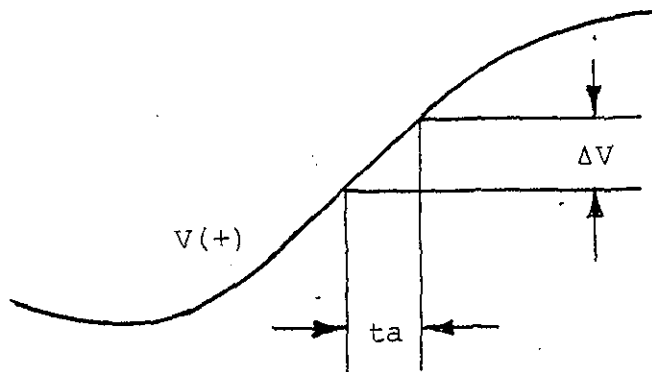


Fig. 4-8 APERTURE TIME AND AMPLITUDE UNCERTAINTY

As illustrated in Fig. 4-8, aperture time and amplitude uncertainty are related by the time rate of change of the analog signal. For the particular case of a sinusoidal signal to

be converted, the maximum rate of change occurs at the zero crossing of the waveform and the amplitude change is:

$$\Delta V = \frac{d}{dt} (V \sin wt)_{t=0} \times t_a \quad (4-1a)$$

$$\Delta V = V w t_a \quad (4-1b)$$

$$\text{giving } \frac{\Delta V}{V} = w t_a = 2 \pi f t_a. \quad (4-2)$$

From this result we can determine the aperture time required to digitize a 30 Hz signal to 12 bits resolution (a resolution of 1 part in 4096 or 0.0244%).

$$t_a = \frac{V}{V} \times \frac{1}{2 f} = \frac{.000244}{6.28 \times 30} = 1.3 \times 10^{-6}$$

This result indicates that to remain within 1 bit of resolution (0.0244%) we require an aperture time of 1.3 microseconds to process analog signals varying at a rate of 30 Hertz. It can be seen that the system would require fast A/D converters plus extremely fast computational capability to accommodate this configuration of sensors and analog subsystem. By using multiplexing and sample and hold circuitry we can however reduce the number of A/D converters required to one and alleviate the aperture and processing requirements imposed above.

The operation of sampling to be used by the instrument is illustrated in Fig. 4-9 which shows an analog signal and a train of sampling pulses. The pulses are provided by the central processing unit. A switch connects the analog signal for a very short period of time to the hold circuitry charging a capacitor and storing the sampled voltage until the next sample is required. This type of sampler is called sample and hold.

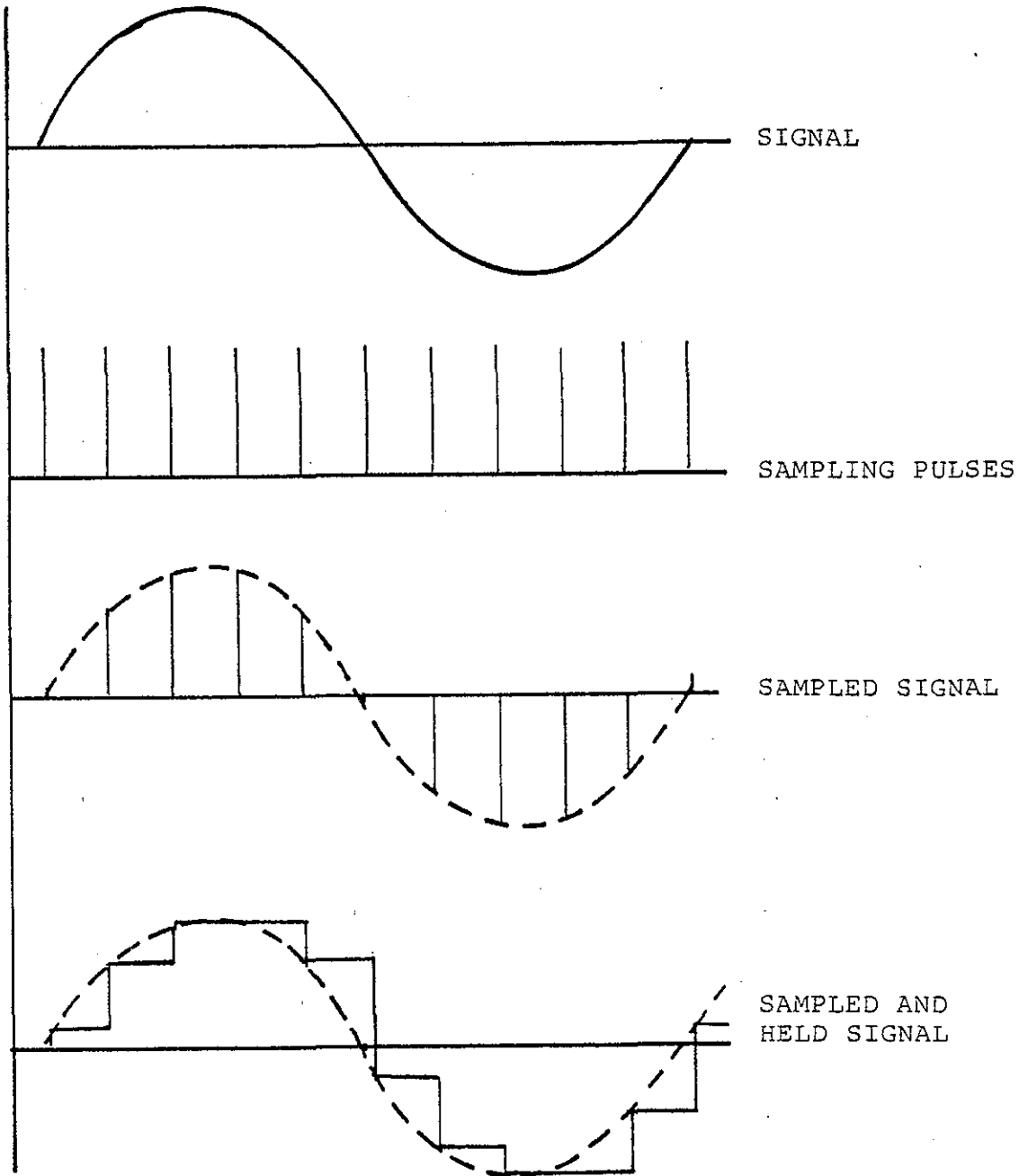


Fig. 4-9 SIGNAL SAMPLING PROCESS

## A) Sampling Rate Errors

The process of uniformly sampling a function of continuous time can yield a significant source of error if the sampling period  $T$  is selected too large [Ref. 4-4, 4-5]. This error can be illustrated by considering an analog signal  $x_a(t)$  that has the Fourier representation [Ref. 4-6]

$$x_a(t) = \frac{1}{2\pi} \int_{-\infty}^{\infty} X_a(j\Omega) e^{j\Omega t} d\Omega \quad (4-3a)$$

$$X_a(j\Omega) = \int_{-\infty}^{\infty} x_a(t) e^{-j\Omega t} dt \quad (4-3b)$$

The sequence  $x(n)$  with values  $x(n) = x_a(nT)$  is said to be derived from  $x_a(t)$  by periodic sampling and  $T$  is the sampling period. The reciprocal of  $T$  is called the sampling frequency or sampling rate. In order to determine the sense in which  $x(n)$  represents the original signal  $x_a(t)$ , it is convenient to relate  $X_a(j\Omega)$ , the continuous-time Fourier transform of  $x_a(t)$ , to  $X(e^{j\Omega})$ , the discrete-time Fourier transform of the sequence  $x(n)$ . From (4-3a) we note that

$$x(n) = x_a(nT) = \frac{1}{2\pi} \int_{-\infty}^{\infty} X_a(j\Omega) e^{j\Omega nT} d\Omega \quad (4-4)$$

From the discrete-time Fourier transform we also obtain the representation [Ref. 4-4]

$$x(n) = \frac{1}{2\pi} \int_{-\pi}^{\pi} X(e^{j\omega}) e^{j\omega n} d\omega \quad (4-5)$$

To relate the equations (4-4) and (4-5) we can express (4-4) as a sum of integrals over intervals of length  $2\pi/T$ , as in

$$x(n) = \frac{1}{2\pi} \sum_{r=-\infty}^{\infty} \int_{(2r-1)\pi/T}^{(2r+1)\pi/T} X_a(j\Omega) e^{j\Omega nT} d\Omega \quad (4-6)$$

Each term in the sum can be reduced to an integral over the range  $-\pi/T$  to  $+\pi/T$  by a change of variables to obtain

$$x(n) = \frac{1}{2\pi} \sum_{r=-\infty}^{\infty} \int_{-\pi/T}^{\pi/T} X_a \left[ j\left(\Omega + \frac{2\pi r}{T}\right) \right] e^{j\left(\Omega + \frac{2\pi r}{T}\right)nT} d\Omega \quad (4-7a)$$

$$x(n) = \frac{1}{2\pi} \sum_{r=-\infty}^{\infty} \int_{-\pi/T}^{\pi/T} X_a(j\Omega + j\frac{2\pi r}{T}) e^{j\Omega nT} e^{j2\pi r n} d\Omega \quad (4-7b)$$

If we now change the order of integration and summation and note that  $e^{j2\pi r n} = 1$  for all integer values of  $r$  and  $n$ , we obtain

$$x(n) = \frac{1}{2\pi} \int_{-\pi/T}^{\pi/T} \left[ \sum_{r=-\infty}^{\infty} X_a(j\Omega + j\frac{2\pi r}{T}) \right] e^{j\Omega nT} d\Omega \quad (4-8)$$

By substituting  $\Omega = \omega/T$  we get

$$x(n) = \frac{1}{2\pi} \int_{-\pi}^{\pi} \left[ \frac{1}{T} \sum_{r=-\infty}^{\infty} X_a\left(\frac{j\omega}{T} + j\frac{2\pi r}{T}\right) \right] e^{j\omega n} d\omega \quad (4-9)$$

which is identical in form to equation (4-5). We can therefore make the identification (equating like terms of (4-5) and (4-9))

$$X(e^{j\omega}) = \frac{1}{T} \sum_{r=-\infty}^{\infty} X_a\left(\frac{j\omega}{T} + j\frac{2\pi r}{T}\right) \quad (4-10)$$

We can also express (4-10) in terms of the analog frequency variable  $\Omega$  (where  $\Omega = \omega/T$ ) as

$$X(e^{j\omega T}) = \frac{1}{T} \sum_{r=-\infty}^{\infty} X_a(j\Omega + j\frac{2\pi r}{T}) \quad (4-11)$$

The last two equations clearly reveal the relationship between the continuous-time Fourier transform and the Fourier transform of a sequence derived by sampling. For example, if  $X_a(j\Omega)$  is as depicted in Fig. 4-10a then  $X(e^{j\omega})$  will be as shown in Fig. 4-10b when the sampling period  $T$  is too long and as shown in Fig. 4-10c if  $T$  is short enough.

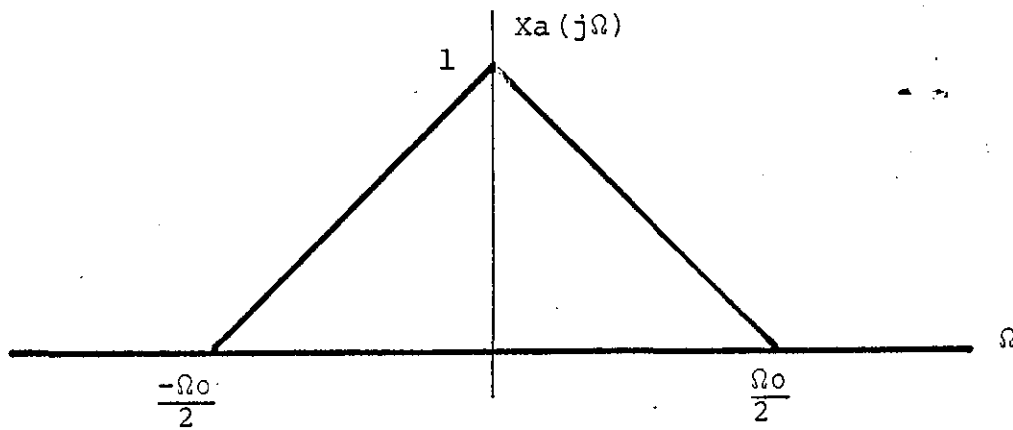
From Fig. 4-10c it is obvious that if  $\frac{\Omega_{OT}}{2} < \pi$ , i.e., we sample at a rate at least twice the highest frequency of  $X_a(j\Omega)$ , then  $X(e^{j\omega})$  is identical to  $X_a(\omega/T)$  in the interval  $-\pi \leq \omega \leq \pi$  and can be recovered from the samples  $x_a(nT)$  by an appropriate interpolation formula.

For the remote magnetic indicator instrument designed in previous chapters, the analog signals are filtered with a low pass section reducing frequency content above 30 Hz. The sampling rate must therefore exceed 60 Hz ( $T < 16.67$  m.s.) to enable accurate dynamic operation of the system.

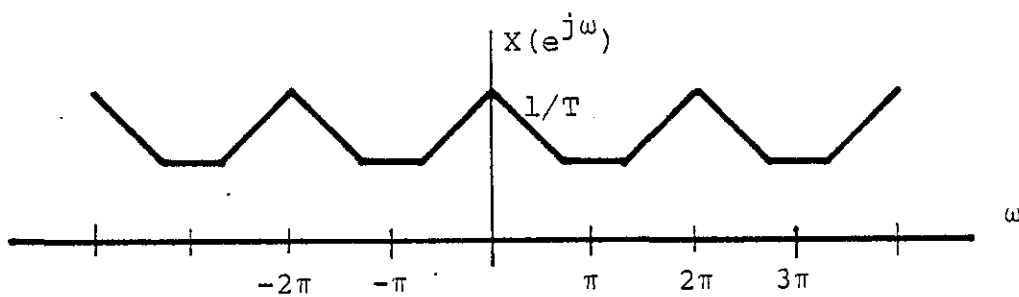
Laboratory measurements of sampling rates on the functional microprocessor based instrument revealed that the analog subsystem operated at a sampling rate of 62.5 Hz (16 m.s.) indicating that the algorithm execution rate supported a system bandwidth of 31.25 Hz. If frequency content of the analog signals is less than 31.25 Hz there is no error due to sampling.

#### B) Analog Multiplexer Induced Error

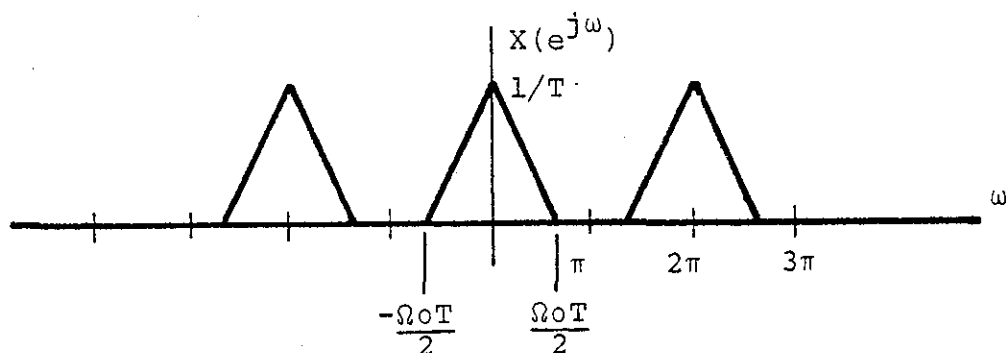
The analog multiplexer of Fig. 4-7 selectively connects one analog transducer output at a time to the input of the sample and hold subsystem. The Datel Systems, Inc., multiplexer [Ref. 4-7] selected for the remote magnetic indicator experiment features eight MOS-FET switches with associated driver circuits,



(a) Fourier transform as a continuous-time signal



(b) Fourier transform of the discrete-time signal obtained by periodic sampling ( $T$  is too large)



(c) Same as (b) except  $T$  is short enough

Fig. 4-10 FOURIER TRANSFORMS OF CONTINUOUS AND DISCRETE-TIME SIGNALS



FET pull-up to reduce propagation delays and all of the necessary decoding logic to enable random channel addressing with a four bit parallel binary input.

Several important parameters are used to characterize analog multiplexers and can contribute error.

#### 1) Transfer Accuracy

Transfer accuracy is a function of the source impedance, switch resistance, load impedance (if the multiplexer is not buffered) and the signal frequency. It expresses the input to output error as a percentage of the input. In our case the system configuration predicates a maximum error due to transfer accuracy of (+0.01%) yielding an error term of

$$\underline{+0.0001} \times 2.5 \text{ Volts} = \underline{+25} \text{ mV}$$

#### 2) Settling Time

This parameter defines the time elapsed from the application of a full scale step input to the time when the output has entered and remained within a specified error band around its final value. In our case the selected multiplexer has a maximum settling time of 1 microsecond to +0.01% full scale (F.S.) Since the control system selecting channels is implemented using a microprocessor, the minimum time between analog subsystem commands will always be greater than 3.0 microsecond<sup>6</sup>. The multiplexer will therefore always have settled to the final value before the sample and hold circuit (following this subsystem) can be activated with no error due to the settling time parameter.

---

<sup>6</sup>One machine cycle time for the 2650 microprocessor with 1 MHz clock frequency.

## 3) Throughput Rate

The highest rate at which the multiplexer can switch from channel to channel at its specified accuracy is in this case 500 kHz. Since this rate is more than four orders of magnitude greater than the operational rate of the subsystem there is no error due to throughput rate limitations.

## 4) Input Leakage Current

The amount of signal coupled to the output as a percentage of input signal applied to all OFF channels together can be calculated by considering the maximum leakage current specified from OFF channels to the ON channel. In our case the maximum error signal can be calculated

$$\text{Error} = [ 4 (8 \text{ na} \times 2000 \text{ ohms source imped.})^2 ]^{\frac{1}{2}}$$

$$\text{Error} = 32 \text{ microvolts}$$

Note that in this case the voltage levels are statistically independent allowing an R.S.S. of error sources to calculate total error [Ref. 4-8, 4-9].

## C) Sample and Hold Circuit Induced Errors

The sample and hold subsystem consists of a switch and capacitor arrangement as shown in Fig. 4-11. The Datel Systems, Inc., model SHM-IC-1 integrated circuit sample and hold device [Ref. 4-10] features a self-contained high gain differential input amplifier, a digitally controlled electronic switch and a high input impedance buffer amplifier. The external components used with the sample and hold circuit in the solid state remote magnetic indicator instrument consisted of the 0.001 $\mu$ f holding capacitor and a 100K offset trimpot. By connecting

the output back to the negative input of the input amplifier (Fig. 4-11), the sample and hold subsystem operated in a unity gain, noninverting mode. When the switch is closed, the unit is in the sampling or tracking mode (Digital Control = 0 Volts), and will follow a changing input signal.

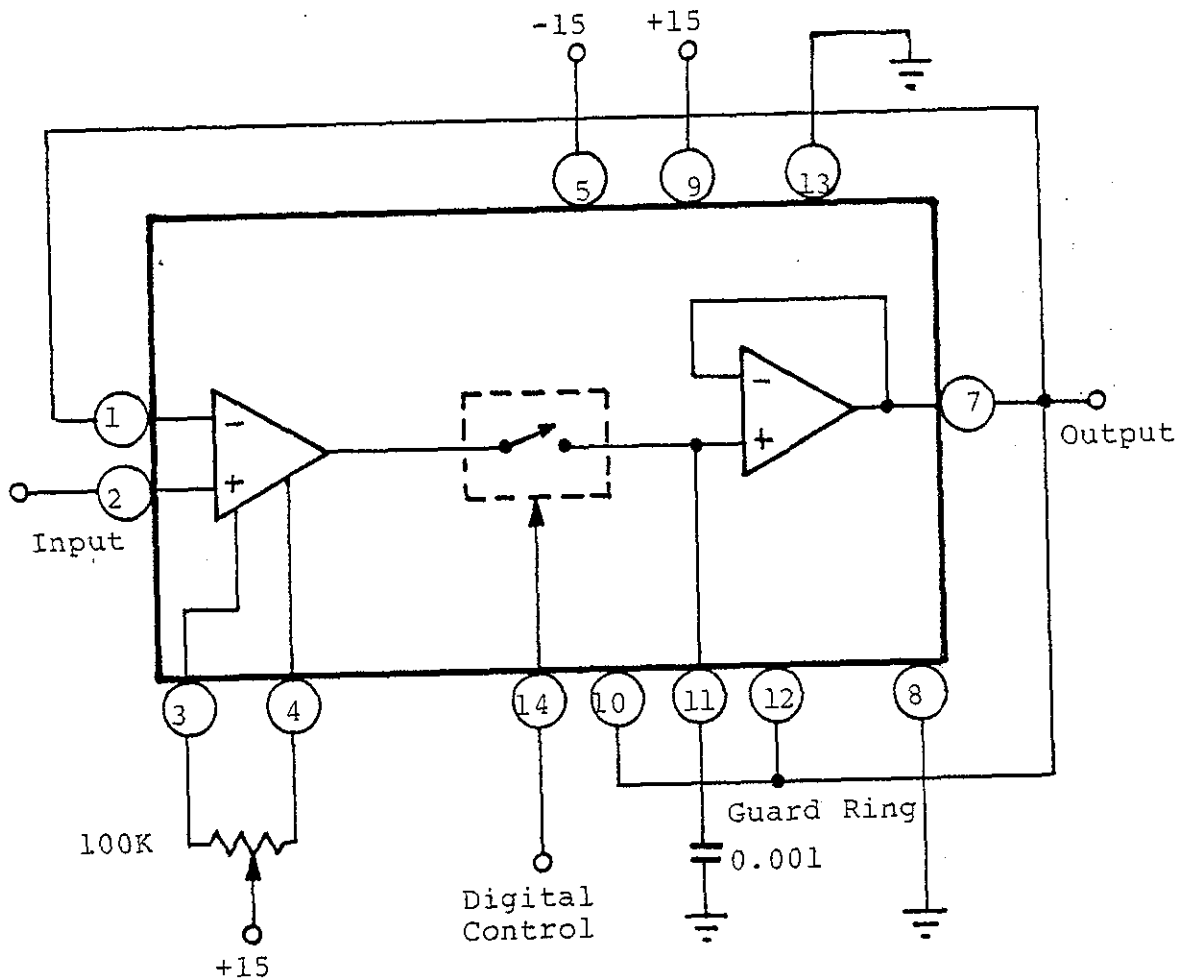


Figure 4-11 SAMPLE AND HOLD SUBSYSTEM

When the switch opens the unit is in the hold mode and retains a voltage on the capacitor for some period of time depending on capacitor and switch leakage. Sample and hold devices are characterized by a number of important parameters that must be considered in the design of a data acquisition subsystem.

#### 1) Acquisition Time

The time lapse between the time that the sample command is given to the point where the output enters and remains within a specified error band around the input value is specified to be less than 4 microseconds time to transit from 0 to 0.1% of 10 Volts with  $C = 0.001 \mu\text{f}$  [Ref. 4-10]. This implies that the control signals emanating from the central processor should allow at least 4  $\mu\text{s}$  acquisition time prior to entering the hold mode. We note that the sample and hold subroutine (Appendix B) executes the instruction

IORI, R3 H'80' READY TO HOLD,

a two machine cycle instruction prior to sending the hold control signal. This instruction delays control signal transmission by  $(2 \times 3 \mu\text{s}) = 6 \mu\text{s}$  allowing the sample and hold circuit ample time to settle with no appreciable error due to the acquisition time parameter.

#### 2) Hold Mode Voltage Droop

The maximum change in output voltage as a function of time is specified to be 50 mv/sec maximum using a 0.001  $\mu\text{f}$  polystyrene capacitor. Since the maximum total accumulated time to completion of the analog to digital conversion can be calculated as

5 Instructions (11 machine cycles)	= 33 $\mu$ s
1 Analog to Digital Conversion	= 20 $\mu$ s
3 Instructions if Conversion not synchronized with instructions (7 machine cycles)	= <u>21</u> $\mu$ s
	74 $\mu$ s

we can then compute droop error to be  $50 \text{ mv/sec} \times (74 \times 10^{-6})$   
 $\text{sec} = 3.73 \text{ mv.}$

### 3) Aperature Delay

The maximum time lapse between the time of hold signal receipt to opening of the switch is specified to be 50 nsec, an insignificant length of time in the instrument. There is therefore no error due to aperature delay.

### 4) Offset Error

Although the maximum offset error is specified to be 20 mv maximum [Ref. 4-10], the error was eliminated using the 100K trimpot offset adjustment. There was no appreciable offset error contribution due to the sample and hold circuit.

### 5) Gain Error

The gain error of a sample and hold circuit is apparent during the sample mode when the transfer function of the total amplifier deviates from the ideal unity slope condition (Fig. 4-12). In the noninverting unity gain mode, the specified gain error is  $\pm 0.05\%$  maximum yielding a signal error of

$$(\pm 0.0005) \times 5.0 \text{ V} = 250 \text{ mV}$$

This error can, however, be eliminated with the gain

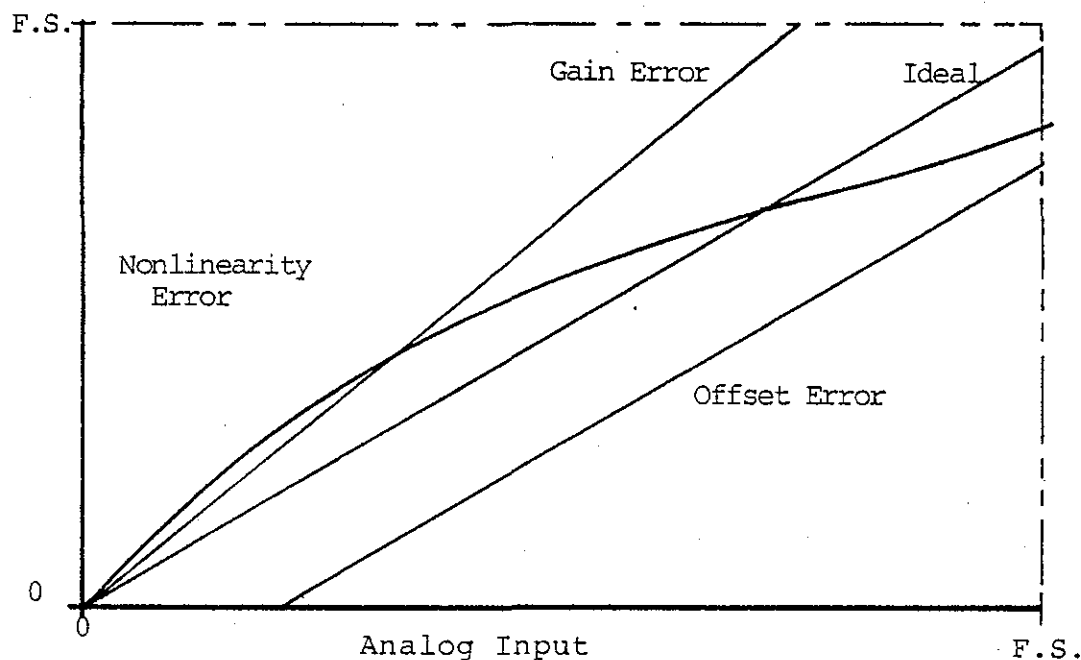


Fig. 4-12 GAIN, OFFSET AND LINEARITY ERRORS

adjustment available at the analog to digital converter. There will therefore be no appreciable net gain error due to the analog subsystem.

#### 6) Nonlinearity Error

Nonlinearity error is apparent in the sample and hold circuit if the transfer function departs from a linear curve (Fig. 4-12). In the noninverting unity gain mode with a 0.001  $\mu\text{f}$  holding capacitor the maximum nonlinearity is 0.01% resulting in a worst case signal uncertainty of  $(.0001) \times 2.5 \text{ Volts} = 25 \text{ mV}$ .

#### 7) Hold Mode Feedthrough

This error appears due to input signal appearing at the output when the unit is in the hold mode. Although the

feedthrough varies with signal frequency and the expected signal frequencies are substantially lower than the upper frequency limits of the sample and hold device (30 Hz max. versus several kiloHertz), we consider the worst case feedthrough of 0.01% [Ref. 4-10] or 25 mV.

#### D) Analog to Digital Converter Induced Errors

The A/D Converter selected for the solid state magnetic indicator instrument (Datel ADC-MA12B1B) [Ref. 4-11] uses the successive approximation technique to achieve excellent linearity and speed. Important parameters that potentially contribute errors are addressed below.

##### 1) Resolution Error

The smallest analog change that can be distinguished by the A/D converter is

$$\text{Least Significant Bit (LSB)} = \frac{\text{Full Scale}}{2^n}$$

$$\text{LSB} = \frac{5}{2^{12}} = 1.22 \text{ mV}$$

this uncertainty manifests itself as an error in computing by limiting the precision of any calculation.

##### 2) Linearity Error

The maximum deviation from a straight line drawn between the end points of the converter transfer function are specified in [Ref. 4-11] to be  $\pm 1/2$  LSB (in our case  $\pm 1.22$  mV of analog signal).

### 3) Accuracy Error

The input to output error of the A/D converter is specified in [Ref. 4-11] to be  $\pm 0.012\%$  F.S.  $\pm 1/2$  LSB or

$$\pm(0.00012) \times 5.00V \pm 1.22 \text{ mV} = \pm 1.82 \text{ mV Worst Case}$$

In reality, the two error terms are unrelated and the

$$\text{Rss Error} = \pm \left[ (.00012 \times 5V)^2 + (1.22\text{mV})^2 \right]^{1/2}$$

$$\text{RSS Error} = \pm 1.36 \text{ mV}$$

### 4) Offset Error and Gain Error

Both the offset error and gain error were adjusted to zero using the trimming potentiometers (Fig. 4-7) and the calibration procedure outlined in Ref. 4-11. A reference signal of plus  $1/2$  LSB (1.22 mV) was applied to the converter and the offset trimming potentiometer adjusted until the output flickered equally between logic "0" and logic "1". The gain was then adjusted by setting the converter input to full scale minus  $1-1/2$  LSB (4.99817 Volts) and the gain trimming potentiometer was adjusted until the output flickered between logic "111...110" and logic "111...111". The above steps were repeated until no appreciable error in gain or offset was evident.

#### 4-4 PROCESSING ERRORS

Errors in processing data accrue due to several sources including imprecision and truncation. Since the microprocessor selected for the instrument is inherently an eight bit device, single precision calculations are conducted with eight bits and double precision calculations are conducted with a total



of sixteen bits. This section addresses the effects of computational precision and truncation in the various subroutines and relates these to overall computational accuracy. The various subroutines are analyzed in chronological order as they appear in the main program.

A) Subroutine "SAMP"

The sample subroutine (delineated in Fig. 3-6a) selects and digitizes analog signals by controlling respective analog subsystem modules. During the first portion of this subroutine, A/D converter data bits are stored in two consecutive bytes<sup>7</sup> in the computer memory. The A/D conversion precision of 12 bits is thereby preserved.

The second, third and fourth operations of the sample subroutine convert the unipolar binary format of the data to sign magnitude format, adds offset quantities and merely changes the signs of the Hx and Hy data. The operations are conducted in a double precision manner and precision of the data remains unaltered.

Correction of x axis orthogonality error is the final operation of the sample subroutine. Equation (3-1) is implemented at this point using a table lookup (for the sin function), multiplication and addition. The final result can be expressed as

$$Hx = Hx' + Hy \sin \epsilon$$

---

<sup>7</sup>A byte is accepted terminology for an eight bit data quantity.

where the respective quantities have the following forms

$$Hx^1 = x_1 + \sum_{i=1}^{11} a_i 2^i$$

$$Hy = x_2 + \sum_{j=1}^{11} a_j 2^j$$

$$\text{Sin } \epsilon = \sum_{k=1}^8 a_k 2^{-k}$$

and

$x_1, x_2$  are sign bits

$a_{i,j,k}$  equal 0 or 1 depending on whether the respective term is to exist or not

We can analyze the effects of imprecision and truncation by noting that the sin function has eight significant binary bits resulting in a resolution of  $1/256$  or  $90^\circ/256 = 0.352^\circ$ .

The relative error in  $\text{sin } \epsilon$  is computed by Dahlquist [Ref. 4-12] as follows

let  $\tilde{a}$  = the approximate value of  $\text{sin } \epsilon$   
 $a$  = the exact value of  $\text{sin } \epsilon$

then the relative error in  $\tilde{a}$  is

$$(\tilde{a} - a)/a \text{ if } a \neq 0$$

Since data in the sin table has been truncated, maximum relative error can be as large as  $\pm(1/2^{12})$  or  $\pm 0.02\%$ .

From the definition of relative error we obtain the following relationships between exact, estimate and estimated

relative error

$$\tilde{a} = a + ar = a(1 + r)$$

If  $a_1$ , and  $a_2$  have relative errors of  $\pm 0.39\%$  and  $\pm 0.02\%$ , respectively, then

$$\begin{aligned}\tilde{a}_1 \tilde{a}_2 &= a_1(1 \pm 0.0039) a_2(1 \pm 0.00024) \\ &= a_1 a_2 (1 \pm 0.0039)(1 \pm 0.00024)\end{aligned}$$

Thus, the relative error in  $\tilde{a}_1 \tilde{a}_2$  is

$$\begin{aligned}(1 \pm 0.0039)(1 \pm 0.00024) - 1 &= \\ \pm(0.0039) \pm(0.0039)(0.00024) \pm(0.00024) & \\ \approx \pm(0.0041) &\end{aligned}$$

Since the maximum value of  $\sin \epsilon$  to be encountered occurs when the orthogonality error ( $\epsilon$ ) is 1 degree,  $\sin \epsilon = 0.017$  maximum. The maximum value for  $H_y$  can be 0.6 gauss or 2048 units. Maximum error due to imprecision in the product  $H_y \sin \epsilon$  is then

$$\begin{aligned}Er \text{ Max} &= (2048 \times 0.017)(1 + .0041) - (2048 \times 0.017) \\ &= 0.1427 \text{ units}\end{aligned}$$

Since only the integer portion is retained in the final product, insignificant error can be attributed to imprecision of the  $\sin \epsilon$  term in this case. Orthogonality error will be adequately corrected.

B) Subroutines ROTX and ROTY

These subroutines were developed in Chapter III and implement the equation of 2-11 required to compute horizontal

0-2

x and y magnetic field components. Equations to be implemented by the respective subroutines are

$$\begin{aligned} H_x = & H_{xm} \cos(\text{pitch}) + H_{ym} \sin(\text{pitch}) \sin(\text{roll}) \\ & + H_{zm} \sin(\text{pitch}) \cos(\text{roll}) \end{aligned} \quad (4-12)$$

and

$$H_y = H_{ym} \cos(\text{roll}) - H_{zm} \sin(\text{roll}) \quad (4-13)$$

where  $H_{xm}$ ,  $H_{ym}$  and  $H_{zm}$  are measured field components made available from the magnetometer via the analog subsystem.

Since the transcendental functions are implemented using table lookup and are limited in precision to 8 bits, imprecision in these variables will dominate in generating error. In particular, the sin/cos terms will have relative error in the order of  $\pm 1/256$  or  $\pm 0.39\%$  while the measured field data has relative uncertainty of only  $\pm 1/4096$  or  $\pm 0.02\%$ . Multiplications will result in addition of the bounds for the relative error as illustrated in section 4-4A above.

The transcendental terms above are limited in magnitude to 1.0 maximum while the field measurements can be 0.60 gauss max. In this case the individual product terms of (4-12) and (4-13) can have maximum errors of

$$E_r = (2048)(1 + 0.0041) - (2048) = 8.4 \text{ units}$$

Errors in  $H_y$  and  $H_x$  (4-12 and 4-13) will be maximum when roll and pitch are at 45 degrees and the fields are equal. In this case the error in  $H_y$  will be

$$E_{Hy} = [(0.707)(2048)(1 + 0.0041) - (0.707)(2048)] - [(0.707)(2048)(1 - 0.0041) - (0.707)(2048)]$$

$$E_{Hy} = 4.94 - 5.94 = 11.87 \text{ units}$$

Similarly, maximum error in Hx can be calculated as

$$E_{Hx} = [(0.707)(2048)(1.0041) - (0.707)(2048)] \times 3$$

$$E_{Hx} = 17.8 \text{ units maximum}$$

It should be noted that these error terms are worst case and peak at multiples of 45 degrees in yaw.

### C) Subroutines COSY and SINY

These two subroutines compute the angle between the x axis sensor (when projected onto the horizontal plane) and the north-south horizontal vector of earth's magnetic field. The first two operations of these subroutines perform double precision multiplication and division. Since the data variables involved are 12 bits in length and the computations performed preserving 16 bits, no error is introduced.

The "ANGL" subroutine called by the above two subroutines computes the desired (x axis to horizontal vector) angle by completing an associative table look up procedure. The task required is to match a given data quantity either  $(Hx^2/Hh^2)$  or  $(Hy^2/Hh^2)$  with the contents of a memory cell. The address of this cell is then the required angle.

Since the table is limited in precision to 16 bits there are obviously cases where an interpolation is required to

ascertain the true address<sup>9</sup>. The function stored in tabular form is  $\cos^2\theta$  where  $\theta$  varies from 45 to 90 degrees. Maximum error will therefore be induced while attempting to locate solutions (angles near 90 degrees if inadequate precision is provided. Error in this region due to resolution of tabular data can be examined by noting the entries in Table 4-8

$\theta$	$\cos^2\theta$	Most Significant Binary Bit ( $2^{-X}$ )
90	0	-
89	0.000305	12
88	0.001218	9
87	0.00274	8

Table 4-8  $\cos^2\theta$  AND MOST SIGNIFICANT BINARY DIGITS

provided to indicate the relative magnitudes of  $\cos^2\theta$  in the region of  $\theta = 90$  degrees. We observe that the most significant binary digit affected at 89 degrees is binary decimal digit 12 implying that the resolution of  $H_x^2/H_h^2$  or  $H_y^2/H_h^2$  (the argument of  $\cos^2\theta$ ) must be accurate to at least  $1/2^{12}$  or 0.024%.

Considering the horizontal field of earth's magnetic vector as observed in laboratory experimentation at this latitude, we note that  $H_h$  is 730 units. At a heading of 89 degrees,  $H_x = 730 \cos 89 = 12.7$  units. The argument would therefore be

$$\text{ARG} = H_x^2/H_h^2 = \frac{(12.7)^2}{(730)^2} = 0.000305$$

<sup>9</sup>The procedure determines the relative address by linear interpolation, then selects the closest address as the required angle for the solution.

Since, the squaring and division operations are conducted in double precision, precision is preserved and the algorithm should be able to resolve heading to at least one degree over all portions of the compass.

#### D) Errors Due to the Remaining Subroutines

Since all of the remaining subroutines work with data that has been rounded to a precision representing 1 degree or better and the computations involve addition or subtraction in double precision binary or binary coded decimal (BCD) format, we note that there will be no further appreciable error due to truncation or rounding.

#### 4-5 MEASUREMENT ERROR SUMMARY

Errors due to sensors and measurement of their respective outputs were discussed in sections 4-2 and 4-3 above. Before proceeding with the analysis of errors, the total signal inaccuracy due to contribution from the many sources above will be summarized in Table 4-10. Total instrument error can then be computed by considering the propagation and enhancement of these errors during the computation process.

Since the errors in Table 4-9 are stochastically independent, we can compute error for any given signal level by finding the RSS of respective error sources. In this manner, the instrument error can be evaluated by considering all input signals with errors superimposed to produce an erroneous computation of heading.

PARAMETER	ERROR	COMMENT
1. Magnetometer		
Offset	≈0	Corrected by software
Orthogonality	≈0	Corrected by software
Noise	Negligible	
Gain	+0.01%	Proport. to signal level
Linearity	±0.01%	
2. Analog Subsystem		
Sampling	Negligible	Sampling rate & filtering adequate
Multiplexer		
Transfer Accuracy	±0.01%	Proport. to signal level
Settling Time	≈0	
Rate	≈0	
Input Leakage	≈0	
Sample and Hold		
Acquisition	≈0	
Hold	4mV	
Aperture Delay	≈0	
Offset	≈0	Corrected by software
Gain	≈0	Corrected by software
Nonlinearity	+0.01%	Proport. to signal level
Feedthrough	±0.01%	Proport. to signal level and frequency
A/D Converter		
Resolution	+1.2mV	
Accuracy	±1.4mV	
Offset	≈0	
Gain	≈0	

Table 4-9 SENSOR AND ANALOG SUBSYSTEM ERROR SUMMARY



## 4-6 SAMPLE ERROR ANALYSIS

Orthogonality correction using the algorithmic method can be verified by computing expected error prior to correction and comparing measured system output with the error prediction. Assuming that the angle between the x and y sensors exceeds 90 degrees as in Fig. 4-13, we can proceed to compute error by noting the following relationships

$$\begin{aligned} H_x &= H_h \cos(+\psi) \\ H_y &= H_h \sin(\psi) \\ H_{x_1} &= H_x \cos \epsilon - H_y \sin \epsilon \\ \text{True Yaw} = \psi_T &= \cos^{-1} \left( \frac{H_x}{(H_x^2 + H_y^2)^{\frac{1}{2}}} \right) \end{aligned}$$

Computed yaw

$$\begin{aligned} \psi_m &= \cos^{-1} \left[ \frac{H_x \cos \epsilon - H_y \sin \epsilon}{(H_x \cos \epsilon - H_y \sin \epsilon)^2 + H_y^2)^{\frac{1}{2}}} \right] \\ &= \cos^{-1} \left[ \frac{H_h \cos \psi \cos \epsilon - H_h \sin \psi \sin \epsilon}{[(H_h \cos \psi \cos \epsilon - H_h \sin \psi \sin \epsilon)^2 + H^2 h \sin^2 \psi]^{\frac{1}{2}}} \right] \end{aligned}$$

Using small angle approximations with  $\epsilon \approx 0.79^\circ$

$$\cos \epsilon \approx 1 \text{ and } \sin \epsilon \approx 0.014$$

then

$$\psi_m = \cos^{-1} \left[ \frac{H_h \cos \psi - 0.014 \sin \psi}{[H_h^2 (\cos \psi - 0.014 \sin \psi)^2 + H_h^2 \sin^2 \psi]^{\frac{1}{2}}} \right]$$

Computed error

$$\text{Error} = \psi_m - \psi$$

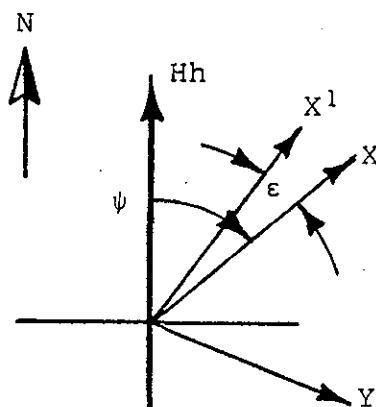


Fig. 4-13 ANGLE (X - Y) &gt; 90°

We can now evaluate computed yaw angle ( $\psi_m$ ) given a particular yaw ( $\psi$ ) and the horizontal field vector (Hh). Heading error for horizontal field vector of 730 units at various yaw angles with pitch and roll angles of zero degrees is tabulated in Table 4-10 and plotted along with actual measured yaw error (data taken during experimentation of Chapter V) in Fig. 4-14.

Heading (Degrees)	Computed Error (Degrees)	Heading (Degrees)	Computed Error (Degrees)
90	0.8	290	0.7
70	0.7	270	0.8
50	0.5	250	0.7
30	0.2	230	0.5
10	0.0	210	0.2
350	0.0	190	0.0
330	0.2	170	0.0
310	0.5	150	0.2
		130	0.5

Table 4-10 COMPUTED HEADING ERROR WITH Hh = 730 UNITS

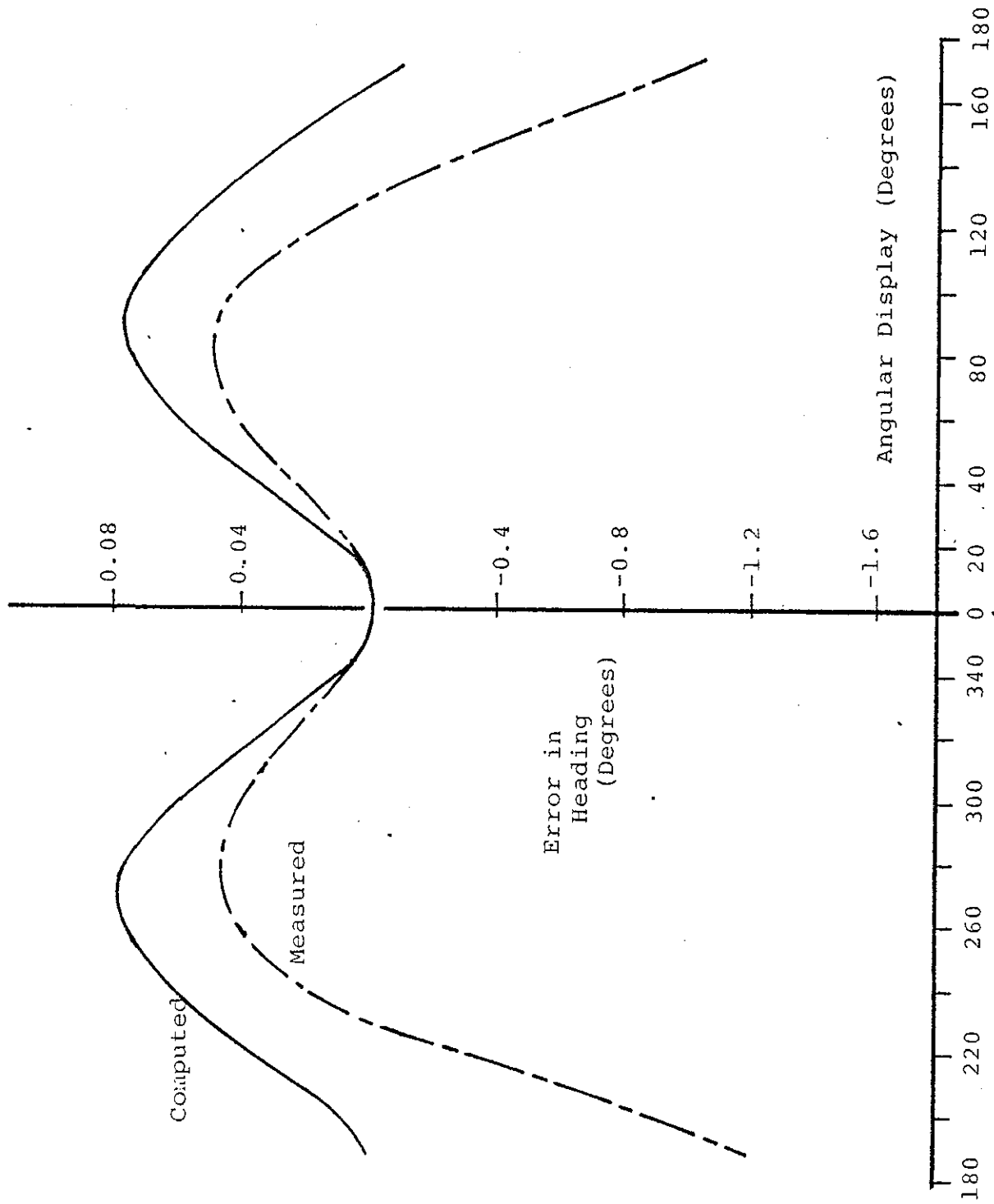


Fig. 4-14 COMPARISON OF COMPUTED AND MEASURED ORTHOGONALITY INDUCED ERROR

#### 4-7 CONCLUSIONS

The preceding error analysis has identified potential error sources along with relative magnitudes of error to be expected. Magnetometer sensor and analog subsystem errors were identified and analyzed individually. During this analysis it became apparent that errors due to sensor offset and nonorthogonality dominated and would severely limit total instrument performance. The relative magnitudes of these errors and their mode of contribution would have degraded system capacity.

By carefully characterizing the offset and orthogonality error it was determined that these systematic errors could be reduced by appropriate programming. A need to identify the extent of each error unique to the laboratory instrument imposed a need to evaluate the instrument empirically. Using earth's magnetic field and the laboratory test fixture (described in Chapter V) to provide control inputs each of the parameters was identified and measured. An algorithm with the empirically determined correction coefficients was included in the final system to reduce the error and to improve final system performance. The remaining potential error sources were tabulated and relative magnitudes noted.

Processing errors due to register precision and truncation were analyzed by considering pertinent subroutines individually. It was noted that the relative error bounds add when multiplying variables with relative error. In addition, it was noted that error accrued during processing is proportional to sensor signal levels involved. The final uncertainty is then proportional to actual aircraft attitude with error increasing as displacement from level flight occurs. Computational error is also noted to increase at particular headings causing the error function to peak at specific yaw angles.

The sample error analysis clearly shows that a correlation between sensor nonorthogonality induced error and measured (uncorrected) data exists. By predicting and computing an error function prior to experimentally verifying the result we gain confidence that the sensor characteristics derived empirically in previous sections are correct.

## CHAPTER V

LABORATORY EVALUATION OF THE ATTITUDE INDEPENDENT  
REMOTE MAGNETIC INDICATOR AND HEADING INSTRUMENT

## 5-1 INTRODUCTION

This chapter addresses laboratory evaluation of the microprocessor based computer designed to implement the heading measurement instrument. An integral part of this instrument was the three axis fluxgate magnetometer used to implement the attitude independent remote magnetic indicator of Chapter II. The laboratory evaluation was designed to investigate empirically the effects of physical parameters that would otherwise be impossible to assess.

Although phenomena such as noise, magnetic field gradient, sensor orthogonality errors and offset errors can be predicated, combined effects on the proposed instrument and remote magnetic indicator are best evaluated in the laboratory. In addition, it was noted that errors due to sensor offset and nonorthogonality could be corrected by software included with the sample subroutine. Determination of the effectiveness of this correction technique necessitated laboratory measurements of the errors (to determine correction constants) and comparison of data prior to and following corrections.

The chapter begins by discussing laboratory test apparatus designed to evaluate the instrument. Actual data measured and recorded during experimentation is then presented in both tabular and graphic form to facilitate comparison and evaluation. Finally, the laboratory data is discussed and it is concluded that the remote magnetic indicator used with the heading measurement instrument results in a viable alternative to conventional heading measurement systems. The microprocessor based

computer implementation of the instrument has added unique sensor measurement correction ability that enhances performance of otherwise marginal sensors. In this manner limitations in systems performance that now exist due to sensor inadequacy can be minimized without incurring the burden of using more expensive sensors.

## 5-2 TEST APPARATUS

### A) Electronic Subsystem

The microprocessor based computer (illustrated in photos 5-1 and 5-2) was constructed on printed circuit boards consisting of a central processing card, two memory cards (2K bytes capacity each) and an output board. A separate analog subsystem card contained the multiplexer, sample and hold, analog to digital converter and trimming potentiometers. The circuit cards were all organized with edge connectors and mounted vertically into a hand wired backplane assembly as shown in photos 5-1 and 5-2.

The card in the left foreground of photo 5-1 served as the output display with three seven-segment displays displaying significant figures of system heading. A small printed circuit in the right foreground of photo 5-1 contained potentiometers used to generate analog signals proportional to roll and pitch signals (simulating gyroscope outputs). Cards shown vertically mounted in photo 5-2 can be identified from right to left as the analog subsystem, two memory cards and the central processing card. The large integrated circuit shown on the CPU card is the Signetics 2640 microprocessor.

### B) Sensor Assembly

To evaluate the effects of combined aircraft pitch, roll

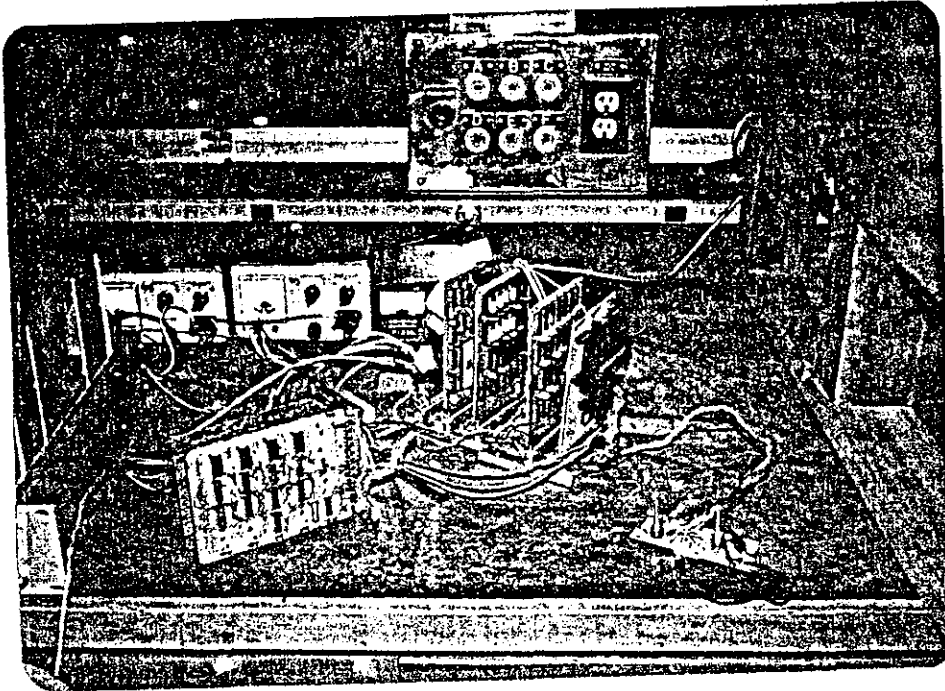


Photo 5-1 MICROPROCESSOR BASED HEADING COMPUTER

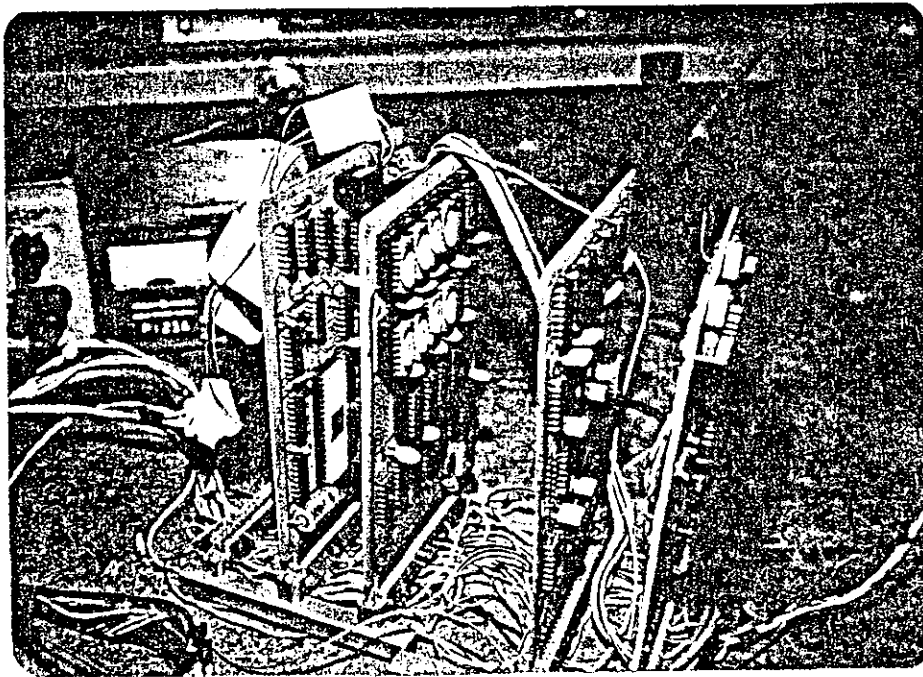


Photo 5-2 CENTRAL PROCESSOR, MEMORY AND  
ANALOG SUBSYSTEM



and yaw a three axis gimbal apparatus was required. In addition, since angular measurements were required, a means of measuring angular rotation in each of the three axes was provided. The gimbal apparatus as illustrated in photos 5-3 and 5-4 was fitted with large protractors centered on the rotation axes. Pointers were provided to enable angular rotation measurements on the respective protractor scales. Since the angular precision on each protractor scale resolved angular position to 0.5 degrees, angular measurements to a resolution of at least 0.5 degrees were possible. Angular position was measured by estimating the decimal place of each measurement with accuracy to  $\pm 0.5$  degrees ensured.

Since the three axis magnetometer (housed in the rectangular block of photos 5-3 and 5-4) measured ambient magnetic fields the test apparatus was constructed of nonferrous material. This ensured that local fields due to residual magnetic fields in the test apparatus would be minimized. In addition, since the material had low permeability, there would be little deformation of the local field causing error due to changing field gradient.

The sensor package shown in photos 5-3 and 5-4 was physically mounted such that the sensors were centered as close to the center of the gimbal as possible. This precaution ensured that measurement error due to sensor translation was minimized<sup>1</sup>. During instrument evaluation, the entire gimbal assembly and sensor were leveled and mounted in a Helmholtz coil assembly as illustrated in photo 5-5. Although the coils were not activated during experimentation, the rotations in heading were

---

<sup>1</sup>Since the local magnetic field has a nonzero gradient, field measurements include a component due to translation of the sensor axes. This component of measurement produces unacceptable error in a system designed to measure field components that change due to rotation.

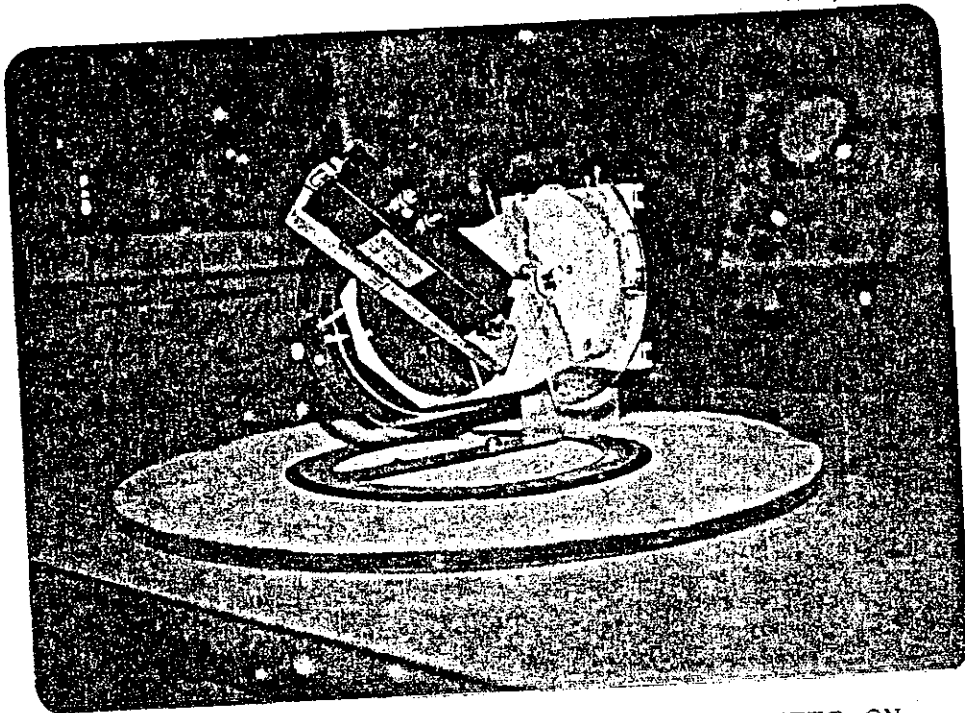


Photo 5-3 MAGNETOMETER SENSOR MOUNTED ON  
GIMBALLED TEST FIXTURE

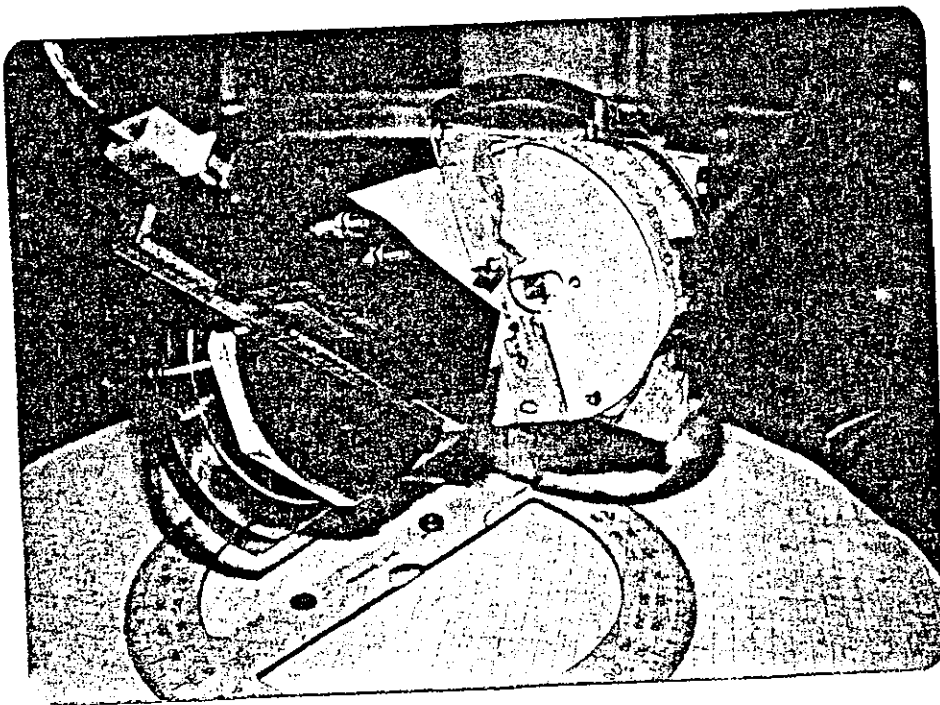


Photo 5-4 SENSOR AND GIMBAL ASSEMBLY WITH PROTRACTORS

carefully controlled since the gimbal assembly was an integral part of the Helmholtz coil fixture with the vertical rotation axis serving as the system yaw axis.

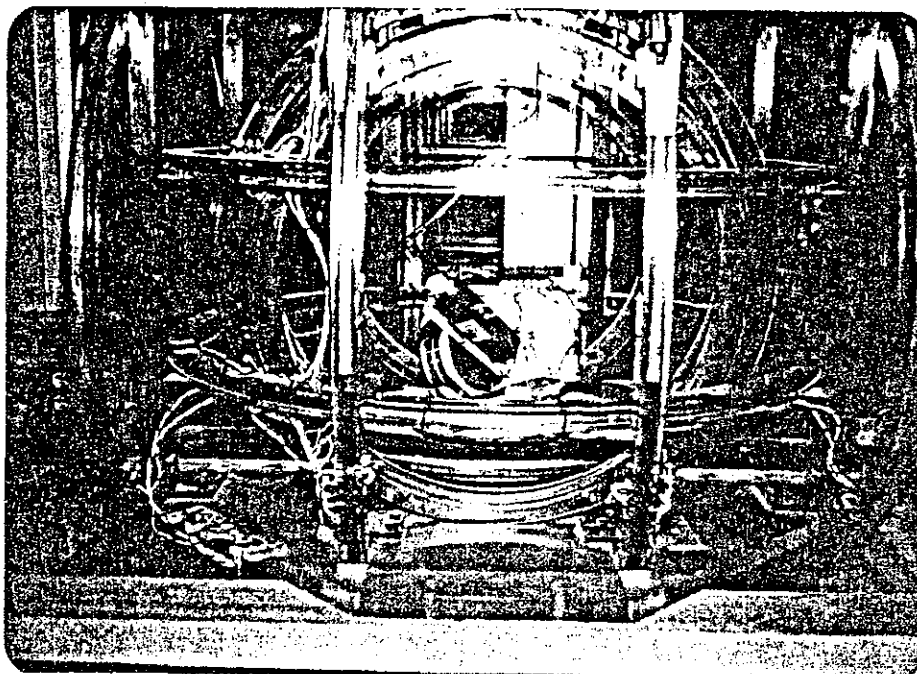


Photo 5-5 TEST FIXTURE MOUNTED IN HELMHOLTZ COIL ASSEMBLY

### 5-3 HEADING MEASUREMENTS WITH NO OFFSET CORRECTION

By maintaining heading of the test fixture constant (no rotation about the vertical axis) and varying both pitch and roll angle, the instrument display was observed to vary. This variation gave a direct measure of instrument error since a constant heading was maintained and a constant display was to be expected.

Data variations were recorded in Tables 5-1 and 5-2 and plotted on Figures 5-1 and 5-2. With only  $\pm 10$  degree variation in pitch combined with  $\pm 30$  degree variation in roll we note that the heading display varies 14 degrees. Obviously,

Roll Angle (Degrees)	$\theta = 0^\circ$	$\theta = 10^\circ$	$\theta = -10^\circ$
-30	000	353	4
-20	000	354	2
-10	359	357	0
0	359	359	358
10	359	000	355
20	358	002	354
30	358	004	353

Table 5-1 HEADING COMPUTED AT A FIXED YAW ANGLE  
WITH NO OFFSET CORRECTION

Roll Angle (Degrees)	$\theta = 0^\circ$	$\theta = 10^\circ$	$\theta = -10^\circ$
-30	46	52	38
-20	45	49	41
-10	45	47	43
0	45	45	43
10	45	43	46
20	44	42	47
30	44	41	49

Table 5-2 HEADING COMPUTED AT A FIXED YAW ANGLE  
WITH NO OFFSET CORRECTION

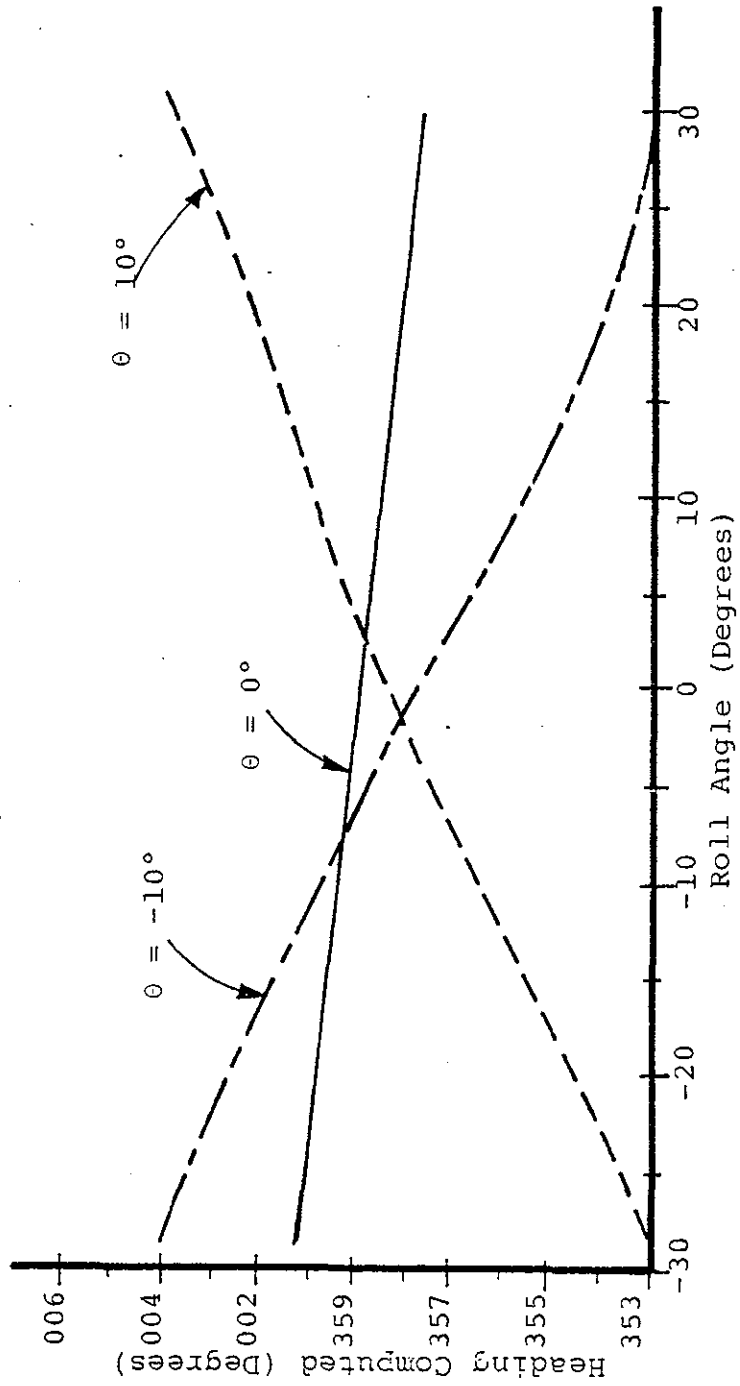


Fig. 5-1 HEADING COMPUTED AT A FIXED YAW ANGLE WITH VARYING  $\theta$  AND  $\phi$  (NO OFFSET CORRECTION)

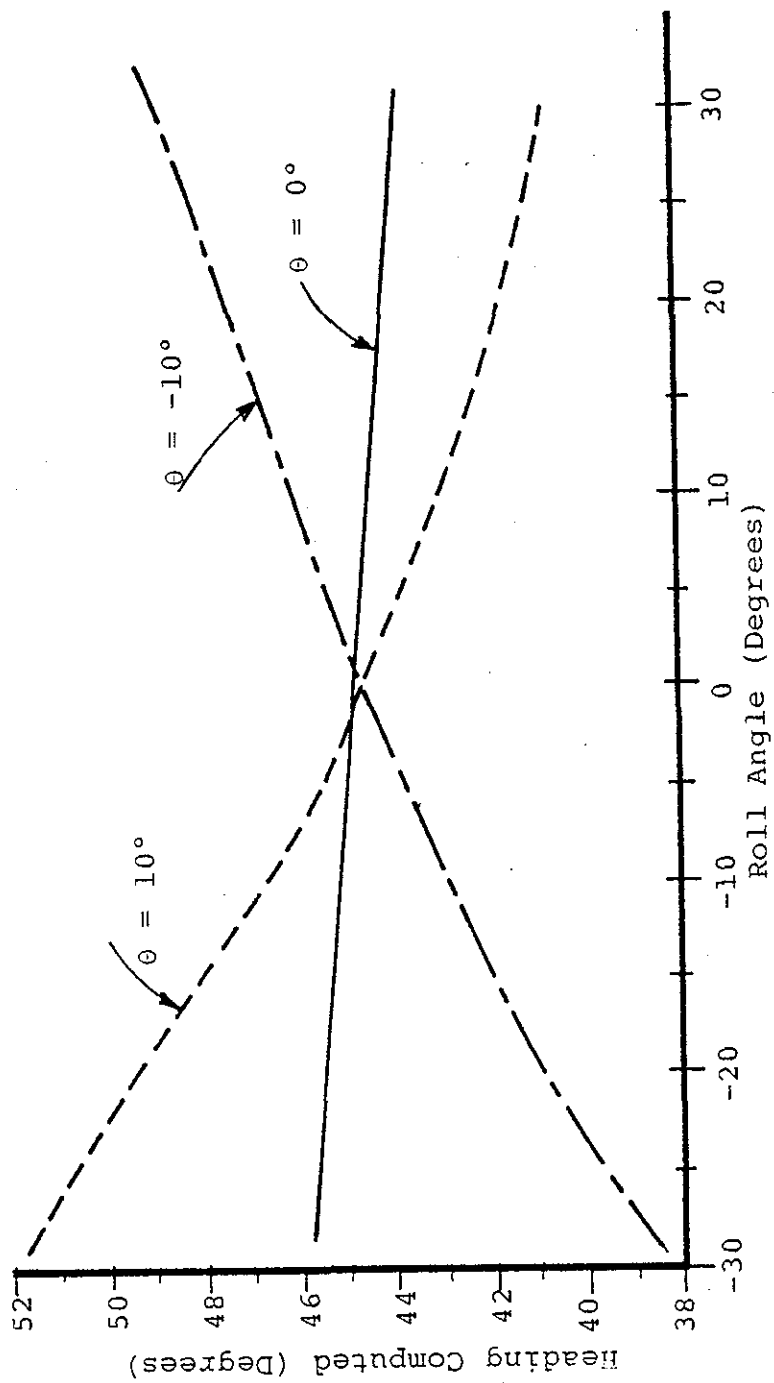


Fig. 5-2 HEADING COMPUTED AT A FIXED YAW ANGLE WITH VARYING  $\theta$  AND  $\phi$  (NO OFFSET CORRECTION)

instrument operation indicated excessive error requiring more elaborate sensors or correction of a sensor inadequacy.

#### 5-4 HEADING MEASUREMENTS TO INVESTIGATE ORTHOGONALITY ERROR

System performance was evaluated by initially aligning the sensors with zero pitch and roll angle. Sensor Z was positioned vertically with positive direction downwards. By observing the Z axis output<sup>2</sup> as the test fixture was rotated about the vertical axis, adjustments were made in pitch and roll angle to minimize coning of the Z axis. Angular measurements on the respective roll and pitch axis protractors were then made to establish the initial reference attitude angles.

Heading measurement accuracy was evaluated by rotating the test fixture in the horizontal plane until the display flickered between (XX9) and (XX9+1). The rotation was then continued a very small amount until a steady display (multiple of 10 degrees) was observed<sup>3</sup>. Measurements ranging from 0 to 350 degrees were made by recording angular position required to produce specific heading data displays. Sets of data were recorded at various combinations of pitch and roll then tabulated in Tables 5-3 through 5-8. Relative error was computed by determining angular position expected at each display value and then computing the difference in angular positions. Errors at the roll extremes of  $\pm 44$  degrees are plotted for pitch angles of plus and minus 20 degrees on Fig. 5-3 through 5-6 inclusive.

---

<sup>2</sup>A special subroutine was used to display Z axis data directly in BCD format on the seven bar output display.

<sup>3</sup>This measurement technique ensured that all heading measurements were made identically. In addition, error due to system imprecision was reduced.

Data in Tables 5-5, 5-6 and Fig. 5-3, 5-4 were recorded with no sensor orthogonality error correction implemented. Data in Tables 5-7, 5-8 and Fig. 5-5, 5-6 was recorded with the sensor orthogonality correction implemented. Comparison of these data indicate that considerable improvement in accuracy is achieved by correcting sensor orthogonality error.

#### 5-5 CONCLUSIONS

Laboratory evaluation of the heading measurement instrument has shown that the algorithms developed in previous chapters are viable. Operation of the device in a laboratory environment has enabled empirical evaluation of the system under adverse combinations of noise, field gradient and sensor plus instrument error sources.

Test apparatus described in section 5-2 served to enable controlled simulation of roll, pitch and yaw rotations. The apparatus was nonmagnetic in nature and contributed insignificant error due to field perturbation. Mounting of protractors and pointers on the test apparatus made angular measurements possible to a precision of at least  $\pm 0.5$  degrees.

Effects of sensor offsets were evaluated in section 5-3 by recording system heading computations when only roll and pitch varied. Since the variations in Figures 5-1 and 5-2 prior to offset correction exceed the maximum excursions of Figures 5-3 and 5-4 by at least a factor of two (angular excursions in first set also less than in the record) and we note that offset errors were corrected prior to recording data in the second set of data, we conclude that offset in magnetometers can be a



PITCH ANGLE 0 DEGREES  
 ROLL ANGLE 0 DEGREES

Heading Displayed (Degrees)	Angular Position (Degrees)	Relative Error (Degrees)
10	275.3	0.3
30	295.2	0.2
50	315.4	0.4
70	335.5	0.5
90	355.5	0.5
130	34.8	-0.2
150	54.3	-0.7
170	74.0	-1.0
190	94.0	-1.0
210	114.4	-0.6
230	135.0	0.0
250	155.5	0.5
270	174.7	-0.3
290	195.5	0.5
310	215.2	0.2
330	235.2	0.2
350	254.7	-0.3

Table 5-3 REFERENCE DATA MEASUREMENTS OF HEADING  
 TAKEN WITH NO ORTHOGONALITY CORRECTION

PITCH ANGLE 0 DEGREES

ROLL ANGLE 0 DEGREES

Heading Displayed (Degrees)	Angular Position (Degrees)	Relative Error (Degrees)
10	276.6	-0.4
30	296.6	-0.4
40	306.7	-0.3
50	316.7	-0.3
60	327.2	+0.2
70	337.0	0.0
90	355.9	-1.1
130	37.0	0.0
160	67.2	0.2
190	96.8	-0.2
220	126.9	-0.1
250	157.0	0.0
280	186.9	-0.1
310	216.6	-0.4
340	246.9	-0.1
350	256.4	-0.6

Table 5-4 HEADING MEASUREMENTS WITH OFFSET AND  
ORTHOGONALITY CORRECTIONS MADE

Heading Displayed (Degrees)	Roll = 44°		Roll = 20°		Roll = -20°		Roll = -44°	
	Angular Position	Error	Angular Position	Error	Angular Position	Error	Angular Position	Error
10	276.3	1.3	276.5	1.5	275.0	0.0	274.0	-1.0
30	296.3	1.3					293.6	-1.4
40			306.1	1.1	304.0	-1.0		
50							313.8	-1.2
60	325.8	0.8						
70			335.6	1.6	334.3	-0.7	333.8	-1.2
90	355.0	0.0	354.0	-1.0	353.1	-1.9	353.0	-2.0
130	34.3	0.7	34.3	-0.7	34.6	-0.4	34.4	-0.6
160	64.5	-0.5	64.0	-1.0	65.0	0.0	65.0	0.0
190	94.3	-0.7	94.6	-0.4	95.0	0.0	95.5	0.5
220	125.2	0.2	125.3	0.3	126.0	1.0	126.5	1.5
250	156.6	1.6	156.2	1.2	156.7	1.7	157.0	2.0
280	186.6	1.6	186.8	1.8	186.5	1.5		
310	216.8	1.8	216.8	1.8	215.9	0.9	215.9	0.9
340	246.0	1.0	246.8	1.8	245.0	0.0		
350							224.9	-0.1

TABLE 5-5 HEADING MEASUREMENTS AT PITCH = 20° WITH NO ORTHOGONALITY CORRECTION

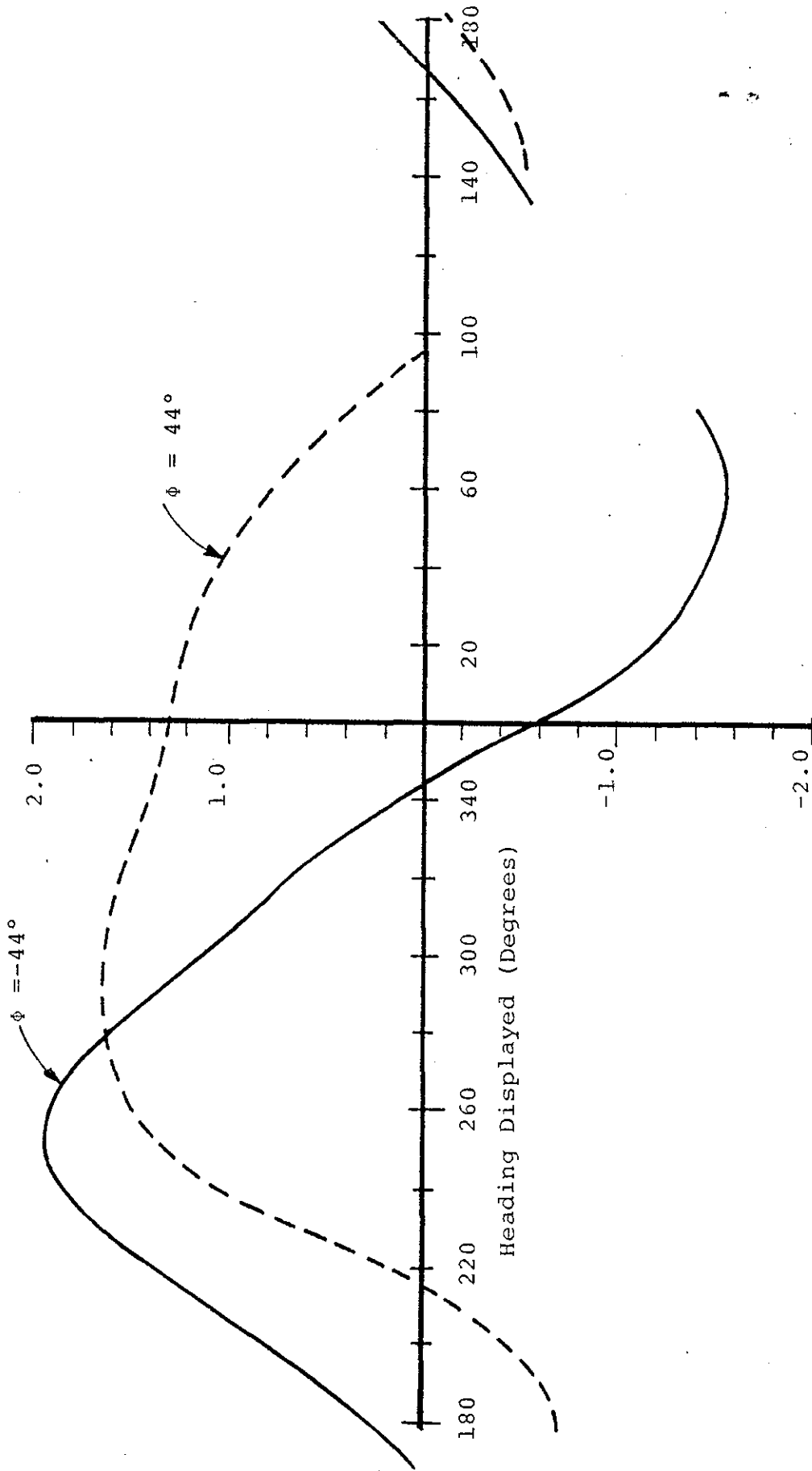


Fig. 5-3 HEADING MEASUREMENT ERROR AT PITCH = 20°  
(NO ORTHOGONALITY CORRECTION)

REPRODUCIBILITY OF THE ORIGINAL PAGE IS POOR

Heading Displayed (Degrees)	Roll = 44°		Roll = 20°		Roll = -20°		Roll = -44°	
	Angular Position	Error	Angular Position	Error	Angular Position	Error	Angular Position	Error
10	276.1	1.1	275.1	0.1	274.2	-0.8	273.7	-1.3
30	296.2	1.2	295.9	0.9			293.6	-1.4
50	316.4	1.4	316.1	1.1			314.1	-0.9
70	336.5	1.5	336.4	1.4	335.5	0.5	334.6	-0.4
90	355.5	0.5	355.3	0.3	355.0	0.0	354.2	-0.8
130	36.0	1.0	36.4	1.4	135.7	0.7	135.7	0.7
150	55.3	0.3	55.9	0.9			55.8	0.8
170	74.5	-0.5	75.6	0.6			75.5	0.5
190	94.9	-0.1	95.3	0.3	95.5	0.5	95.5	0.5
210	115.0	0.0	115.4	0.4			115.6	0.6
220					125.5	0.5		
230	135.0	0.0	135.6	0.6			136.0	1.0
250	155.6	0.6	155.4	0.4	155.5	0.5	155.7	0.7
270	174.8	-0.2	174.8	-0.2			175.0	0.0
290	195.6	0.6	195.4	0.4			195.3	0.3
310	215.5	0.5	215.3	0.3	214.6	-0.4	214.5	-0.5
330	235.7	0.7	235.1	0.1			234.2	-0.8
350	255.6	0.6	255.2	0.2			253.8	-1.2

Table 5-6 HEADING MEASUREMENTS AT PITCH = -20° WITH NO ORTHOGONALITY CORRECTION

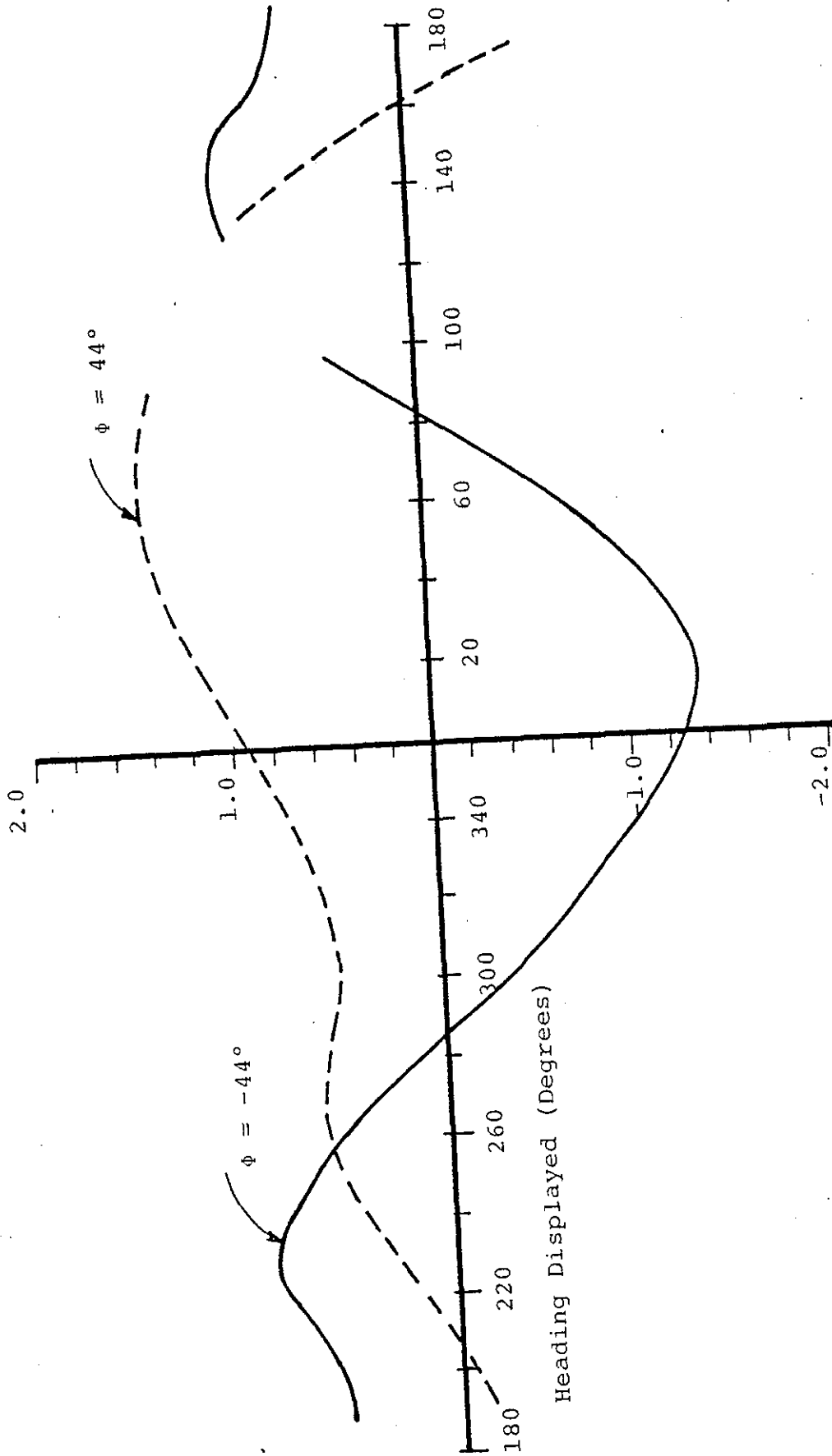


Fig. 5-4 HEADING MEASUREMENT ERROR AT PITCH =  $-20^\circ$   
(NO ORTHOGONALITY CORRECTION)

Heading Displayed (Degrees)	Roll = 0°		Roll = 44°		Roll = -44°	
	Angular Position	Error	Angular Position	Error	Angular Position	Error
20	287.3	0.3	287.5	0.3	286.3	-0.7
40	307.2	0.2	307.5	0.3	306.0	-1.0
60	327.0	0.0	327.9	0.7	325.9	-1.1
80	346.3	-0.7	347.5	0.3	345.6	-1.4
90	355.9	-1.1	357.0	0.2	356.2	-1.8
140	46.9	-0.1	47.0	-0.2	46.5	-0.5
160	67.0	0.0	67.3	0.1	67.1	0.1
180	86.6	-0.4	86.5	-0.7	87.0	0.0
200	107.0	0.0	107.3	0.1	108.1	1.1
220	127.6	0.6	127.3	0.1	128.3	1.2
240	147.2	0.2	147.4	0.2	148.5	1.5
260	167.0	0.0	167.1	-0.1	168.5	1.5
280	187.3	0.3	187.1	-0.1	188.5	1.5
300	207.2	0.2	207.1	-0.1	208.0	1.0
320	227.3	0.3	227.0	-0.2	227.5	0.5
340	247.4	0.4	247.3	+0.1	247.4	0.4
0	266.4	-0.6	267.0	-0.2	266.0	-1.0

Table 5-7 HEADING MEASUREMENTS AT PITCH = 20°  
WITH OFFSET AND ORTHOGONALITY CORRECTION  
MADE

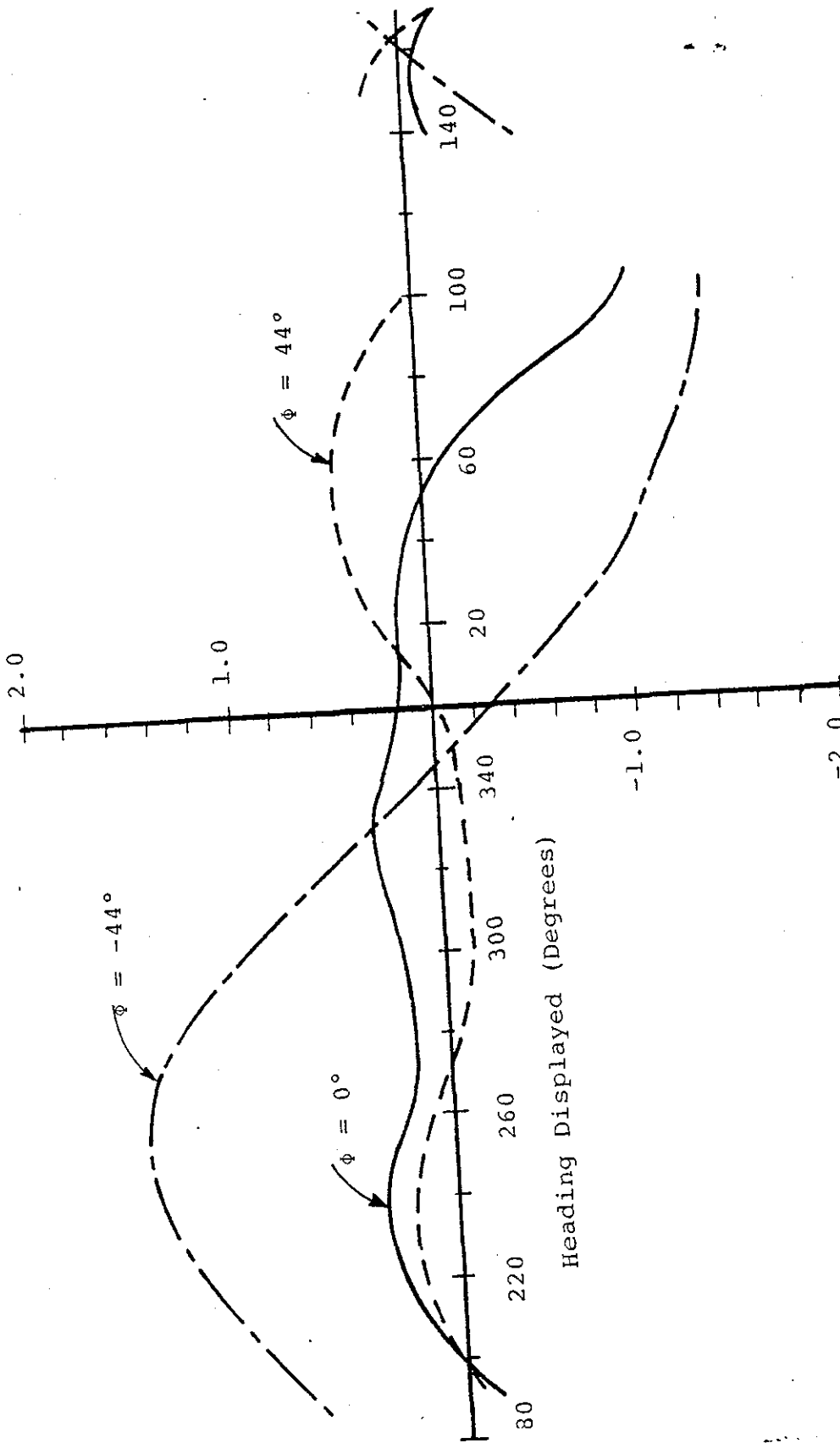


Fig. 5-5 HEADING MEASUREMENT ERROR AT PITCH - 20°  
(OFFSET AND ORTHOGONALITY ERROR CORRECTED)



Heading Displayed (Degrees)	Roll = 44°		Roll = -44°	
	Angular Position	Error	Angular Position	Error
20	287.0	-0.4	286.5	-0.3
40	307.0	-0.4	306.7	-0.1
60	327.0	-0.4	326.8	0.0
80	347.0	-0.4	346.8	0.0
90	356.7	-0.7	355.6	-0.2
140	47.8	0.4	48.0	1.2
160	67.7	0.3	68.0	1.2
180	87.0	-0.4	87.8	1.0
200	107.6	0.2	108.0	1.2
220	127.7	0.3	128.0	1.2
240	147.8	0.4	147.4	0.6
260	167.6	0.2	167.2	0.4
280	187.6	0.2	187.0	0.2
300	207.1	-0.3	206.5	-0.3
320	227.1	-0.3	226.6	-0.2
340	247.1	-0.3	246.9	0.1
0	266.3	-0.9	266.0	-0.8

TABLE 5-8 HEADING MEASUREMENTS AT PITCH = -20° WITH  
OFFSET AND ORTHOGONALITY ERROR CORRECTED

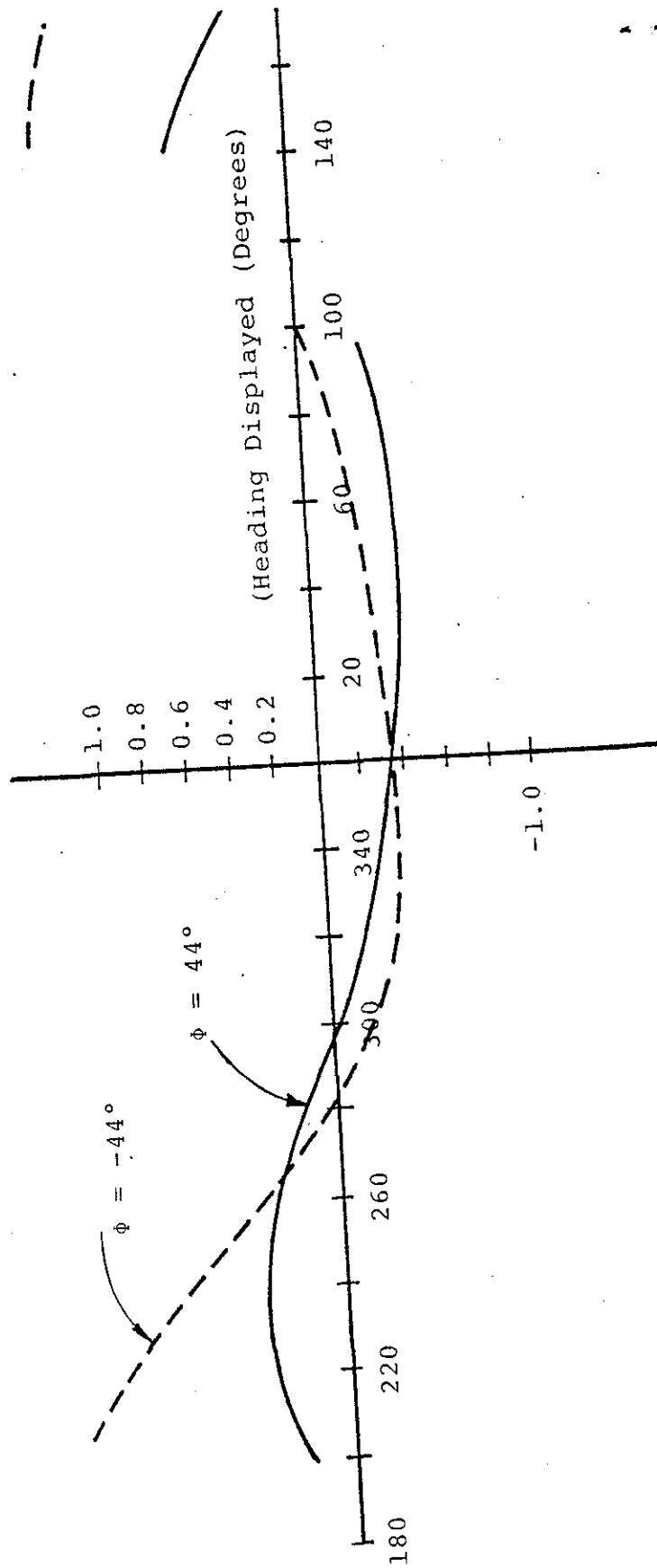


Fig. 5-6 HEADING MEASUREMENT ERROR AT PITCH =  $-20^\circ$   
(OFFSET AND ORTHOGONALITY CORRECTED)

major error source<sup>4</sup>. Additionally, we note that the correction of offset error in sensors has been successful. Experimental results have verified that not only can offset errors be determined (Chapter IV), but a suitable algorithm can be implemented in the computer to improve system operation. It is postulated that offset error correction can be extended to include correction of varying offset values (functions of temperature and supply voltage) by monitoring error causing variables (example temperature) and computing correction constants prior to offset correction as above.

Errors induced by sensor nonorthogonality were predicted in Chapter IV section 4-2 and verified by plotting expected error along with measured error in Fig. 4-14. The curves of Fig. 4-14 were plotted for heading rotations with no pitch or roll angle. To evaluate system performance and the effect of orthogonality error with combined angular rotations, measurements of heading error were plotted in Fig. 5-3 through 5-6 inclusive.

Comparison of these data indicate that maximum excursions of error as a function of heading are significantly less when orthogonality corrections are made. It is also postulated that data could be improved further by similarly correcting orthogonality error in the Z axis sensor<sup>5</sup>.

In summary, the experimental evaluation has provided insight into the operation of an attitude independent remote magnetic indicator and heading computer in the "real world"

---

<sup>4</sup>This corroborates the observations predicted during error analysis in Chapter IV.

<sup>5</sup>We note that the error excursions are functions of pitch and roll and that Z axis data is used in the rotation algorithm.

environment complete with all contributing error sources. The error analysis evolved during development of the system has proven adequate in that an operational system was developed. Major error sources were measurable as predicted and the means of reducing their effects were successfully implemented. Correction of sensor offset and orthogonality error required an empirical evaluation of the respective sensor. These evaluations were performed, the errors characterized, correction coefficients determined, and correction algorithms implemented.

Successful implementation of these corrections was evidenced by significant reductions in system error. The correction methods presented can be extended in future with the net result that less demand is required of physical sensors if the sensor parameters can be established empirically prior to completion of instrument design. Utilization of a microprocessor in the instrument has added the computational flexibility required to facilitate accommodation of sensors with varying error magnitudes.

## APPENDIX A

This appendix lists the instruction set of the Signetics 2650 microprocessor chip used to implement the heading instrument.

Instruction	Length (bytes)	Operation	Register	Condition	Notes
<b>LOAD/STORE INSTRUCTIONS</b>					
LODZ	1	Load Register Zero	r		
LODI	2	Load Immediate	v		
LODR	2	Load Relative	v		
LODA	3	Load Absolute	(*ja, X)		
STRZ	1	Store Register Zero	r		
STR	2	Store Relative	(*ja)		
STRA	3	Store Absolute	(*ja, X)		
<b>ARITHMETIC INSTRUCTIONS</b>					
ADDZ	1	Add to Register Zero	r		
ADDI	2	Add Immediate	v		
ADDR	2	Add Relative	v		
ADDA	3	Add Absolute	(*ja, X)		
SUBZ	1	Subtract from Register Zero	r		
SUBR	2	Subtract Relative	v		
SUBA	3	Subtract Absolute	(*ja, X)		
<b>LOGICAL INSTRUCTIONS</b>					
ANDZ	1	And to Register Zero	r		
ANDI	2	And Immediate	v		
ANDR	2	And Relative	v		
ANDA	3	And Absolute	(*ja, X)		
IORZ	1	Inclusive or to Register Zero	r		
IORI	2	Inclusive or Immediate	v		
IORR	2	Inclusive or Relative	v		
IORA	3	Inclusive or Absolute	(*ja, X)		
EOXZ	1	Exclusive or to Register Zero	r		
EOXI	2	Exclusive or Immediate	v		
EOXR	2	Exclusive or Relative	v		
EOXA	3	Exclusive or Absolute	(*ja, X)		
<b>COMPARISON INSTRUCTIONS</b>					
COMZ	1	Compare to Register Zero	r		
COMI	2	Compare Immediate	v		
COMR	2	Compare Relative	v		
COMA	3	Compare Absolute	(*ja, X)		
<b>ROTATE INSTRUCTIONS</b>					
RRR	1	Rotate Register Right	r		
RLR	1	Rotate Register Left	r		
<b>BRANCH INSTRUCTIONS</b>					
BCR	2	Branch on Condition True Relative	(*ja)		
BCFR	2	Branch on Condition False Relative	(*ja)		
BCRA	3	Branch on Condition True Absolute	(*ja, X)		
BCFA	3	Branch on Condition False Absolute	(*ja, X)		
BKR	2	Branch on Register Non-Zero Relative	(*ja)		
BKRA	3	Branch on Register Non-Zero Absolute	(*ja, X)		
BRR	2	Branch on Incrementing Register Relative	(*ja)		
<b>INPUT/OUTPUT INSTRUCTIONS</b>					
WRD	1	Write Data	r		
RED	1	Read Data	r		
WRC	1	Write Control	r		
REC	2	Read Control	r		
WRE	2	Write Extended	v		
REDE	2	Read Extended	v		
<b>MISCELLANEOUS INSTRUCTIONS</b>					
HALT	1	Halt, Enter Wait State			
DAR	2	Decimal Adjust Register	r		
TMR	2	Test Under Mask Immediate	v		
NOF	1	No Operation			
<b>PROGRAM STATUS INSTRUCTIONS</b>					
LPSU	1	Load Program Status, Upper	r		
LPSL	1	Load Program Status, Lower	r		
SPSU	1	Store Program Status, Upper	r		
SPSL	1	Store Program Status, Lower	r		
CPSU	2	Clear Program Status, Upper, Selective	v		
CPSL	2	Clear Program Status, Lower, Selective	v		
PPSU	2	Preset Program Status, Upper, Selective	v		
PPSL	2	Preset Program Status, Lower, Selective	v		
TPSU	2	Test Program Status, Upper, Selective	v		
TPSL	2	Test Program Status, Lower, Selective	v		
<b>BRANCH/RETURN INSTRUCTIONS</b>					
BIR	3	Branch on Incrementing Register Absolute	(*ja)		
BDR	3	Branch on Decrementing Register Relative	(*ja)		
BDRR	3	Branch on Decrementing Register Absolute	(*ja)		
BXA	3	Branch Indexed Absolute, Unconditional	(*ja, X)		
ZBR	2	Zero Branch Relative, Unconditional	(*ja)		
<b>SUBROUTINE BRANCH/RETURN INSTRUCTIONS</b>					
BSTR	2	Branch to Subroutine on Condition True, Relative	(*ja)		
BSFR	2	Branch to Subroutine on Condition False, Relative	(*ja)		
BSTA	3	Branch to Subroutine on Condition True, Absolute	(*ja)		
BSFA	3	Branch to Subroutine on Condition False, Absolute	(*ja)		
BSNR	2	Branch to Subroutine on Non-Zero Register, Relative	(*ja)		
BSNAR	3	Branch to Subroutine on Non-Zero Register, Absolute	(*ja)		
BSXA	3	Branch to Subroutine, Indexed, Unconditional	(*ja, X)		
RETC	1	Return From Subroutine, Conditional	v		
RETE	1	Return From Subroutine and Enable Interrupt, Conditional	v		
ZBSR	2	Zero Branch to Subroutine Relative, Unconditional	(*ja)		



## APPENDIX B

This appendix contains a listing of the assembly language program used to implement the remote magnetic indicator heading algorithm. The program was assembled on the A2650 cross assembler program operational on the HP 2100 computer at the University of Santa Clara.



REPRODUCIBILITY OF THE ORIGINAL PAGE IS POOR

PIP ASSEMBLER VERSION 500 LEVEL 1 HEADING INSTRUMENT ASSEMBLY PROGRAM 1976 PAGE 2

LINE	ADDR	LAB	H1	B2	H3	H4	FRNGR	SOURCE
3								*****
4	0000	R0	EUU	0				*****
5	0601	R1	EUU	1				*****
6	0002	R2	EUU	2				*****
7	0003	R3	EUU	3				*****
8	0000	UN	EUU	0				*****
9	0000	Z	EUU	0				*****
10	0001	P	EUU	1				*****
11	0002	R	EUU	2				*****
12	0000	FU	EUU	0				*****
13	0001	GT	EUU	1				*****
14	0001	C	EUU	1				*****
15	0002	LF	EUU	2				*****
16	0003	UN	EUU	3				*****
17	0002	CUM	EUU	2				*****
18	0010	RS	EUU	H+02*				*****
19	0008	WC	EUU	H+10*				*****
20	000F	LOWR	EUU	H+0A*				*****
21	00F0	UPPR	EUU	H+0F*				*****
22	0040	FLAG	EUU	H+40*				*****
23	0020	II	EUU	H+20*				*****
24	00FE	NSAM	EUU	H+FF*				*****
25	0001	NSB	EUU	1				*****
26	0002	LSB	EUU	2				*****
27	0004	THA	EUU	4				*****
28	0008	PHI	EUU	8				*****
29	0010	SBIT	EUU	16				*****
30								*****
31		DATA	RES	H+450*				*****
32	0450	DATA	RES	10				*****
33	045A	DATM	RES	10				*****
34	0464	LUPS	RES	1				*****
35	0464	TEMP	RES	2				*****
36	0457	SIND	RES	2				*****
37	0457	SINR	RES	2				*****
38	0469	HM2	RES	2				*****
39	0466	SIGN	RES	1				*****
40	0460	MAX	RES	2				*****
41	046E	MY2	RES	2				*****
42	0470	MY2	RES	2				*****
43	0472	MY2	RES	2				*****
44	0474	MY2	RES	2				*****
45	0475	MY2	RES	2				*****
46	0477	MY2	RES	2				*****
47	0479	MY2	RES	2				*****
48	047D	MY2	RES	2				*****
49	047D	MY2	RES	2				*****
50	047E	MY2	RES	1				*****
51	047F	MY2	RES	1				*****
52	0481	MY2	RES	2				*****
53	0483	MY2	RES	2				*****
54	0485	MY2	RES	1				*****

RAW DATA  
CORRECTED DATA  
HM SQUARED DATA  
HX SQUARED DATA

DATA STORAGE IN RAM

OUTPUT  
OUTPUT



REPRODUCIBILITY OF THE ORIGINAL PAGE IS POOR

PIP ASSEMBLER VERSION SCU LEVEL 1 HEADING INSTRUMENT ASSEMBLY PROGRAM 1976 PAGE 4

LINE ADDR LABEL B1 B2 B3 B4 ERROR SOURCE

82	0598		CE CF 00 01	DATA	H1CE,CF,00,01,02,03,04,05,06,07
			D2 D3 03 04		
			D5 06 07		
83	05A3		D8 09 09 DA	DATA	H1D8,09,09,DA,0B,DC,DD,0D,0E,0F,E0
			D8 0C 0D DD		
			DE DF E0		
84	05AE		E1 E1 E2 E3	DATA	H1E1,E1,E2,E3,E4,E5,E6,E7,E8
			E3 E4 E5 E6		
			E6 E7 E8		
85	05H9	05H9	FF FF FF FF	DATA	H1FF,FF,FF,FF,FF,FF,FF,FF
			FF FF FF FF		
			FF FF		
86	05C3		FF FF FF FF	DATA	H1FF,FF,FF,FF,FF,FF,FF,FF
			FF FF FE FF		
			FE FE FE FF		
87	05C0		FE FE FD FD	DATA	H1FE,FD,FD,FD,FC,FC,FC,FC
			FD FC FC FC		
			FC FC		
88	0507		F8 F8 F8 FA	DATA	H1F8,F8,F8,FA,FA,FA,FA
			FA FA F9 F9		
			F9 FA		
89	05E1		F8 F7 F7 F7	DATA	H1F8,F7,F7,F7,F6,F6,F5,F5,F4,F4
			F6 F6 F5 F5		
			F4 F4		
90	05E8		F4 F3 F3 F2	DATA	H1F4,F3,F3,F2,F1,F1,F0,EF,EF
			F2 F1 F1 F0		
			EF EF		
91	05F5		EE EF FD ED	DATA	H1EE,EE,ED,ED,EC,EB,EB,EA,EA,E9,EB,EB
			EC EB EB EA		
			E4 E9 EB EA		
92	0601		E7 E6 E6 E5	DATA	H1E7,E6,E6,E5,E4,E3,E3,E2,E1,E1
			E4 E3 E3 E2		
			E1 E1		
93	0608		E0 DF 0E 0D	DATA	H1E0,DF,DF,0D,0D,0C,0B,0A,09,09
			0D 0C 0B 0A		
			09 09		
94	0615		08 07 06 05	DATA	H108,07,06,05,04,03,02,01,00
			04 03 03 02		
			01 00		
95	061F		CF CE C0 CC	DATA	H1CF,CE,C0,CC,CA,C9,C8,C7,C6
			CB CA C9 C8		
			C7 C6		
96	0629		C5 C4 C3 C2	DATA	H1C5,C4,C3,C2,C1,C0,BF,BE,BD,BC
			C1 CA BF BE		
			BD BC		
97	0633		H8 BA H9 BA	DATA	H1B8,BA,H9,BA,B7,H6,H5,H3,H2,H1
			H7 B6 B5 B3		
			H2 B1		
98	063D		R0 AF AE AD	DATA	H1B0,AF,AE,AD,AB,AA,A9,AR,A7,A6,A4
			AB AA A9 AR		
			A7 A6 A4		
99	0648		A3 A2 A1 9F	DATA	H1AJ,A2,A1,9F,9E,9D,9C,9B,9A,98,97,95
			9E 9D 9C 9B		
			99 9C 97 95		

REPRODUCIBILITY OF THE ORIGINAL PAGE IS POOR

PIP ASSEMBLER VERSION SCU LEVEL 1 HEADING INSTRUMENT ASSEMBLY PROGRAM 1976 PAGE 5

LINE	ADDR	LABL	H1	H2	H3	H4	B4	ERROR	SOURCE
100	0654		94	93	92	90			DATA
			8F	8E	8C	88			H194,93,92,90,8F,8E,8C,88,8A,88
			84	84					
101	065F		87	86	84	83			DATA
			82	80	7F	7E			H187,86,84,83,82,80,7F,7E,7C,7A
			7C	78					
102	0668		7A	78	77	75			DATA
			74	73	71	70			H17A,78,77,75,74,73,71,70,6E,6D,6C
			6E	60	6C				
103	0673		6A	69	67	66			DATA
			64	63	61	60			H16A,69,67,66,64,63,61,60,5F,5D,5C
			5F	50	5C				
104	067E		5A	59	57	56			DATA
			54	53	51	50			H15A,59,57,56,54,53,51,50,4E,4D
			4E	40					
105	068H		4A	4A	48	47			DATA
			45	44	42	41			H14A,4A,4A,47,45,44,42,41,3F,3E,3C
			3F	3C					
106	0693		3B	39	38	3A			DATA
			35	33	31	30			H13B,39,3A,36,35,33,31,30,2E,2D
			2E	20					
107	069D		2B	2A	28	27			DATA
			25	24	22	20			H12B,2A,2A,27,25,24,22,20,1F,1D
			1F	10					
108	06A7		1C	1A	19	17			DATA
			15	14	12	11			H11C,1A,19,17,15,14,12,11,0F,0E
			0F	0F					
109	06B1		0C	0A	09	07			DATA
			06	04	03	01			H10C,0A,09,07,06,04,03,01,00
			00						
110	06BA	06BA	7F	74	77	72			COSM
			6E	69	65	61			H17F,78,77,72,6E,69,65,61,5C,58,54
			5C	54	54				
111	06C5		50	4C	47	43			DATA
			3F	3C	38	34			H150,46,47,43,3F,3C,38,34,31,20,2A
			31	20	2A				
112	06D0		27	23	20	1D			DATA
			1B	1A	15	13			H127,23,20,1D,1B,18,15,13,11,0E,0C
			11	0F	0C				
113	06D8		0B	09	07	0A			DATA
			04	03	02	01			H10H,09,07,06,04,03,02,01,01,00,00,00,00
			01	00	00	00			
			00						
114	06E8	06E8	FF	FF	12	9F			COSL
			2F	C5	63	0A			H1FF,68,12,9E,2F,C5,63,0A,B7,72,38,0C
			47	72	38	0C			
115	06F4		F0	E3	E8	FF			DATA
			28	6C	C3	32			H1FU,E3,E8,FF,28,6C,C3,32,B9,59,15,EC
			H9	54	15	EC			
116	0700		F0	F2	22	72			DATA
			F2	73	26	FA			H1E0,F2,22,72,26,FA,F4,10,52,88
			F4	1	52	8A			

REPRODUCIBILITY OF THE ORIGINAL PAGE IS POOR

PIP ASSEMBLER VERSION SCU LEVEL 1 HEADING INSTRUMENT ASSEMBLY PROGRAM 1976 PAGE 6  
 LINE ADDR LARL U1 B2 H3 B4 FRROR SOURCE

```

117 070C      43 F5 CD CC      DATA      H:43,F5,C0,CC,F1,3E,B3,4F,13,00,
      F1 3E H3 4F      13 00
118 0716      01 02 04 04      BCD      H:01,02,04,08,16,32,64,00,
      16 32 04 00      SINE DATA      H:031
119 071E      03              ORG      H:7501
120
121
122
123
124
125
126
127
128
129 0750      76 23      PPSU      I1
130 0752      75 FF      CP5L      HIFF*
131 0754      77 02      PPSL      COM
132 0756      04 FF      LODI,H0
133 0758      50          WRTU,H0
134 0759      74 FF      CP5L      HIFF*
135
136 075B      3F 07 40      ** STANT MAIN PROGRAM
137 075D      3F 0A E6      MAIN
138 075E      3F 0A 71      BSTA,UN SAMP
139 0761      3F 0A 09      BSTA,UN ROTX
140 0764      3F 07 70      BSTA,UN ROTY
141 0767      3F 0A 97      BSTA,UN WVEC
142 076A      3F 0A 97      BSTA,UN WICH
143 076D      1F 07 58      BSTA,UN WUTA
144
145
146 0770      77 02      WICH      COM
147 0772      0C 04 70      LODA,H0
148 0775      EC 04 6E      COMA,H0
149 0778      10 08 14      BCTA,ST
150 077B      1E 08 2B      BCTA,LT
151 077E      0C 04 71      LODA,H0
152 0781      EC 04 6F      COMA,H0
153 0784      10 08 14      BCTA,ST
154 0787      1F 08 2B      BCTA,UN
155
156
    
```

LS BITS

LS BITS

LS BITS

LS BITS

LS BITS

LS BITS

LS BITS

REPRODUCIBILITY OF THE ORIGINAL PAGE IS POOR

PIP ASSEMBLER VERSION SCU LEVEL 1 HEADING INSTRUMENT ASSEMBLY PROGRAM 1976 PAGE 7

```

LINE  ADDR  LA=L  H1  H2  H3  H4  C  R  R  O  R  SOURCE
158
159
160
161
162
163
164
165
166
167
168
169
170
171
172
173
174
175
176
177
178
179
180
181
182
183
184
185
186
187
188
189
190
191
192
193
194
195
196
197
198
199
200
201
202
203
204
205
206
207
208
209

0x6
H17501
*****
* A SUBROUTINE TO SAMPLE DATA FROM ALL SENSORS *****
* REGISTER "0" CONTROLS SAMPLE/HOLD & MIX
* BITS 0,1,62 SELECT HX, HY, HZ, TIME, P1
* DATA IS STORED IN DOUBLE PRECISION FORM
* BEGINNING AT "DATA" WITH HX(HSB) FOLLOWED BY
* HX(LSB), HY, HZ, PITCH, ROLL
* (1) CONVERTS A/D DATA TO SIGN MAGNITUDE
* (2) CHANGES SIGN OF HY & HZ (ORIENTATION)
* (3) CORRECTS FOR OFFSET ERROR
* EXIT WITH CORRECTED DATA IN TABLE "DATA"
*****
***** BEGIN SUBROUTINE *****
SAMP  L001,R1  -1      DATA INDEX
      L001,R2  5      LOOP COUNTER
      L001,R3  1      1ST SAMPLE
      CPSL    C,WC
NEXT  WTL,R3  H180*   SELECT & SAMPLE DATA
      ION1,R3  H180*   READY TO HOLD
      WTL,R3  F3      HOLD DATA
      L001,R0  M180*   RESET A/D
      WTL,R0  R0      START A/D
      WTL,R0  R0      READ L50
      REDD,R0  M101*   BRANCH BACK IF EOC=1
      TML,R0  T51     EOR1,R0  H1FF
      BCIN,N  T51     AND1,R0  UP4
      EOR1,R0  H1FF   STRA,R0  DATA-1,P1,* STORE L5 1/3
      AND1,R0  UP4    REDC,R0  EOR1,R0  H1FF
      STRA,R0  DATA-1,P1,* STORE MSH
      REDC,R0  EOR1,R0  DATA-1,P1,* POINT TO NEXT DATA
      ADD1,P3  1      POINT TO CHAN. ONLY
      AND1,R3  LOWK   TEST LOOP COUNTER
      HRR,R2  NEXT
*****
* CONVERT TO SIGN MAGNITUDE *****
PPSL  WCL    ENAHF CARRY
      L001,R2  -1     INDEX
      L001,P3  7      LOOP COUNTER
      LODA,R0  DATA+2,* GET MSB OF DATA
      BCIN,N  KSTU   BR. IF SIGN=1
      STRZ   H1
      EORZ   R0     CLEAR HP
      PPSL   C      SET UP FOR SUIT.
      SUBA,R0  DATA+2,* SUB. L5 BITS
      STRA,R0  DATA+2,* STORE NEW DATA
      EORZ   R0
      SUBZ   H1     SUB. MS BITS
      TOR1,R0  H1801  SET SIGN=1 (NEG)

```

REPRODUCIBILITY OF THE ORIGINAL PAGE IS POOR

PIP ASSEMBLER VERSION SCU LEVEL 1 HEADING INSTRUMENT ASSEMBLY PROGRAM 1976 PAGE 9

LINE ADDR LABEL HI B2 HJ B4 ERROM SOURCE

```

210 07F2 CE 54 59
211 07F5 18 0A
212 07F7 07F7
213 07F9 CE 64 5A
214 07FC 0E 24 50
215 07FF CE 64 5A
216 0802 0802 FB 5A
217 0804
218 0807 0C 04 5C
219 080A 0D 04 5E
220 080C 24 50
221 080E 25 80
222 0811 CC 04 5C
223 0814 CD 04 5E
224 0816 07 00
225 0819 3F 0A 2A
226 081B 07 02
227 081E 3F 0B 2A
228 0820 07 04
229 0823 3F 0B 2A
230 0826 C0
231 0829 07 07
232 082B
233 082E 3F 0F 4B
234 0831 17
235 0834
236

```

STRAR0 DATM+R2 STORE NS BITS

BCIRUN FINI SIGN BIT = 0

ANDIR0 H7FF STORE NEW DATA

STRAR0 DATM+R2 GET LS DATA

LODA+R0 DATA+R2\*\* STORE AS NEW DATA

STRAR0 DATM+R2

BRBR+R3 CONT

\* CHANGE SIGN OF HY SHZ (SENSOR ORIENTATION)

LODA+R0 DATM+2 CHANGE SIGN OF HY & HZ

LODA+R1 DATM+4

EORIR0 H+801

EORIR1 H+801

STRAR0 DAT+2

STRAR1 DATM+4

\* CORRECT FOR OFFSET ERROR IN HY, HZ & HZ CHANNELS

LODI+R3 0 DO HX 1ST

BSTARUN 0FST HY

LODI+R3 2

BSTARUN 0FST HZ

LODI+R3 4

BSTARUN 0FST

NOP

LODI+R3 7

\* CORRECT FOR ORTHOGONALITY ERROR IN HA AXIS

BSTARUN 0RTH

RETCUN

\*\*\*\*\*

REPRODUCIBILITY OF THIS ORIGINAL PAGE IS POOR

PIP ASSEMBLER VERSION SCU LEVEL 1 HEADING INSTRUMENT ASSEMBLY PROGRAM 1976 PAGE 9

```

LINE ADDR LABEL n1 DP H3 H4 FROM SOURCE
230 082A 082A 0F 04 5A
231 082B 082B 0F 04 5A
232 082C 082C 0F 04 5A
233 082D 082D 0F 04 5A
234 082E 082E 0F 04 5A
235 082F 082F 0F 04 5A
236 0830 0830 0F 04 5A
237 0831 0831 0F 04 5A
238 0832 0832 0F 04 5A
239 0833 0833 0F 04 5A
240 0834 0834 0F 04 5A
241 0835 0835 0F 04 5A
242 0836 0836 0F 04 5A
243 0837 0837 0F 04 5A
244 0838 0838 0F 04 5A
245 0839 0839 0F 04 5A
246 083A 083A 0F 04 5A
247 083B 083B 0F 04 5A
248 083C 083C 0F 04 5A
249 083D 083D 0F 04 5A
250 083E 083E 0F 04 5A
251 083F 083F 0F 04 5A
252 0840 0840 0F 04 5A
253 0841 0841 0F 04 5A
254 0842 0842 0F 04 5A
255 0843 0843 0F 04 5A
256 0844 0844 0F 04 5A
257 0845 0845 0F 04 5A
258 0846 0846 0F 04 5A
259 0847 0847 0F 04 5A
260 0848 0848 0F 04 5A
261 0849 0849 0F 04 5A
262 084A 084A 0F 04 5A
263 084B 084B 0F 04 5A
264 084C 084C 0F 04 5A
265 084D 084D 0F 04 5A
266 084E 084E 0F 04 5A
267 084F 084F 0F 04 5A
268 0850 0850 0F 04 5A
269 0851 0851 0F 04 5A
270 0852 0852 0F 04 5A
271 0853 0853 0F 04 5A
272 0854 0854 0F 04 5A
273 0855 0855 0F 04 5A
274 0856 0856 0F 04 5A
275 0857 0857 0F 04 5A
276 0858 0858 0F 04 5A
277 0859 0859 0F 04 5A
278 085A 085A 0F 04 5A
279 085B 085B 0F 04 5A
280 085C 085C 0F 04 5A
281 085D 085D 0F 04 5A
282 085E 085E 0F 04 5A
283 085F 085F 0F 04 5A
284 0860 0860 0F 04 5A
285 0861 0861 0F 04 5A
286 0862 0862 0F 04 5A
287 0863 0863 0F 04 5A
288 0864 0864 0F 04 5A
289 0865 0865 0F 04 5A

```

```

*****
OFST LODA,R0 DAIN,H3 MS BYTE OF DATA
STRZ R1 SIRIP SIGN
ANDI,R0 H:FF SAVE SIGN
ANDI,R1 H:80
STRA,R0 RSLT
STRA,R1 SAES
LODA,R0 DAIN+1,H3 LS BYTE OF DATA
STRA,R0 RSLT+1
LODA,R0 USET,H3 MS BYTE OF OFFSET
STRA,R0 TEMP
LODA,R0 USET+1,H3
STRA,R0 TEMP+1
LODA,R0 SOST,H3
STRA,R0 STE+1
CPSL COM
PUSL MS BANK=1
BSTA,ON SADI BANK=0
CPSL MS
LODA,R0 RSLT
STRA,R0 DAIN,H3
LODA,R0 RSLT+1
STRA,R0 DAIN+1,H3
RETC,ON
*****
BINARY MULT. FOR A TWO-BYTE INTEGER
MULTIPLY BY A SINGLE BYTE INTEGER
MULTIPLICAND IS IN OPR1+1
MULTIPLIER IS IN OPR2+1
RESULT WILL BE IN RSLT+RSLT+1
(2 BYTES ARE DISCARDED)
*****
BEGIN SIM-ONLINE
SMPY MC SET MODE
EHRZ R0 CLEAR RESULT
STRA,R0 RSLT CLEAR RESULT+1
STRA,R0 OPR1
LODI,H3 B LOAD COUNT
LODA,H2 OPR1+1 GET MULTIPLIER
MHR,R2 RUI, R1 GET RIGHT 4 BIT INTO CARRY
FORZ R0 CLEAR R0
RPL,R0 GET CARRY INTO LSH
MHR,H3 LSH
LODI,H1 Z BRANCH IF C=0
LODA,H0 RSLT+1,H1 INDEX
ADDA,H0 OPR2+1,H1 ADD MULTIPLICAND TO PRODUCT
STRA,H0 RSLT+1,H1
HRR,H1 LOC2 FINISH THE ADD

```



PIP ASSEMBLER WITH IN SOURCE LIVE) 1 HEADING INSTRUMENT ASSEMBLY PROGRAM 1976 PAGE 10

```

LINE ADDR LABEL 01 02 03 04 05 06 07 08 09 10 11 12 13 14 15 16 17 18 19 20 21 22 23 24 25 26 27 28 29 30 31 32 33 34 35 36 37 38 39 40
290 0889 0889 05 FE LOC4 LODI,R1 -2 ROT. THE PRODUCT
291 088H 088B 0D 61 79 LOC5 LODA,R0 RSLT-256*2,R1
292 088E 50 RRR,R0 STRA,R0
293 088F CD 61 79 STRA,R0 RSLT-256*2,R1
294 0892 09 77 BIRR,R1 LDCS BIRR,R1
295 0894 F5 61 BURR,R3 L000 FINISH THE LOOP
296
297 0896 RETC,UN *****
298 *****
299 *****
300 *****
301 *****
302 *****
303 0897 0C 04 00 OUTA LODA,R0 DATM*6 FETCH THETA (MSR)
304 089A C3 ANDI,R0 04R0? SAVE SIGN
305 089M 44 R0 NTH BR. ON NEG THETA
306 089O 1A 14 06 EORA,R0 DATM*H COMPARE SIGNS
307 089F 2C 04 62 BCTR,R0 NPHI
308 08A2 1A 06 BCTR,R0 7
309 08A4 04 07 LDI,R0 7
310 08A6 04 10 WRI,R0 SWIT BOTH POSITIVE
311 08A8 1B 14 BCTR,UN AGL
312 08AA 20 EORZ R0
313 08AB 04 10 WRI,R0 SWIT PHI NEG.
314 08AD 1B 0F BCTR,UN AGL
315 08AF 08AF 2C 04 A2 EORA,R0 DATM*H
316 08B2 19 0A BCTR,P 0PH
317 08B4 04 01 LODI,R0 3
318 08B6 04 10 WRI,R0 SWIT
319 08B8 1B 0A BCTR,UN AGL
320 08BA 04 04 08HA R
321 08BC 04 10 WRI,R0 SWIT
322 08BE 0F 04 CC BCTR,UN L000
323 08C1 05 04 62 WRI,R1 THA
324 08C3 0F 04 62 LODA,R3 DATM*6
325 08C6 3F 04 CC BCTR,UN L000
326 08C9 05 04 WRI,R1 PHI
327 08CA 17 RETC,UN *****
328 *****
329 08CC 07 7E LOD ANDI,R3 047F? *****
330 08CE CF 04 7C LOD STRA,R3 08R2*1 *****
331 08D1 20 R0 LOKZ R0 *****
332 08D2 CC 04 74 STRA,R0 08R2 *****
333 08D5 04 5A LODI,R0 045A *****
334 08D7 CC 04 7A STRA,R0 08R1*1 *****
335 08DA 3F 04 66 BCTR,UN SOPY *****
336 08DD 0C 04 78 LODA,R0 045A *****
337 08E0 3F 04 64 BCTR,UN BCOA *****
338 08E3 25 FF EORI,R1 04FF? *****
339 08E5 *****
340 *****

```

REPRODUCIBILITY OF THE ORIGINAL PAGE IS POOR

PIP ASSEMBLER VERSION 1 IN SCU LEVEL 1 HEADING INSTRUMENT ASSEMBLY PROGRAM 1976 PAGE 11

```

LINE ADDR LABEL MI O2 I3 B4 FRQR SOURCE
342 .....
343 * S.R. ROTX TO CORRECT HX DATA USING ALGORITHM *
344 * HASRXX=COS(PITCH)*SIN(PITCH)+(HYMMSIN( *
345 * *ULL)*ZMCCOS(MULL)) *
346 * * * * *
347 * ENTER WITH "NEW DATA" IN LABEL DATA *
348 * EXIT WITH "OFFIFIED HX IN "DATA" *
349 * CALLS S.M. HZH *
350 * CALLS S.M.S. "SAOD" & "SHPY" TO DO *
351 * STORED MAGNITUDE AND/SUBI AND MULTIPLY *
352 * * * * *
353 ROTX PPSL WC.C
354 LODA,R0 DATM
355 STRZ R1
356 ANDI,R1 R3
357 ANDI,R3 R100
358 SIRA,R3 SIND
359 LODA,R0 SIND,R1
360 ORF7 CC 04 68
361 ORFA R0 R5 R9
362 ORFD CC 04 65
363 ORFO CC 04 7A
364 ORO3 CC 04 5A
365 ORO6 C1
366 ORO7 44 7F
367 ORO9 45 80
368 OROR CC 04 7B
369 OROE C1 04 96
370 OROI CC 04 98
371 ORO14 CC 04 7C
372 ORO17 4F 04 66
373 ORO1A CC 04 77
374 ORO1D CC 04 48
375 ORO20 6C 04 78
376 ORO23 CC 04 9C
377 ORO26 3F 04 40
378 ORO29 CC 04 68
379 ORO2C CC 04 7A
380 ORO2F 3F 04 66
381 ORO32 CC 04 67
382 ORO35 CC 04 7E
383 ORO38 R0 04 46
384 ORO3E CC 04 70
385 ORO41 R0 04 9C
386 ORO44 CC 04 55
387 ORO47 CC 04 66
388 ORO4A 75 67
389 ORO4C 4F 04 78
390 ORO4F CC 04 78
391 ORO52 CC 04 40
392 ORO55 4C 04 77
393 .....
394 .....
395 .....
396 .....
397 .....
398 .....
399 .....
400 .....
401 .....
402 .....
403 .....
404 .....
405 .....
406 .....
407 .....
408 .....
409 .....
410 .....
411 .....
412 .....
413 .....
414 .....
415 .....
416 .....
417 .....
418 .....
419 .....
420 .....
421 .....
422 .....
423 .....
424 .....
425 .....
426 .....
427 .....
428 .....
429 .....
430 .....
431 .....
432 .....
433 .....
434 .....
435 .....
436 .....
437 .....
438 .....
439 .....
440 .....
441 .....
442 .....
443 .....
444 .....
445 .....
446 .....
447 .....
448 .....
449 .....
450 .....
451 .....
452 .....
453 .....
454 .....
455 .....
456 .....
457 .....
458 .....
459 .....
460 .....
461 .....
462 .....
463 .....
464 .....
465 .....
466 .....
467 .....
468 .....
469 .....
470 .....
471 .....
472 .....
473 .....
474 .....
475 .....
476 .....
477 .....
478 .....
479 .....
480 .....
481 .....
482 .....
483 .....
484 .....
485 .....
486 .....
487 .....
488 .....
489 .....
490 .....
491 .....
492 .....
493 .....
494 .....
495 .....
496 .....
497 .....
498 .....
499 .....
500 .....
501 .....
502 .....
503 .....
504 .....
505 .....
506 .....
507 .....
508 .....
509 .....
510 .....
511 .....
512 .....
513 .....
514 .....
515 .....
516 .....
517 .....
518 .....
519 .....
520 .....
521 .....
522 .....
523 .....
524 .....
525 .....
526 .....
527 .....
528 .....
529 .....
530 .....
531 .....
532 .....
533 .....
534 .....
535 .....
536 .....
537 .....
538 .....
539 .....
540 .....
541 .....
542 .....
543 .....
544 .....
545 .....
546 .....
547 .....
548 .....
549 .....
550 .....
551 .....
552 .....
553 .....
554 .....
555 .....
556 .....
557 .....
558 .....
559 .....
560 .....
561 .....
562 .....
563 .....
564 .....
565 .....
566 .....
567 .....
568 .....
569 .....
570 .....
571 .....
572 .....
573 .....
574 .....
575 .....
576 .....
577 .....
578 .....
579 .....
580 .....
581 .....
582 .....
583 .....
584 .....
585 .....
586 .....
587 .....
588 .....
589 .....
590 .....
591 .....
592 .....
593 .....
594 .....
595 .....
596 .....
597 .....
598 .....
599 .....
600 .....
601 .....
602 .....
603 .....
604 .....
605 .....
606 .....
607 .....
608 .....
609 .....
610 .....
611 .....
612 .....
613 .....
614 .....
615 .....
616 .....
617 .....
618 .....
619 .....
620 .....
621 .....
622 .....
623 .....
624 .....
625 .....
626 .....
627 .....
628 .....
629 .....
630 .....
631 .....
632 .....
633 .....
634 .....
635 .....
636 .....
637 .....
638 .....
639 .....
640 .....
641 .....
642 .....
643 .....
644 .....
645 .....
646 .....
647 .....
648 .....
649 .....
650 .....
651 .....
652 .....
653 .....
654 .....
655 .....
656 .....
657 .....
658 .....
659 .....
660 .....
661 .....
662 .....
663 .....
664 .....
665 .....
666 .....
667 .....
668 .....
669 .....
670 .....
671 .....
672 .....
673 .....
674 .....
675 .....
676 .....
677 .....
678 .....
679 .....
680 .....
681 .....
682 .....
683 .....
684 .....
685 .....
686 .....
687 .....
688 .....
689 .....
690 .....
691 .....
692 .....
693 .....
694 .....
695 .....
696 .....
697 .....
698 .....
699 .....
700 .....
701 .....
702 .....
703 .....
704 .....
705 .....
706 .....
707 .....
708 .....
709 .....
710 .....
711 .....
712 .....
713 .....
714 .....
715 .....
716 .....
717 .....
718 .....
719 .....
720 .....
721 .....
722 .....
723 .....
724 .....
725 .....
726 .....
727 .....
728 .....
729 .....
730 .....
731 .....
732 .....
733 .....
734 .....
735 .....
736 .....
737 .....
738 .....
739 .....
740 .....
741 .....
742 .....
743 .....
744 .....
745 .....
746 .....
747 .....
748 .....
749 .....
750 .....
751 .....
752 .....
753 .....
754 .....
755 .....
756 .....
757 .....
758 .....
759 .....
760 .....
761 .....
762 .....
763 .....
764 .....
765 .....
766 .....
767 .....
768 .....
769 .....
770 .....
771 .....
772 .....
773 .....
774 .....
775 .....
776 .....
777 .....
778 .....
779 .....
780 .....
781 .....
782 .....
783 .....
784 .....
785 .....
786 .....
787 .....
788 .....
789 .....
790 .....
791 .....
792 .....
793 .....
794 .....
795 .....
796 .....
797 .....
798 .....
799 .....
800 .....
801 .....
802 .....
803 .....
804 .....
805 .....
806 .....
807 .....
808 .....
809 .....
810 .....
811 .....
812 .....
813 .....
814 .....
815 .....
816 .....
817 .....
818 .....
819 .....
820 .....
821 .....
822 .....
823 .....
824 .....
825 .....
826 .....
827 .....
828 .....
829 .....
830 .....
831 .....
832 .....
833 .....
834 .....
835 .....
836 .....
837 .....
838 .....
839 .....
840 .....
841 .....
842 .....
843 .....
844 .....
845 .....
846 .....
847 .....
848 .....
849 .....
850 .....
851 .....
852 .....
853 .....
854 .....
855 .....
856 .....
857 .....
858 .....
859 .....
860 .....
861 .....
862 .....
863 .....
864 .....
865 .....
866 .....
867 .....
868 .....
869 .....
870 .....
871 .....
872 .....
873 .....
874 .....
875 .....
876 .....
877 .....
878 .....
879 .....
880 .....
881 .....
882 .....
883 .....
884 .....
885 .....
886 .....
887 .....
888 .....
889 .....
890 .....
891 .....
892 .....
893 .....
894 .....
895 .....
896 .....
897 .....
898 .....
899 .....
900 .....
901 .....
902 .....
903 .....
904 .....
905 .....
906 .....
907 .....
908 .....
909 .....
910 .....
911 .....
912 .....
913 .....
914 .....
915 .....
916 .....
917 .....
918 .....
919 .....
920 .....
921 .....
922 .....
923 .....
924 .....
925 .....
926 .....
927 .....
928 .....
929 .....
930 .....
931 .....
932 .....
933 .....
934 .....
935 .....
936 .....
937 .....
938 .....
939 .....
940 .....
941 .....
942 .....
943 .....
944 .....
945 .....
946 .....
947 .....
948 .....
949 .....
950 .....
951 .....
952 .....
953 .....
954 .....
955 .....
956 .....
957 .....
958 .....
959 .....
960 .....
961 .....
962 .....
963 .....
964 .....
965 .....
966 .....
967 .....
968 .....
969 .....
970 .....
971 .....
972 .....
973 .....
974 .....
975 .....
976 .....
977 .....
978 .....
979 .....
980 .....
981 .....
982 .....
983 .....
984 .....
985 .....
986 .....
987 .....
988 .....
989 .....
990 .....
991 .....
992 .....
993 .....
994 .....
995 .....
996 .....
997 .....
998 .....
999 .....
1000 .....

```

REPRODUCIBILITY OF THE ORIGINAL PAGE IS POOR

PDP ASSEMBLER VMS:IN SCU LEVEL 1 HEADING INSTRUMENT ASSEMBLY PROGRAM 1976 PAGE 12

```

LINE  ADDR  LABL  HI B? M3 B4 FRROR SOURCE
394  0958                CC 04 7F
395  0958                17
396
397
398
399
400
401
402  095C                77 04
403  095E                P0
404  095F                CC 04 77
405  0962                CC 04 76
406  0965                07 10
407  0967                65 7F
408  0969                CU 04 7H
409  096C                CE 04 7C
410  096F                51
411  0970                096F
412  0971                52
413  0972                20
414  0973                00
415  0975                F8 12
416  097A                0C 04 76
417  097H                8C 04 7C
418  097E                CC 04 78
419  0981                9C 04 77
420  0984                8C 04 78
421  0987                1F 04 8A
422  098A                0987
423  098D                50
424  098F                CC 04 77
425  0991                0C 04 78
426  0992                50
427  0995                CC 14 76
428                F8 5H
429  0997                17

```

STRA,R0 DATA  
 RETC,UN  
 \*\*\*\*\*  
 \* SUBROUTINE TO SQUARE TWO 2 BYTE VALUES \*\*\*\*\*  
 \* ENTER WITH VALUE IN R1(MSB) & R2(LSB) \*  
 \* EXIT WITH 2 MSB IN RSLT+1 \*\*\*\*\*  
 \*\*\*\*\* BEGIN \*\*\*\*\*  
 500  
 EORZ WC  
 STRA,R0 R0  
 STRA,R0 R0 CLEAR TEMP STORAGE  
 STRA,R0 RSLT+1  
 LODI,R3 16 COUNTER  
 ANDI,R1 H'7F\*  
 STRA,R1 OPR2  
 STRA,R2 OPR2+1  
 RRR,R1 ROTATE MULTIPLIER  
 RRR,R2  
 R0  
 EORZ  
 KRL,R0  
 BRR,R0  
 LODA,R0 NOAD  
 ADDA,R0 RSLT+1  
 STRA,R0 OPR2+1  
 LODA,R0 RSLT+1  
 LODA,R0 RSLT  
 ADDA,R0 OPR2  
 BCTI,UN NOAD+3  
 LODA,R0 RSLT  
 RRR,R0  
 STRA,R0 RSLT  
 LODA,R0 RSLT+1  
 RRR,R0  
 STRA,R0 RSLT+1  
 BRR,R3  
 \*\*\*\*\*  
 ROTATE LS 1/2 RESULT  
 CUNI, MULF, IF WFO.  
 \*\*\*\*\*  
 END OF SUBROUTINE

REPRODUCIBILITY OF THE ORIGINAL PAGE IS POOR

PIP ASSEMBLER VERSION SCU LEVEL 1 HEADING INSTRUMENT ASSEMBLY PROGRAM 1476 PAGE 13

LINE ADDR LABEL HI B2 B3 B4 FROM SOURCE

```

431
432
433
434
435
436
437
438
439
440 0998 77 03
441 099A 07 02
442 099C 05 02
443 099E 1C 0A 16
444
445 09A1 0F 04 70
446 09A4 03
447 09A5 2C 04 7E
448 09A8 1E 04 CA
449 09AB 75 01
450 09AD 0C 04 66
451 09B0 7C 04 78
452 09B3 CC 04 78
453 09B6 0C 04 25
454 09B9 0C 04 77
455 09BC 9C 09 F9
456 09BF 00 04 18
457 09C2 9C 09 F9
458 09C5 20
459 09C6 CC 04 77
460 09C9 17
461 09CA 59CA 06 02
462 09CC 03
463 09CD 1E 0A 02
464 09D0 0E 04 04
465 09D3 AE 04 76
466 09D6 CE 04 76
467 09D9 FA 75
468 09DA 05 01
469 09DD 1C 0A 12
470 09E0 09E0 77 01
471 09E2 05 02
472 09E4 09E4 20
473 09E5 AE 04 76
474 09E8 CE 04 76
475 09E9 FA 77
476 09F0 01
477 09F2 9C 09 FE
478 09F1 00 04 78
479 09F4 9C 09 FE
480 09F7 18 01
481 09F9 09F9 03
482 09FA 09FA CC 04 77

```

```

*****
* S.R. SADC TO PERFORM DOUBLE PRECISION *
* SIGN & MAGNITUDE ADD/SUBT *
* ADDEND (SUBTRACTEND) IN TEMP, F*MP*1 *
* AUGEND (MULTIPLY) IN RSLT, RSLT*1 *
* STEM = SIGN OF TEMP IN TEMP SHFS = SIG *
* CUM HLT IS FLAG. (0=ADD) 1= SUBT *
* SIGNED TOTAL LEFT IN RSLF, RSLT*1 *
*****
SADD PPSL WC*C AMITH WITH CARRY1 SFT CARRY
      LOD1,*3 2 INDEX
      TPLS COM TEST FLAG
      BCTR*UN SSON HK, IF SUBT.
      * START ADD HERE *
      LODA,*0 STEM
      LODZ K3
      BURR,*0 SHFS
      BCTR*N DIFM
      CPSL C
      LODA,*0 TEMP*1
      ADDA,*0 RSLT*1
      STRA,*0 RSLT*1
      LODA,*0 TEMP
      ADDA,*0 RSLT
      BCTR*Z RTRV
      LODA,*1 RSLT*1
      BCTR*Z RTRV
      BURZ K3
      STRA,*0 RSLT
      BCTR*UN C
      LOD1,*2 C
      BCTR,*1 X*E0
      LODA,*0 TEMP-1,R2
      SUBA,*0 RSLT-1,R2
      STRA,*0 RSLT-1,R2
      BURR,*2 SUP1
      TPLS C
      BCTR*UN TZE4
      PPSL C
      LOD1,*2 C
      BURZ K3
      SUBA,*0 RSLT-1,R2
      BURR,*2 SUP2
      STRZ K1
      BCTR*Z SHFS
      LODA,*1 RSLT*1
      BCTR*UN SHFS
      BURR*UN NOW
      LODZ K3
      STRA,*0 RSLT

```

```

DIFR
SUP1
TNEG
SUP2
MTRN
RLOW

```

```

*****
* GET LS BITS *
* ZERO RSLT = POS *
* CTR/INDEX *
* BK, IF BK = TRG *
* FORM TEMP = RSLT *
* HK, IF C = 1 *
* INDEX/CTR *
* FORM 2'S COMPLEMENT *
* IF C = 0 *

```

REPRODUCIBILITY OF THE ORIGINAL PAGE IS POOR

PIP ASSEMBLER VERSION SCU LEVEL 1 HEADING INSTRUMENT ASSEMBLY PROGRAM 1976 PAGE 14

LINE ADDR L A H L A1 R2 R3 R4 FROM SOURCE

```

483 09FD          RETC,UN
484 09FE          IOA1,R0
485 0A00          BCIR,UN
486 0A02          LODA,R0
487 0A05          SUBA,R0
488 0A08          STRA,R0
489 0A0B          BDRR,R2
490 0A0D          TPSL
491 0A0F          HCF,UN
492 0A12          ADI,R0
493 0A14          STRA,R0
494 0A17          RETC,UN
495 0A17          TZER
496 0A17          SSUB
497 0A18          LODI,R2
498 0A1B          EDRA,R0
499 0A1C          BCFA,N
500 0A1E          CP,SL
501 0A21          LODA,R0
502 0A24          ADDA,R0
503 0A26          STRA,R0
504 0A29          JUNK
505 0A2C          STRA,R0
506 0A2F          RETC,UN
507 0A31          RETC,UN
508 0A32          RETC,UN
509 0A35          RETC,UN

* START HERE IF TEMP IN "TEMP" IS NEGATIVE
* FORM DIFFERENCE
* LOOP UNCE
* RESULT IS POS
*****
* START HERE IF SUBTRACTION IS REQUIRED
* I.E. (KSLT,KSLT+1) - (TEMP,TEMP+1)
*****
SIGN OF RESULT
BK, IF SIGNS SAME

```

REPRODUCIBILITY OF THE ORIGINAL PAGE IS PO

PIP ASSEMBLER VERSION IN SCU LEVEL 1 HEADING INSTRUMENT ASSEMBLY PROGRAM 1976 PAGE 15

LINE ADDR LABEL H1 H2 H3 H4 FROM SOURCE

LINE	ADDR	LABEL	H1	H2	H3	H4	FROM	SOURCE
513	0A36	0A36	77	01				* START HERE IF BOTH TERMS SAME SIGN
514	0A38	0A38	0E	64	76			CLUP
515	0A39	0A39	0E	64	64			CLUP
516	0A3E	0A3E	0E	64	76			CLUP
517	0A41	0A41	0E	64	76			CLUP
518	0A43	0A43	0E	64	76			CLUP
519	0A45	0A45	0E	64	76			CLUP
520	0A47	0A47	0E	64	76			CLUP
521	0A49	0A49	0E	64	76			CLUP
522	0A4B	0A4B	0E	64	76			CLUP
523	0A4D	0A4D	0E	64	76			CLUP
524	0A4F	0A4F	0E	64	76			CLUP
525	0A51	0A51	0E	64	76			CLUP
526	0A53	0A53	0E	64	76			CLUP
527	0A55	0A55	0E	64	76			CLUP
528	0A57	0A57	0E	64	76			CLUP
529	0A59	0A59	0E	64	76			CLUP
530	0A5B	0A5B	0E	64	76			CLUP
531	0A5D	0A5D	0E	64	76			CLUP
532	0A5F	0A5F	0E	64	76			CLUP
533	0A61	0A61	0E	64	76			CLUP
534	0A63	0A63	0E	64	76			CLUP
535	0A65	0A65	0E	64	76			CLUP
536	0A67	0A67	0E	64	76			CLUP
537	0A69	0A69	0E	64	76			CLUP
538	0A6B	0A6B	0E	64	76			CLUP
539	0A6E	0A6E	0E	64	76			CLUP
540	0A70	0A70	0E	64	76			CLUP
541								*****

START HERE IF BOTH TERMS SAME SIGN  
 C=1  
 RSLT = TEMP - RSLT

TEST CARRY  
 START 2'S COMPL  
 LOOP TO DO  
 2'S COMPL.

TEST SIGN  
 MIN IF NEG.

SIGN = STEM

\*\*\*\*\*

REPRODUCIBILITY OF THE ORIGINAL PAGE IS POOR

PIP ASSEMBLER VERSION SOURCE L FVEI 1 HEADING INSTRUMENT ASSEMBLY PROGRAM 1976 PAGE 16

```

543 LINE ADDR L AIL B1 B2 B3 B4 FROM SOURCE
544 0A71 0A71 77 04
545 0A73 0C 04 62
546 0A76 C1
547 0A77 45 7F
548 0A79 2C 04 5E
549 0A7C 44 80
550 0A7E 0C 04 70
551 0A81 00 64 49
552 0A84 CC 04 75
553 0A87 00 64 30
554 0A8A CC 04 7A
555 0A8D 0C 04 5E
556 0A90 44 7F
557 0A92 CC 04 78
558 0A95 CC 04 5F
559 0A98 CC 04 7C
560 0A9H 3F 0A 66
561 0A9E 0C 04 77
562 0AA1 CC 04 65
563 0AA4 CC 04 78
564 0AA7 CC 04 66
565 0AAA 0C 04 5C
566 0AAE C1
567 0AH0 CD 04 76
568 0AH3 CC 04 7E
569 0AHE CC 04 5D
570 0A8E 0C 04 7C
571 0AC1 CC 04 7A
572 0AC4 3F 0A 66
573 0AC7 77 02
574 0AC9 3F 0A 66
575 0ACC 0C 04 77
576 0ACF CC 04 71
577 0AD2 0C 04 76
578 0AD5 CC 04 7F
579 0AD8 0C 04 76
580 0AD9 0C 04 75
581 0AD9 0C 04 75
582 0AD9 0C 04 75
583 0AD9 0C 04 75
584 0AD9 0C 04 75
585 0AD9 0C 04 75
586 0AD9 0C 04 75
587 0AD9 0C 04 75
588 0AD9 0C 04 75
589 0AD9 0C 04 75
590 0AD9 0C 04 75
591 0AD9 0C 04 75

```

\*\*\*\*\*  
\* S.N. ROTY TO ADJUST HY DATA USING ALGORITHM \*  
\* HY=HY\*(COS(ROLL)-ZM\*SIN(ROLL)) \*  
\* USES SIGN AND MAGNITUDE DATA FROM TABL MATM \*  
\* STORES NEW DATA INTO DATY, DATY+1 \*  
\* CALLS S.S.S. "SADDH" & "SMPLY" TO PERFORM SIGNED \*  
\* MAGNITUDE ARITHMETIC \*  
\*\*\*\*\*  
\* ROTY PPSL W-C-C \*\*\*\*\*  
LODA,R0 UATM,H GET HOLL ANGLF PHI  
STRZ R1 STRIP OFF SIGN  
ANDI,H1 H17F, DETERMINE SIGN OF PROD.  
EORA,R0 DATM+4  
ANDI,R0 H180,  
STRA,R0 STEM  
LODA,H0 COS,H1 CUS (PHI)  
STRA,H0 COSK  
LODA,H0 SIN,R1 SIN (PHI)  
STRA,H0 OPR1+1 MULTIPLIER  
LODA,H0 DATM+4 GET HZ  
ANDI,H0 H17F, STRIP SIGN  
STRA,H0 OPR2 MULTIPLICAND  
LODA,H0 UATM+5 FORM Z2\*SIN(PHI)  
STRA,H0 OPR2+1 MOVE PRODUCT  
BSTA,UN SPLY  
LODA,H0 RSLT  
STRA,H0 TFMP  
LODA,H0 RSLT+1  
STRA,H0 TFMP+1  
\*\*\*\*\*  
\* BEGIN FORMING 2ND TERM  
LODA,R0 UAT1+2  
STRZ R1  
ANDI,H1 H17F,  
STRA,H1 OPR2  
ANDI,R0 R1R0,  
STRA,R0 SRES  
LODA,H0 DATM+3  
STRA,H0 OPR2+1  
LODA,H0 COSK  
STRA,H0 OPR1+1  
BSTA,UN SPLY  
\*\*\*\*\*  
\* NOW FORM NEW HY  
PPSL COM  
BSTA,UN SADD  
LODA,R0 RSLT  
STRA,H0 DATY  
LODA,H0 RSLT+1  
STRA,H0 UATY+1  
RETCL,UN





REPRODUCIBILITY OF THE ORIGINAL PAGE IS POOR

PIP ASSEMBLER VERSION SOURCE LAYER 1 HEADING INSTRUMENT ASSEMBLY PROGRAM 1976 PAGE 16

LINE ADDR L4HL B1 B2 B3 B4 ERROR SOURCE

```

641
642
643
644
645 0B2B 0B 02
646 0B20 0D 64 6F
647 0B30 CD 64 7B
648 0B33 F9 7A
649 0B35 20
650 0B36 3F 0A 4A
651 0B39 3F 0A 4B
652 0B3C 3F 0C 64
653 0B3F 04 90
654 0B41 77 09
655 0B43 A1
656 0B44 64
657 0B45 C1
658 0B46 3F 0C 7C
659 0B49 17
660

```

\*\*\*\*\*  
\* A SUBROUTINE TO COMPUTE HEADING WHEN \*  
\* ( \*/-)135 < YAW < ( \*/-)145 DEGREES \*  
\*\*\*\*\*  
SINY L001,R1 2 INDEX  
LUP STRA,R0 MY2-1,R1 LOAD OPRI-1,OPRI  
BDAR,R1 LUP  
EORZ R0  
BSTA,UN V1V1 FORM MY2/MH2  
BSTA,UN ANGL FURM\_ARCOS(MY2/MH2)  
BSTA,UN BCDA FURM\_ARCOS(MY2/MH2)  
L001,R0 H\*90\* CONVERT TO HCD  
PP5L C+WC .CALC. 90-ANGLE  
SURZ R1  
DAR,R0  
STAZ R1  
BSTA,UN HDG  
RETC,UN  
\*\*\*\*\*

REPRODUCIBILITY OF THE ORIGINAL PAGE IS POOR

PIP ASSEMBLER VERSION SCU LEVEL 1 READING INSTRUMENT ASSEMBLY PROGRAM 1976 PAGE 19

```

LINE ADDR LABEL M1 M2 M3 M4 EXPON SOURCE
602 0B54 0B54 70
603 0B48 CC 04 77 STRA#0 MSL CLR QUOTIENT
604 0B4E CC 04 78 STRA#0 MSL+1
605 0B51 07 11 LOUJ#3 17 CIR.
606 0B53 0E 04 7C LUDA#2 M#2+1
607 0B56 03 04 7B LUDA#1 M#2
608 0B59 0B59 77 04 PPSL COM+C*W C LOGICAL COMP., C=1, WITH C
609 0B58 F5 06 75 COMJ#1 0
610 0B5D 1C 04 73 BCT#2 ZER
611 0B60 E0 04 79 COMA#1 0PHI
612 0B63 19 14 BCT#01 0TU BK. IF M#2>M#12
613 0B65 1A 05 BCT#ALY 1TU BK. IF M#2<M#12
614 0B67 2E 04 7A COMA#2 0PHI+1 BK. IF M#2>M#12 (LS BITS)
615 0B6A 19 12 BCT#01 0TU
616 0B6C 0C 04 7A LUDA#0 0PHI+1
617 0B6F A2 STRA#0 0PHI+1
618 0B70 0C 04 7A LUDA#0 0PHI
619 0B73 0C 04 79 SUBZ R1
620 0B76 A1 STRA#0 0PHI
621 0B77 CC 04 79 STRA#0 0PHI
622 0B7A 77 01 PPSL C
623 0B7C 19 02 RCT#IN Jmp
624 0B7E 0A 7E 75 01 0TU
625 0B80 0C 04 78 JMP
626 0B83 10 LUDA#0 MSL+1
627 0B84 CC 04 78 STRA#0 MSL+1
628 0B87 0C 04 77 LUDA#0 MSL
629 0B8A 0B 04 77 MGL#R0
630 0B8H CC 04 77 STRA#0 MSL
631 0B8F 51 RRR#R1
632 0B90 52 RRR#R2
633 0B92 F0 47 BUR#R3 LUPI
634 0B95 17 RET#UN
635 0B98 9C 04 70 ZER COMJ#2 0
636 0B9B 1F 04 7E BCF#Z LUPI+7
637 0B9E 0B9E 77 04 RCT#UN 0TU
638 0BA0
639 0BA3
640 0BA6
641 0BA9
642 0BAC
643 0BAE
644 0BB1
645 0BB4
646 0BB7
647 0BB9
648 0BC0
649 0BC3
650 0BC6
651 0BC9
652 0BCB
653 0BCD
654 0BCE
655 0BCF
656 0BD0
657 0BD3
658 0BD6
659 0BD9
660 0BDB
661 0BDE
662 0BDF
663 0BE0
664 0BE3
665 0BE6
666 0BE9
667 0BED
668 0BEF
669 0BF0
670 0BF3
671 0BF6
672 0BF9
673 0BFB
674 0BFE
675 0C01
676 0C04
677 0C07
678 0C0A
679 0C0D
680 0C10
681 0C13
682 0C16
683 0C19
684 0C1C
685 0C1F
686 0C22
687 0C25
688 0C28
689 0C2B
690 0C2E
691 0C31
692 0C34
693 0C37
694 0C3A
695 0C3D
696 0C40
697 0C43
698 0C46
699 0C49
700 0C4C
701 0C4F
702 0C52
703 0C55
704 0C58
705 0C5B
706 0C5E
707 0C61
708 0C64
709 0C67
710 0C6A
711 0C6D
712 0C70
713 0C73

```

\*\*\*\*\*  
\* A SUBROUTINE TO DIVIDE M#2/M#2 OR M#2/M#2 \*  
\* ENTER WITH M#2 OR M#2 IN 0PHI & 0PHI+1 0 \*  
\* EXIT WITH QUOTIENT IN MSL/MSL+1 \*  
\*\*\*\*\*  
DIVI ENRZ M0  
STR#M0 MSL CLR QUOTIENT  
STR#M0 MSL+1  
LOUJ#3 17 CIR.  
LUDA#2 M#2+1  
LUDA#1 M#2  
PPSL COM+C\*W C LOGICAL COMP., C=1, WITH C  
COMJ#1 0  
BCT#2 ZER  
COMA#1 0PHI BK. IF M#2>M#12  
BCT#01 0TU BK. IF M#2<M#12  
BCT#ALY 1TU BK. IF M#2>M#12 (LS BITS)  
COMA#2 0PHI+1  
BCT#01 0TU  
LUDA#0 0PHI+1  
STR#M0 0PHI+1  
LUDA#0 0PHI  
SUBZ R1  
STR#M0 0PHI  
PPSL C  
RCT#IN Jmp  
CPSL C  
LUDA#0 MSL+1  
RRR#R0 MSL+1  
STR#M0 MSL+1  
LUDA#0 MSL  
MGL#R0  
STR#M0 MSL  
RRR#R1  
RRR#R2  
BUR#R3 LUPI  
HERE MSL=COS(Y#\*1)  
RETC#UN  
ZER COMJ#2 0  
BCF#Z LUPI+7  
RCT#UN 0TU  
\*\*\*\*\*  
\*\*\*\*\*  
\* A SUBROUTINE TO CALCULATE THE ARCUS FUNCTION \*  
\* THE ALGORITHM USES SUCCESSIVE APPROXIMATION \*  
\* & TABLE LOOK-UP TO ITERATE TO THE SOLUTION \*  
\* BEGIN WITH ARG. IN MSL/MSL+1 \*  
\* EXIT WITH ARCUS(M) IN RD \*  
\*\*\*\*\*  
MGL PPSL C\*W+C\*W



PIP ASSEMBLER VERSION SCU LEVEL 1 HEADING INSTRUMENT ASSEMBLY PROGRAM 1/7/74 PAGE 21

LINE	ADDR	LABL	M1	M2	M3	M4	PROR	SOURCE
766	0BFC		45 01					SUM1,M1 I
767	0BFE		1F 0C 43					BCFM,UN QUIT
768								START HERE IF COSTEST1 > ARG0.
769	0C01	0C01	F4 02					COM1,M0 C
770	0C03		98 07					BCFM,ED NEQ?
771	0C05		75 01					CPSL C
772	0C07		05 01					ADJ1,M1 I
773	0C09		1F 0C 43					BCFM,UN QUIT
774	0C0C	0C0C	00 06 00					LODA,M0 COS,M1,M1
775	0C0F		C3					STRZ M1
776	0C10		00 66 0A					LODA,M0 COS,M1,M1
777	0C13		77 01					PSL C
778	0C15	A3						SUBZ M3
779	0C16		75 01					CPSL C
780	0C18		50					RRR,R0
781	0C19		75 01					CPSL C
782	0C1A		83					ADDZ M3
783	0C1C		1E 0C 43					COM2 M2
784	0C1D		75 01					BCFM,LT QUIT
785	0C20		75 01					CPSL C
786	0C22		62 01					ADJ1,P1 I
787	0C24		1F 0C 43					BCFM,UN QUIT
788								EXAMINE LS BITS
789	0C27	0C27	75 01					ITLS CPSL C
790	0C29		05 2A					LODI,M1 42
791	0C2B		0E 04 70					LODA,M2 MSLF,M1
792	0C2E		F6 31					COM1,M2 M3,M1
793	0C30		10 0C 43					BCFM,GT QUIT
794	0C33		05 01					ADJ1,M1 I
795	0C35		F6 31					COM1,M2 M3,M1
796	0C37		10 0C 43					BCFM,GT QUIT
797	0C3A		85 01					ADJ1,M1 I
798	0C3C		F6 09					COM1,M2 M3,M1
799	0C3F		10 0C 43					BCFM,GT QUIT
800	0C41		85 01					ADJ1,M1 I
801	0C43	0C43	01					LODZ M3
802	0C44		75 01					CPSL C
803	0C46		04 20					ADJ1,M0 45
804								*****
805	0C48		17					RFIC,MN
806	0C49	0C49	65 28					LODI,M1 40
807	0C4A		00 66 19					LODA,M0 COS,M1,M1
808	0C4F		C3					STRZ M3
809	0C4F		00 66 18					LODA,M0 COS,M1
810	0C52		77 01					PSL C
811	0C54		61					SUBZ M3
812	0C55		75 01					CPSL C
813	0C57		50					RRR,R0
814	0C58		75 01					CPSL C
815	0C5A		83					ADDZ M3
816	0C5B		FC 04 78					COM1,M0 MSLF,M1
817	0C5F		1A 61					BCFM,LT QUIT

BEGIN ITERATION ON LS BITS  
ESTIMATE OF ADDRESS  
1ST ESTIMATE  
2ND EST.  
3D EST.

REPRODUCIBILITY OF THE ORIGINAL PAGE IS POOR

PIP ASSEMBLER VERSION SCU LEVEL 1 HEADING INSTRUMENT ASSEMBLY PROGRAM 1976 PAGE 22

LINE ADDR LABEL R1 R2 R3 R4 FROM SOURCE

```

818 0C60          05 29
819 0C62          1H 5F
820
821
822
823
824
825 0C64 0C64 07 07
826 0C66 0C66 05 00
827 0C68 0C68 75 01
828 0C6A 0C6A 00
829 0C6B 0C6B C2
830 0C6C 0C6C 9A 0A
831 0C6E 0C6E 01
832 0C6F 0C6F 75 01
833 0C71 0C71 84 06
834 0C73 0C73 8F 87 15
835 0C76 0C76 94
836 0C77 0C77 C1
837 0C7A 0C7A 02
838 0C79 0C79 FB 6D
839 0C7B 0C7B 17
840
841

```

LODI,R1 41  
 BCTR,JUN QUIT  
 \*\*\*\*\*  
 \* A SUBROUTINE TO CONVERT BINARY ANGLE TO BCD \*  
 \* ENTR WITH R0=ANGLE(IN) & EXIT R1=BCD FOURIV. \*  
 \*\*\*\*\*  
 BCDA LODI,R3 7 CLR,  
 LODI,R1 0 CLR TOTAL  
 CPSL C CLR, C  
 RRL,R0  
 STRZ R2 MOVE RESULT  
 BCFR,R1 NINC BK, IF MS BIT=0  
 LODZ R1  
 CPSL C  
 ADDI,R0 R1,66 BCD ADD 2 BYTES  
 ADDA,R0 BCD-1,R3 INCR, BCD TOTAL  
 DARR,R0  
 STRZ R1  
 LODZ R2 RESULT TO R0  
 BRRK,R3 BRCH GO BACK TIC DONE  
 NINC \*\*\*\*\* LEAVE WITH BCD EQUIV. OF YAW IN R1  
 \*\*\*\*\* METC,LUN \*\*\*\*\*

PIP ASSEMBLER VERSION SCU LEVEL 1 READING INSTRUMENT ASSEMBLY PROGRAM 1976 PAGE 23

LINE ADDR LABEL N1 N2 N3 B4 FROM SOURCE

```

843
844
845
846
847 UC7C 067C 77 04
848 UC7E 0C 04 7F
849 UC81 1A 1R
850
851 UC83 0C 04 81
852 UC86 1A 1R
853
854 UC88 F5 00
855 UC8A 1B 0C
856 UC8C 04 80
857 UC8E A1
858 UC8F 94
859 UC90 C3
860 UC91 0B 03
861 UC93 0B 00
862 UC95 96
863 UC96 1B 27
864
865
866 UC9A 0C 0B 0B 00
867 UC9A 01
868 UC9B C3
869 UC9C 1B 21
870
871
872 UC9E 0C 0E 0C 04 81
873 UC9E 1A 1P
874

```

```

*****
* A SUBROUTINE TO CALCULATE HEADING & OUTPUT *
* THREE TWO DIGITS PLUS SIGN *
*****
HUG PPSL AC=C SIGN OF HX ?
      LODA,R0 DATA BM, IF NEG
      BCIN,N YAWO
* SOLVE FOR HEADING (HCD FORM) GET HY
      LODA,R0 DATA GET HY
      BCIN,N HYN RM, ON HY=NEG.
* START HERE ON POS, HY & HX
      COMI,M1 0
      BCIN,R0 HYN
      LODI,R0 H1001
      SUBZ M1
      DASH,R0
      SINZ M3
      LODI,R2 H1031
      SUBI,R2 0
      DAR,RP
      ACIN,UN FINP
* ENTER HERE IF HX=POS. & HY=NEG.
HYN LODI,R2 H1001
      LODZ M1
      SINZ M3
      BCIN,UN FINE
* ENTER HERE HX=NEG & HY= +/- TEST SIGN OF HY
YAWO LODA,R0 DATA
      BCIN,N HNY

```

# REPRODUCIBILITY OF THE ORIGINAL PAGE IS POOR

PIP ASSEMBLER VERSION 10.00 SCULVEI 1 HEADING INSTRUMENT ASSEMBLY PROGRAM 1976 PAGE 24

```

LINE ADDR L=NL H1 H2 H3 H4 H5 H6 H7 H8 H9 H0
876      0CA3      04 80
877      0CA5      75 01
878      0CA7      84 66
879      0CA9      H1
880      0CAA      94
881      0CAC      C3
882      0CAC      06 01
883      0CAE      H6 66
884      0CB0      H6 00
885      0CB2      96
886      0CB3      1B 04
887
888
889      0CB5      0C H5
890      0CB7      0C H7
891      0CB8      A1
892      0CB9      94
893      0CBA      C3
894      0CBC      06 01
895      0CCE      A6 00
896      0CCE      96
897
898
899      0CC1      HCRF
900      0CC1      26 FF
901      0CC3      06 01
902      0CC3      27 FF
903      0CC5      17 02
904      0CC7      17
905
906
907
908
909
910
911      0E40      0E 40
912      0E43      0E 04 62
913      0E46      45 80
914      0E48      4B 7F
915      0E4A      CD 04 80
916      0E4C      0E 65 00
917      0E50      CC 04 69
918      0E53      0E 65 49
919      0E56      CC 04 7A
920      0E59      CC 04 7E
921      0E5C      03 04 5F
922      0E5F      CC 04 78
923      0E62      CC 04 7C
924      0E65      3F 08 66
925      0E68      0C 04 77
926      0E6H      0D 04 78
927      0E6F      CC 04 79

* ENTER HERE IF HX=NEG & HY=POS
  LODI,R0 H1B01
  CPSL C
  ADDI,R0 H166
  ADDI,R1
  DAK,R0
  STRZ R3
  LODI,R2 H1011
  ADDI,R2 H166
  ADDI,R2 0
  DAK,R2
  BCTR,RUN FINE
* ENTER HERE IF HX & HY = NEG
  NHY
  DO LODI,R0 H1B01
  SUBZ R1 SUB. YAW1 LSR
  DAK,R0
  STRZ R3
  LODI,R2 H1011
  SUBI,R2 0
  DAK,R2

* ***** HEADOUT OF DATA *****
  FINE
  WRITE,R2 HSR MSB OUT
  EORI,R3 H1FF LSR OUT
  WRITE,R3 LSB
  RETC,RUN
* *****
  ORG H1E40
* *****
* S.M. TO CALC. THE HZ COMPONENT IN X-Z PLANE *
  HZ=HY*SI(Phi) + HZ*COS(Phi)
* EXIT WITH HZ IN UPK210PR2+1
* *****
  HZR1 LODA,R1 DAIM+8 GET PHI
  LODA,R2 DAIM+8
  ANDI,R1 H1B01 SAVE SIGN
  ANDI,R2 H1FF1 STRI SIGN
  STRA,R1 TRUF HULU SIGN
  LODA,R0 SIN,R2 SIN(PHI)
  STRA,R0 SINR
  LOGA,P0 COS,R2 COS(PHI)
  STRA,R0 UPK1+1 HZ
  LODA,R0 DAIM+4
  LODA,R1 DAIM+5
  STRA,R0 UPK2+1
  BSTR,UN SWPT
  LODA,R0 HSL1
  LODA,R1 HSLI+1
  STRA,R0 ANUP

```

REPRODUCIBILITY OF THE ORIGINAL PAGE IS POOR

25

PIP ASSEMBLER DECK IN SCU LEVEL 1 HEADING INSTRUMENT ASSEMBLY PROGRAM 1-76 PAGE

LINE ADDR I AIL D1 D2 D3 D4 FADDR SOURCE

928	0E71					CD 04 7A	STRA,R1	BRUF	
929	0E74					CC 04 89	LODA,R0	STNR	
930	0E77					CC 04 7A	STRA,R0	OPR1+1	
931	0E7A					CC 04 5C	LODA,R0	UATM+2	MY
932	0E7D					DD 04 5D	LODA,R1	UATM+3	
933	0E80					C2	STRZ	R2	
934	0E81					44 7F	ANDI,R0	H7F1	
935	0E83					46 8C	ANDI,R2	H780	
936	0E85					7E 04 0D	LODA,R2	TRUF	DETERMINE SIG
937	0E88					CC 04 7A	STRA,R0	OPR2	
938	0E8B					CC 04 7C	STRA,R1	OPR2+1	
939	0E8F					CE 04 7E	STRA,R2	SRES	
940	0E91					3F 04 0D	BSTA,UN	SMPY	HY=SIN(PHI)
941	0E94					0C 04 09	LODA,R0	ARUF	
942	0E97					00 04 7A	LODA,R1	TEMP	
943	0E9A					CC 04 75	STRA,R0	TEMP+1	
944	0E9D					CD 04 00	STRA,R1	COM	AUD
945	0E9E					75 02	OPSL	COM	
946	0EA2					20	OPRZ	R0	HZ=COS(PHI)=PUS
947	0EA3					CC 04 7D	STRA,R0	STEM	
948	0EA6					1F 09 0B	BSTA,UN	SADD	
949	0EA9					0C 04 77	LODA,R0	RSLT	
950	0EAC					00 04 7B	LODA,R1	RSLT+1	
951	0EAF					CC 04 7A	STRA,R0	OPR2	
952	0EB2					CD 04 7C	STRA,R1	OPR2+1	
953	0EB5					77 02	PPSL	COM	
954	0EB7					17	RETC,MIN		



REPRODUCIBILITY OF THE ORIGINAL PAGE IS POOR

PIP ASSEMBLER VERSION SCU LEVEL 1 HEADING INSTRUMENT ASSEMBLY PROGRAM 1976 PAGE 26

LINE	ADDR	LABEL	B1	B2	B3	B4	ERROR SOURCE
956							
957							
958							
959							
960							
961							
962							
963							
964	0E1B	ORTH	75	01			
965	0E1A	CPSL	0C	04	5C		
966	0E1D	LODA,R0	0D	04	5D		
967	0E1E	LODA,R1	0E	07	1E		
968	0E1C	LODA,R2	0E	07	1C		
969	0E14	STRZ	C3				
970	0E17	ANDI,R0	44	7F			
971	0E18	ANDI,R3	47	80			
972	0E1A	STR,R0	CC	04	7A		
973	0E1B	STR,R1	CC	04	7C		
974	0E1D	STR,R2	CE	04	7E		
975	0E14	BSTA,UN	CF	04	66		
976	0E17	LODA,R0	0C	04	5A		
977	0E1A	LODA,R1	0D	04	5B		
978	0E1D	STRZ	C2				
979	0E1E	ANDI,R0	44	7F			
980	0E1E	ANDI,R2	46	80			
981	0E1E	STR,R0	CC	04	65		
982	0E1E	STR,R1	CD	04	66		
983	0E1B	STR,R2	CE	04	70		
984	0E1B	CPSL	75	02			
985	0E1D	BSTA,UN	3F	04	78		
986	0E1F	LODA,R0	0C	04	77		
987	0E1F	LODA,R1	0D	04	78		
988	0E1F	STR,R0	CC	04	5A		
989	0E1F	STR,R1	CC	04	5B		
990	0E1F	STR,R2	CC	04	5D		
991	0E1F	REF,UN	77	02			
992							
993							

TOTAL ASSEMBLY ERRORS = 0

\*\*\*\*\*  
 \* S.H. TO CORRECT NONORTHOGONALITY ERRORS IN HX \*  
 \* ENTER ONCE EACH SAMPLE CORRECTING HX SAMPLE \*  
 \* HX=HX(MEAS) \* HY=MEASJ(SIN(ERROW) \*  
 \* LOCATE SIN(ERROW) IN SINE \*  
 \* USES "SMPLY" TO FORM PRODUCT & "SADD" TO SUM \*  
 \* EXIT WITH MODIFIED HX IN DATA,DATA+1 \*  
 \*\*\*\*\*

ORTH CPSL C  
 LODA,R0 DATA+2 HY MSB  
 LODA,R1 DATA+3 HY LSB  
 LODA,R2 SINE SIN(ERROW)  
 STRZ R3 STRIP SIGN  
 ANDI,R0 R17F1 SAVE SIGN  
 ANUI,R3 H\*801  
 STR,R0 DRR2  
 STR,R1 URR2+1  
 STR,R2 OPR1+1  
 STR,R3 SWES SIGN OF HY\*(SIN(ERROW)  
 BSTA,UN SMPLY FORM PROD.  
 LODA,R0 DATM HX MSB  
 LODA,R1 DATM+1 HX LSB  
 STRZ R2  
 ANDI,R0 R17F1  
 ANUI,R2 H\*801  
 STR,R0 TFMP  
 STR,R1 TFMP+1  
 STR,R2 STEA FORM SUM  
 CPSL COM  
 BSTA,UN SADD  
 LODA,R0 RSLT  
 LODA,R1 RSLT+1 MODIFIED HX  
 STR,R0 DATA  
 STR,R1 DATA+1  
 PPSP COM  
 REF,UN  
 \*\*\*\*\*  
 END

## APPENDIX C

The transcendental functions used throughout the heading computation algorithm were implemented using a table look up procedure. To generate the respective look up tables in computer memory data was first generated using algol programs. This technique expedited modifications to tabular data and provided output data in a convenient (hexadecimal) format.

Programs that calculated  $\text{Cos}(\theta)$  and  $\text{Cos}^2(\theta)$  to eight bit and sixteen bit resolution respectively are included.

REPRODUCIBILITY OF THE  
ORIGINAL PAGE IS POOR

REPRODUCIBILITY OF THE  
ORIGINAL PAGE IS POOR

PAGE 001

```

001 00000 HPAI 4, "RP"
002 00000 BFGT,
003 00001 A.....
004 00001 A A PROGRAM TO GENERATE A COS*COS TABLE FOR A
005 00001 A MICROPROCESSOR BASED SYSTEM
006 00001 A ANGLE, COS(ANGLE), AND DATA IN
007 00001 A BOTH BINARY AND HEX FORMAT IS TABULATED
008 00001 A.....
009 00001 INTRGR A,B,C,D,E,F
010 00010 RPAI THETA,STHETA,AP,ASTH
011 00020 RPAI ARRAY AN(0:256,0:1)
012 21070 INTRGR ARRAY VAL(0:15):="0","1","2","3","4","5",
013 21102 "6","7","8","9","A",
014 21107 "B","C","D","E","F"
015 21114 INTRGR ARRAY MULT(0:3):="8.4,2,1"
016 21124 INTRGR ARRAY HEX(0:256,0:3)
017 23136 WRITE (A,*(1:1))
018 23175 WRITE (A,*(//,4X,"A",5X,"THETA",4X,"COS*COS",5X,
019 23226 "BINARY",14X,"HEX",//))
020 23242 WRITE (A,*(5X,"(ADD)",3X,"(DEG)",18X," DATA ",//))
021 23276 FOR A:= 45 TO 90 DO
022 23304 BEGIN
023 23304 AX:=A
024 23310 THETA:= AX*PI/180
025 23316 STHETA:=(COS(THETA))^2
026 23330 HI:=0
027 23332 HSTH:=STHETA
028 23336 WHILE HI<17 DO
029 23341 BEGIN
030 23342 STH:= 2*HSTH
031 23350 IF STH>1 THEN
032 23355 BEGIN
033 23355 AN(A,HI:=1)
034 23367 STH:=HSTH-1
035 23375 END ELSE AN(A,HI):=0
036 23435 HI:=HI+1
037 23440 END
038 23441 HI:=0
039 23443 FOR C:=0 TO 3 DO
040 23451 BEGIN
041 23451 HI:=4*C
042 23455 FI:=0
043 23457 FOR F:=0 TO 3 DO
044 23465 BEGIN
045 23465 FI:=F*MULT(F)*AN(A,HI)
046 23520 HEX(A,C):= VAL(F)
047 23533 END
048 23537 END
049 23543 THETA:= THETA*180/PI
050 23553 WRITE (B,*(5X,15,2(3X,FA,6),3X,10(1,5X,4A2),A,
051 23604 THETA,STHETA, FOR HI= 0 TO 15 DO
052 23620 AN(A,HI), FOR C:= 0 TO 3 DO HEX(A,C))
053 23653 ENDF
054 23657 ENDA
PROGRAM= 0236A3 ERRORS=000

```

REPRODUCIBILITY OF THE  
ORIGINAL PAGE IS POOR

A	THETA	COS*COS	BINARY	HEX
(ADDR.)	(DEG)		DATA	
45	45.00000	.500000	0111111111111111	7 F F F
46	46.00000	.482550	0111101110001000	7 8 8 8
47	47.00000	.465122	0111011100010010	7 7 1 2
48	48.00000	.447736	0111001010011110	7 2 9 E
49	48.99999	.430413	0110111000101111	6 E 2 F
50	50.00000	.411176	0110100111000101	6 9 C 5
51	51.00000	.396044	0110010101100011	6 5 6 3
52	52.00001	.379039	0110000100001000	6 1 0 8
53	53.00000	.362181	0101110010110111	5 C 8 7
54	54.00000	.345491	0101100001110010	5 8 7 2
55	55.00000	.328990	0101010000111000	5 4 3 8
56	56.00000	.312697	0101000000001100	5 0 0 C
57	57.00000	.296632	0100101111110000	4 8 F 0
58	58.00000	.280814	0100011111100011	4 7 E 3
59	58.99999	.265244	0100001111101000	4 3 E 8
60	60.00001	.250060	0011111111111111	3 F F F
61	61.00000	.235040	0011110000101011	3 C 2 8
62	62.00000	.220403	0011100001101100	3 8 6 C
63	63.00000	.206107	0011010011000011	3 4 C 3
64	64.00000	.192149	0011000100110010	3 1 3 2
65	65.00000	.178606	0010110110111001	2 D 8 9
66	66.00000	.165435	0010101001011001	2 A 5 9
67	66.99998	.152671	0010011100010101	2 7 1 5
68	68.00000	.140330	0010001111101100	2 3 E C
69	69.00000	.128427	0010000011100000	2 0 E 0
70	70.00000	.116978	0001110111110010	1 D F 2
71	71.00000	.105965	0001101100100010	1 8 2 2
72	72.00000	.095491	0001100001110010	1 8 7 2
73	73.00000	.085481	0001010111100010	1 5 E 2
74	73.99998	.075976	0001001101110011	1 3 7 3
75	75.00000	.066987	0001000100100110	1 1 2 6
76	76.00000	.058526	0000111011111011	0 E F 8
77	77.00002	.050603	0000110011110100	0 C F 4
78	78.00000	.043227	0000101100010000	0 8 1 0
79	79.00000	.036408	0000100101010010	0 9 5 2
80	80.00000	.030154	0000011110111000	0 7 8 8
81	81.00000	.024472	0000011001000011	0 6 4 3
82	82.00000	.019349	0000010011110101	0 4 F 5
83	83.00000	.014852	0000001111001101	0 3 C 0
84	84.00002	.010926	0000001011001100	0 2 C C
85	84.99998	.007596	0000000111100001	0 1 F 1
86	86.00000	.004866	0000000100111110	0 1 3 E
87	87.00000	.002739	0000000010110011	0 0 8 3
88	88.00000	.001218	0000000001001111	0 0 4 F
89	89.00000	.000305	0000000000010011	0 0 1 3
90	90.00000	.000000	0000000000000000	0 0 0 0

REPRODUCIBILITY OF THE  
ORIGINAL PAGE IS POOR

PAGE 001

```

001 00000 HPAI ,I , "RPH"
002 00000 HPGIN
003 00001 &*****
004 00001 & A PROGRAM TO GENERATE A COS TABLE FOR A
005 00001 & MICROPROCESSOR BASED SYSTEM
006 00001 & ADDRESS, ANGLE, COS(ANGLE), AND DATA IN
007 00001 & BOTH BINARY AND HEX FORMAT IS TABULATED
008 00001 &*****
009 00001 INTEGER A,B,C,D,E,F;
010 00010 RFAI THETA,STHETA,AR,HSTH;
011 00020 RFAI ARRAY AN(0:256,0:16);
012 21070 INTEGER ARRAY VAL(0:15):="0","1","2","3","4","5",
013 21102 "6","7","8","9","A","B",
014 21107 "C","D","E","F";
015 21114 INTEGER ARRAY MULTI(0:15):=8+4+2+1;
016 21124 INTEGER ARRAY HEX(0:256,0:1);
017 23136 WRITE (A,*(I(H));
018 23175 WRITE (6,*(//,9X,"A",5X,"THE TA",4X,"COS(THETA)",2X," BINARY",6X,"HEX",
019 23240 /));
020 23243 WRITE (A,*(5X,"(ADDR)",3X,"(DEG)",18X," DATA ",//));
021 23277 FOR A:= 45 TO 90 DO
022 23305 BEGIN
023 23305 AR:=AI
024 23311 THETA:= AR*PI/180;
025 23317 STHETA:= COS(THETA);
026 23323 H:=0;
027 23325 HSTH:=STHETA;
028 23331 WHILE H<9 DO
029 23334 BEGIN
030 23335 HSTH:= 2*HSTH
031 23343 IF HSTH>1 THEN
032 23350 BEGIN
033 23350 AN(A,B):=1;
034 23362 HSTH:=HSTH-1;
035 23370 ENI ELSE AN(A,B):=0;
036 23403 H:=B+1;
037 23406 ENI
038 23407 H:=0;
039 23411 FOR C:=0 TO 3 DO
040 23417 BEGIN
041 23417 D:=4*C;
042 23450 F:=0;
043 23452 FOR E:=0 TO 7 DO
044 23460 BEGIN
045 23460 F:=F*MULT[F]*AN(A,B)*E;
046 23513 HEX(A,C):= VAL(F);
047 23526 ENI;
048 23532 ENI;
049 23536 THETA:= THETA*180/PI;
050 23546 WRITE (6,*(5X,"(S",15,2(3X,FR,6),3X,HF1,0,5X,242),A,THETA,STHETA,
051 23605 FOR H:=0 TO 7 DO AN(A,B),FOR D:=0 TO 1 DO HEX(A,D));
052 23646 ENI;
053 23652 ENI;

```

PROGRAM= 023656 ERRORS=000

REPRODUCIBILITY OF THE  
ORIGINAL PAGE IS POOR  
ORIGINAL PAGE IS POOR

A (ADDR.)	THETA (DEG)	COS(THETA)	BINARY DATA	HEX
45	45.00000	.707107	1.11.1.1	8 5
46	46.00000	.694659	1.11...1	8 1
47	47.00000	.681998	1.1.111.	A E
48	48.00000	.669131	1.1.1.11	A 8
49	48.99999	.656059	1.1.1111	A 7
50	50.00000	.642788	1.1.1.1..	A 4
51	51.00000	.629320	1.1...1	A 1
52	52.00001	.615662	1...111.1	9 0
53	53.00000	.601815	1...11.1.	9 A
54	54.00000	.587785	1...1.11.	9 6
55	55.00000	.573576	1...1.1.1.	9 2
56	56.00000	.559193	1...1111	8 F
57	57.00000	.544639	1...1.11	8 B
58	58.00000	.529919	1...1111	8 7
59	58.99999	.515038	1...1.11	8 3
60	60.00001	.500000	.1111111	7 F
61	61.00000	.484810	.11111..	7 C
62	62.00000	.469471	.1111...	7 8
63	63.00000	.453991	.111.1...	7 4
64	64.00000	.438371	.111.....	7 0
65	65.00000	.422618	.11.11...	6 C
66	66.00000	.406737	.11.1...	6 8
67	66.99998	.390731	.11.1.1..	6 4
68	68.00000	.374607	.1.11111	5 F
69	69.00000	.358348	.1.1.1.11	5 8
70	70.00000	.342020	.1.1.1.111	5 7
71	71.00000	.325568	.1.1.1.11	5 3
72	72.00000	.309017	.1.1.1111	4 F
73	73.00000	.292372	.1.1.1.1.	4 A
74	73.99998	.275637	.1...111.	4 6
75	75.00000	.258819	.1....1.1.	4 2
76	76.00000	.241922	.1111.1	3 0
77	77.00002	.224951	.111.1	3 9
78	78.00000	.207912	.11.1.1	3 5
79	79.00000	.190809	.11.....	3 0
80	80.00000	.173648	.1.11...	2 C
81	81.00000	.156435	.1.1.1...	2 8
82	82.00000	.139173	.1.1.111	2 3
83	83.00000	.121849	.111111	1 F
84	84.00002	.104528	.11.1.1.	1 A
85	84.99998	.087156	.1.1.11.	1 6
86	86.00000	.069757	.1.1.1.1	1 1
87	87.00000	.052336	.1.1.1.1	0 D
88	88.00000	.034900	.1.1.1.	0 8
89	89.00000	.017452	.1.1.1.	0 4
90	90.00000	.000000	.....	0 0

## BIBLIOGRAPHY

- [1-1] C. C. Kalweit, "The ESRO 1 attitude measurement system," *IEEE Trans. Aerosp. Electron. Syst.*, vol. AES-7, pp. 132-141, Jan. 1971.
- [1-2] G. A. Korn and T. M. Korn, *Mathematical Handbook for Scientists and Engineers*. New York: McGraw-Hill, 1961, sec. 14.10-2.
- [1-3] E. V. Condon and H. Odishaw, *Handbook of Physics*, 2nd ed., 1967, ch. 2-3.
- [1-4] S. H. Crandall, *Dynamics of Mechanical and Electromechanical Systems*. New York: McGraw-Hill, 1968, pp. 42-152.
- [1-5] M. Kayton and W. Fried, *Avionics Navigation Systems*. New York: Wiley, 1969.
- [1-6] S. Chapman and J. Bartel, *Geomagnetism*, vol. II, New York: Oxford Univ. Press, 1940.
- [1-7] Vestine *et al.*, "The geomagnetic field, its description and analysis," Dept. Terrestrial Magnetism, Carnegie Inst. Technol., Pittsburgh, PA., publ. 580, ch. 2, 1947.
- [1-8] E. Irving, *Paleomagnetism and Its Application to Geology and Geophysical Problems*. New York: Wiley, 1964, ch. 3.
- [1-9] F. D. Stacey, *Physics of the Earth*. New York: Wiley, 1969, ch. 5.
- [1-10] D. R. Hartman, D. J. Tskey, and G. L. Friedberg, "A system for digital aeromagnetic interpretation," *Geophysics*, vol. 36, pp. 891-918, Oct. 1971.
- [1-11] M. L. Hill, "Introducing the electrostatic autopilot", *Astronaut. Aeronaut.*, pp. 24-31, Nov. 1972.
- [1-12] R. Markson, "Practical aspects of electrostatic stabilization," *Astronaut. Aeronaut.*, pp. 44-49, Apr. 1974.

BIBLIOGRAPHY (Continued)

- [2-1] R. Pietila and W. R. Dunn, Jr., "A Vector Autopilot System," *IEEE Transactions on Aerospace and Electronic Systems*, vol. AES-12, No. 3, May, 1976.
- [2-2] G. A. Korn and T. M. Korn, *Electronic Analog Computer*, McGraw-Hill, 2nd ed., 1956.
- [2-3] E. A. Parrish, Jr., and Y. C. Lee, "A microcomputer preprocessor/postprocessor for analog signals," *IEEE Trans. on Industrial Electronics and Control Instrumentation*, vol. IECI-21, No. 1, Feb. 1974, pp. 38-41.
- [3-1] R. Allan, "Components: Microprocessors Galore," *IEEE Spectrum*, vol. 13, no. 1, Jan. 1976, pp. 50-56.
- [3-2] G. Kaplon, "Industrial Electronics to Boost Productivity," *IEEE Spectrum*, vol. 13, no. 1, Jan. 1976, pp. 87-90.
- [3-3] H. Falk, "Computers: Poised for Progress", *IEEE Spectrum*, vol. 13, no. 1, Jan. 1976, pp 44-49.
- [3-4] D. Christianson, "Technology '76", *IEEE Spectrum*, vol. 13, no. 1, Jan. 1976, pp 42-43.
- [3-5] W. Myers, "Key Developments in Computer Technology: A Survey", *Computer, IEEE Computer Society*, vol 9, no. 11, Nov. 1976, pp 48-77.
- [3-6] E. A. Terrero, "Focus on Microprocessors", *Electronic Design* 7, March 29, 1976, pp 58-64.
- [3-7] R. Noyce, "From Relays to MPU's", *Computer, IEEE Computer Society*, vol. 9, no. 12, Dec. 1976, pp 26-29.
- [3-8] E. R. Garren, "Applying Microprocessors and Microcomputers", *Modern Data*, Feb. 1975, pp. 54-57.
- [3-9] D. N. Kaye, "How to Pick a Microprocessor, a Mini or Anything in Between", *Electronic Design* 16, Aug. 1975, pp. 26-30.



BIBLIOGRAPHY (Continued)

- [3-10] T. A. Seim, "Microprocessors Aid Experimentation in Scientific Laboratory", *Computer Design*, Sept. 1976, pp. 83-89.
- [3-11] M. Teener and W. Liles, "Microcomputers, Where the Action Really is", *Modern Data*, Feb. 1975, pp. 49-53.
- [3-12] H. D. Scott and R. A. Smoak, "A Microcomputer Controller for a Nuclear Pool Reactor", *IEEE Trans. on Industrial Electronics and Control Instrumentation*, vol. IECI-22, no. 1, Feb. 1975, pp. 15-18.
- [3-13] A. Osbourne and Associates, "An Introduction to Microcomputers", Adam Osbourne and Associates, Inc., Berkeley, CA. 1975.
- [3-14] M. H. Lewin, "Integrated Microprocessors", *IEEE Trans. on Circuits and Systems*, Vol. CAS-22, no. 7, July 1975, pp. 577-585.
- [3-15] R. K. Jurgen, "The Microprocessor: In the Driver's Seat", *IEEE Spectrum*, vol. 12, no. 6, June 1975, pp. 73-77.
- [3-16] C. Newcombe, "How to Evaluate Microprocessor Instruments", *IEEE Spectrum*, vol. 13, no. 4, April 1976, pp. 38-55.
- [3-17] S. Sheikh, "A Programmable Digital Control System for Copying Machines", *IEEE Trans. on Industrial Electronics and Control Instrumentation*, vol. IECI-21, no. 1. Feb. 1974, pp. 25-33.
- [3-18] D. L. Smith, "The Problem with Programmable Controllers", *IEEE Trans. on Industrial Electronics and Control Instrumentation*, vol. IECI-21, no. 2, May 1974. pp. 50-52.
- [3-19] H. Falk, "Self Contained Microcomputers Ease System Implementation", *Computer, IEEE Spectrum*, vol. 11, no. 12, Dec. 1974, pp. 53-54.
- [3-20] A. R. Ward, "LSI Microprocessors and Microcomputers: A Bibliography", *Computer, IEEE Computer Society*, vol. 7, no. 7, July 1974.

BIBLIOGRAPHY (Continued)

- [3-21] A. R. Ward "LSI Microprocessors and Microcomputers: A Bibliography Continued", *Computer, IEEE Computer Society*, vol. 9, no. 1, Jan. 1976, pp. 42-53.
- [3-22] *Signetics 2650 Microprocessor Manual*, Signetics Corporation, Sunnyvale, CA. 1975.
- [3-23] A.V.Oppenheim and R.W.Schafer, *Digital Signal Processing*, Prentice Hall, N.J., 1975.
- [3-24] C.E.Shannon, "Communication in the Presence of Noise", *Proc. IRE*, vol. 37, No. 1 (Jan. 1949), pp 10-21.
- [3-25] *Engineering Product Handbook (A/D and D/A Converters)*, Datel Systems Incorporated, 2nd Printing. Canton, Massachusetts.
- [3-26] *Analog-Digital Converter Data Sheets*, Analog Devices, Inc., Norwood, Massachusetts.
- [3-27] *Analog-Digital Converter Data Sheets*, Burr-Brown Research Corp., Tucson, AZ.
- [3-28] User's Guide to A/D Converters. *Electronic Products*, Dec. 1976.
- [3-29] T.R.Blakeslee, *Digital Design with Standard MSI and LSI*, Wiley-Interscience Pub., John Wiley & Sons, 1975.
- [3-30] J. B. Peatman, *The Design of Digital Systems*, McGraw-Hill, 1972.
- [3-31] H. W. Gschwind, *Design of Digital Computers*, Springer-Verlag, N.Y., 1967.
- [3-32] The Signetics 2650 Assembler Version SCU Level 1 (Signetics part number 2650 AS1000/1100) operational on the HP2100 computer at the University of Santa Clara.
- [3-33] C.McGowan "Structured Programming:A Review of Some Practical Concepts", *IEEE Computer*, Vol 8, No.6, June, 1975
- [3-34] *Three Axis Fluxgate Magnetometer Specification*, Model 9200C. Develco, Inc., Mountain View, CA.
- [3-35] *Analog to Digital Converter Specification*, Model ADC-MA12B2B. Datel Systems, Inc., Canton, Mass.

BIBLIOGRAPHY (Continued)

- [3-36] Telephone conversations with Dr. Opher of Develco Inc., during summer of 1976.
- [3-37] G. Dahlquist and A. Bjorck, *Numerical Methods*, Prentice Hall, 1974.
- [3-38] C.V. Ramamoorthy, J.R. Goodman and K.H. Kim, "Some Properties of Iterative Square-Rooting Methods Using High Speed.
- [4-1] Telephone conversation with Develco magnetometer project engineer, Ronald Warkentine, November 3, 1976.
- [4-2] P.E. Gise, "A Cylindrical Thin-Film Magnetometer Sensor", PhD Thesis, University of Santa Clara, 1976.
- [4-3] Telephone Conversation with Ronald Warkentine (project engineer) at Develco, November 24, 1976.
- [4-4] J.A. Cadzow, *Discrete Time Systems*, Prentice-Hall, Inc., Englewood Cliffs, New Jersey, 1973.
- [4-5] A.V. Oppenheim, R.W. Schafer, *Digital Signal Processing*, Prentice-Hall, Inc., Englewood Cliffs, N.J., 1975.
- [4-6] S. Mason and H.J. Zimmerman, *Electronic Circuits, Signals and Systems*, John Wiley & Sons, Inc., New York, 1960.
- [4-7] Model MM-8, *8 Channel Analog Multiplexer Data Sheets*, Datel Systems, Inc., Canton, Mass., 1975
- [4-8] B.A. Barry, *Engineering Measurements*, J. Wiley, & Sons, Inc., N.Y., 1964.
- [4-9] M.B. Stout, *Basic Electrical Measurements*, Prentice-Hall, Inc., N.J., 1960.
- [4-10] Model SHM-IC-1, *Sample and Hold Integrated Circuit*, Datel Systems, Inc., Canton, Mass., 1975.
- [4-11] Model ADC-MA12B1B, *Analog to Digital Converter Data Sheets*, Datel Systems, Inc., Canton, Mass., 1974.
- [4-12] G. Dahlquist, *Numerical Methods*, Prentice-Hall, Inc., Englewood Cliffs, N.J., 1974.

